The CMB foregrounds according to Planck

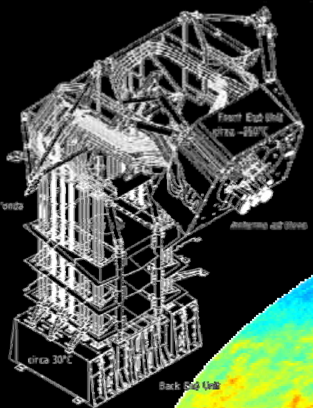

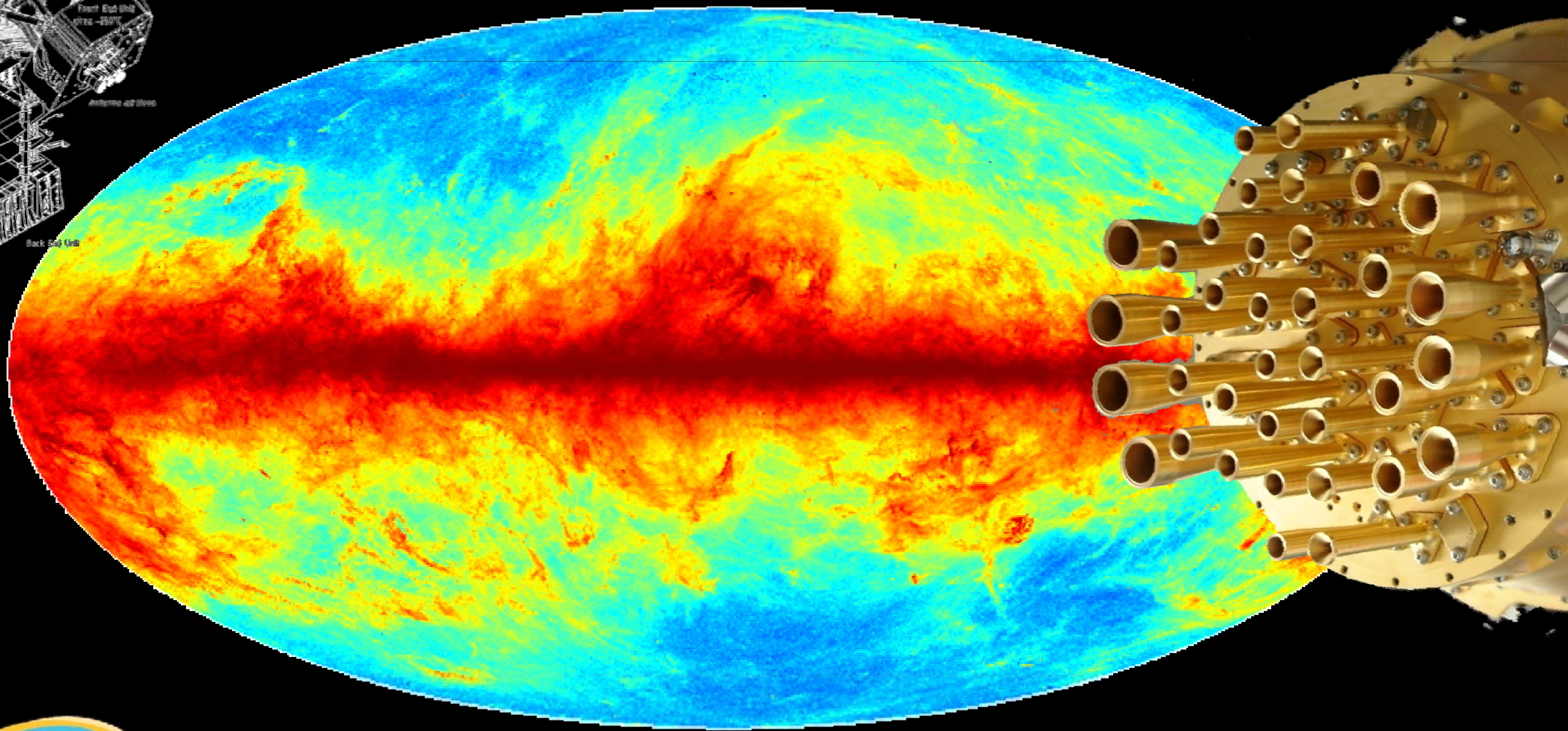

the first 295 days of survey

HFI PLANCK

F. R. Bouchet, IAP

Planck Goals in perspective

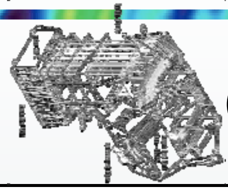

("Blue Book", twice better than requirements)

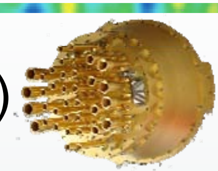

PLANCK	LFI			HFI					
Center Freq (GHz)	30	44	70	100	143	217	353	545	857
Angular resolution (FWHM arcmin)	33	24	14	10	7.1	5.0	5.0	5	5
Sensitivity in I [μK.deg] [$\sigma_{pix}\ \Omega_{pix}^{1/2}$]	3.0	3.0	3.0	1.1	0,7	1.1	3.3	33	3.0

WMAP Center Freq.	23	33	41	61	94
Angular resolution (FWHM arcmin)	49	37	29	20	12,6
Sensitivity in I [μK.deg], 1 yr (8 yr)	12.6 (4.5)	12.9 (4.6)	13.3 (4.7)	15.6 (5.5)	15.0 (5.3)

The aggregated sensitivity of Planck core CMB channels is ~0.5μK.deg in T (nominal mission – 14months)

NB: Anticipated survey duration is now ~30 months, so final sensitivity ~0.33 μK.deg in T (approx 1000 years of WMAP 60+90GHz aggregated sensitivity of 10.8 μK.deg in1yr)

HFI cut-away

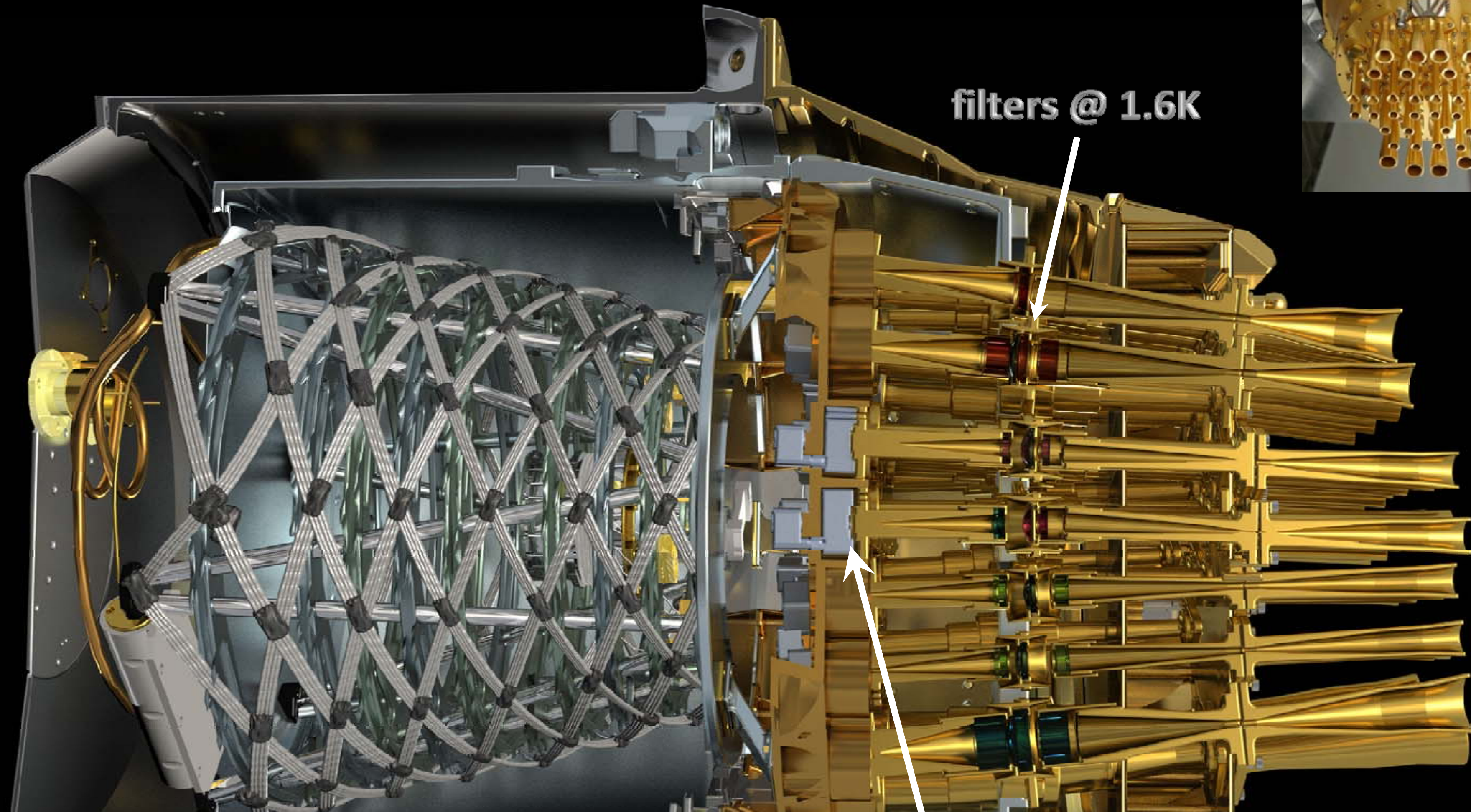

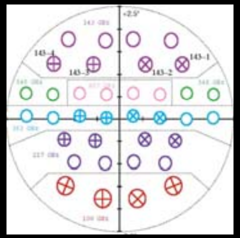


DUSTING IT OFF...
AFTER 16 YEARS
OF HOPES & WORK

Ariane 5 ECA Launch • HERSCHEL – PLANCK *- May 14, 2009*

Tension subsides...

Picture by Ganga

Trajectory of Planck from launch until 6 June 2010

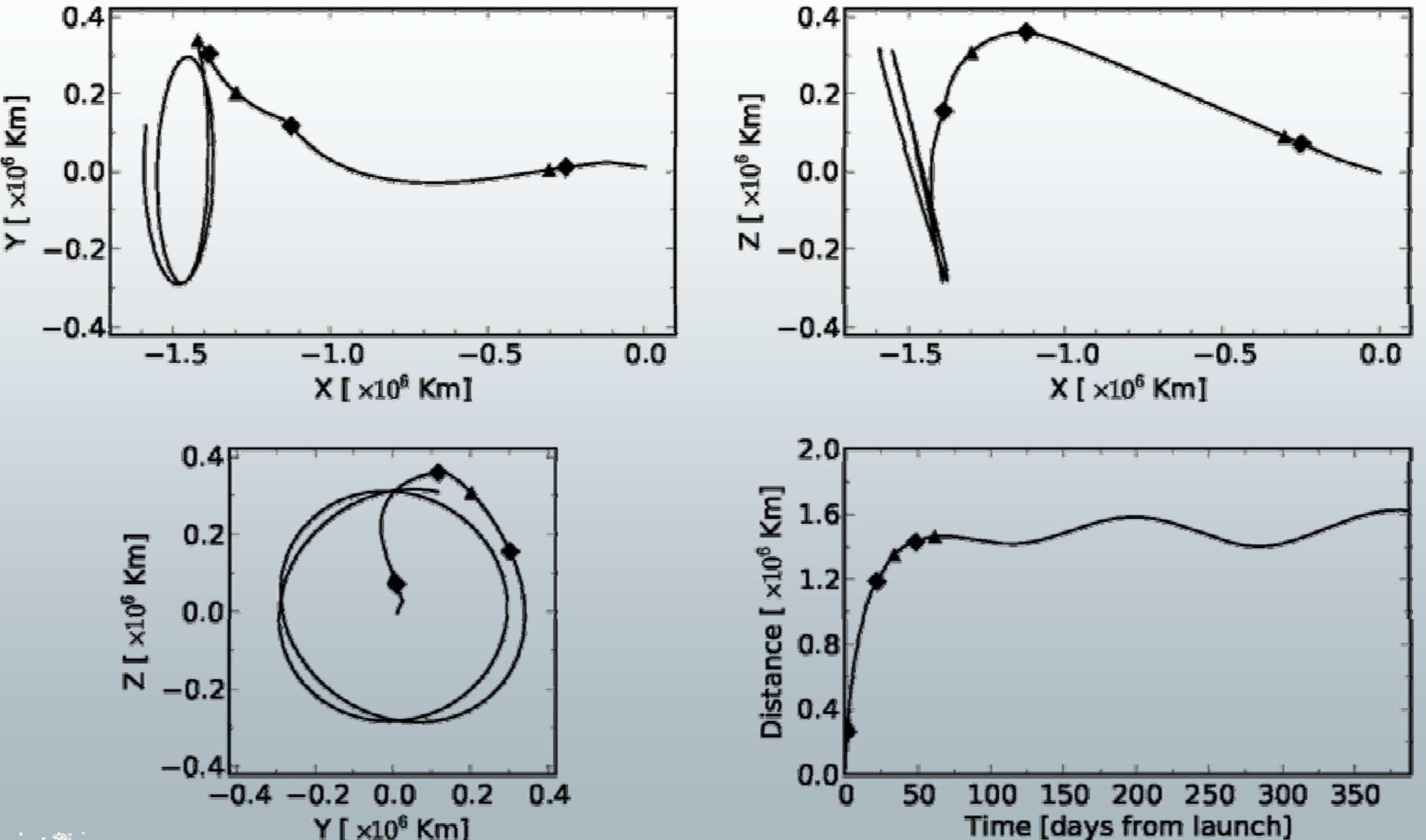

4th Press Release (05/07/2010)

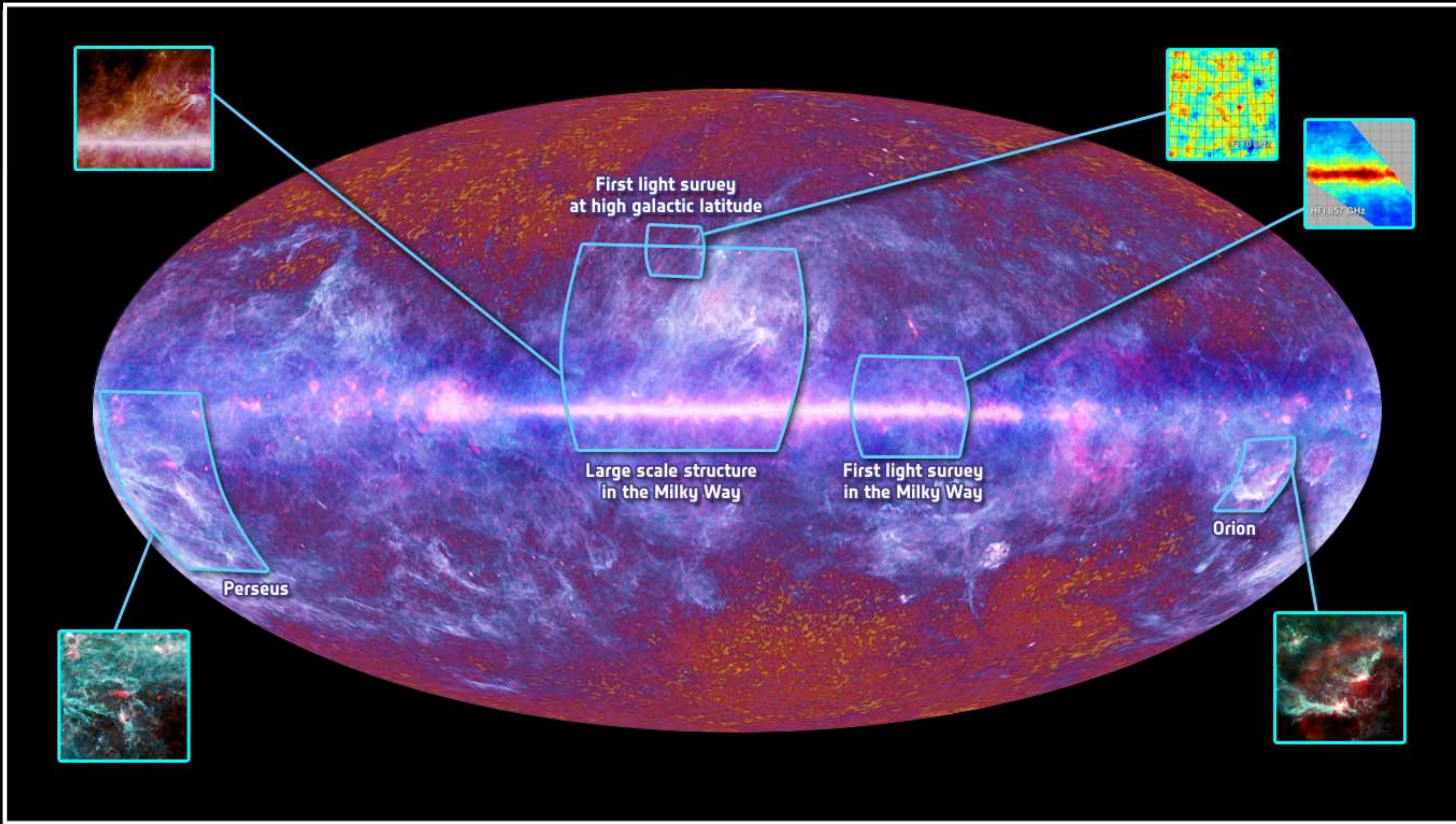

The Planck one-year all-sky survey

esa

Overall

- Instrument very stable, continuously mapping the sky, with essentially no hiccups from the beginning of the first light survey on the 13th August 2009, till today.
- Ground (good)expectations on sensitivities confirmed in flight
- Surprise of Glitch rate!

- The data acquired till June 7^{th}, ie the nearly ten months of survey data provide complete coverage of the sky by all detectors (by roughly 3 days more than the minimum duration needed),
  - *but only limited redundancy. Indeed the overlap between the two consecutive six-month surveys is only about 60%.*

- DX4 was released on July 17th 2010 to LFI & ERCSC team, DR2 (CMB-removed) to all Planck collaboration on 08/02, characterisation continued till very recently.

Cumulated integration time

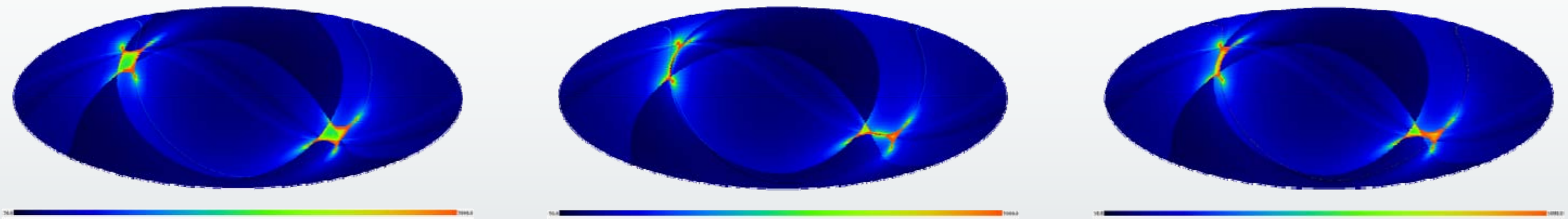

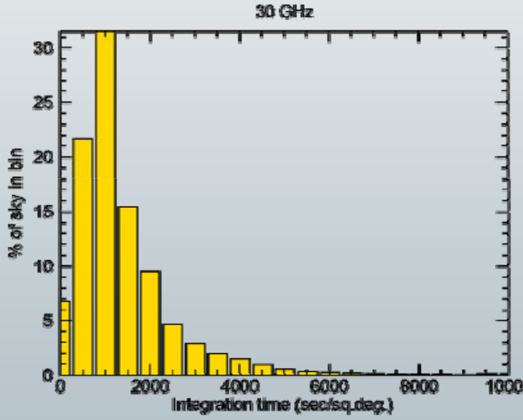

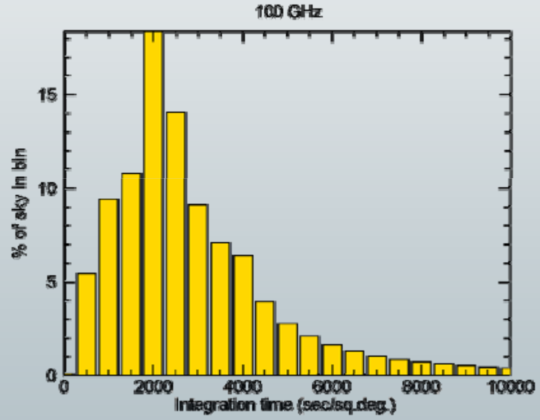

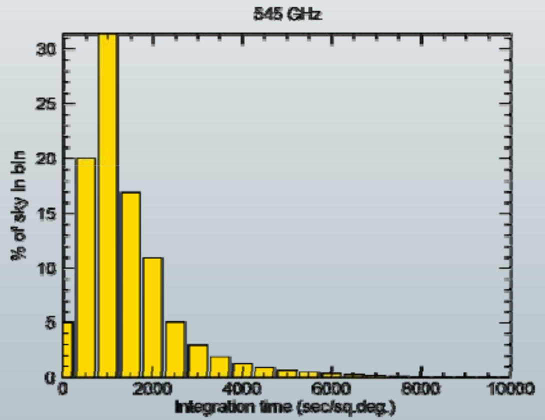

	30 GHz	100 GHz	545 GHz	
Mean[a]	2293	4575	2278	sec deg^2
Minimum	440	801	375	sec deg^2
$<$ half Mean[b]	14.4	14.6	15.2	%
$>$ 4$\times$ Mean[c]	1.6	1.5	1.2	%
$>$ 9$\times$ Mean[d]	0.41	0.42	0.41	%

HFI Data Processing Centre flow

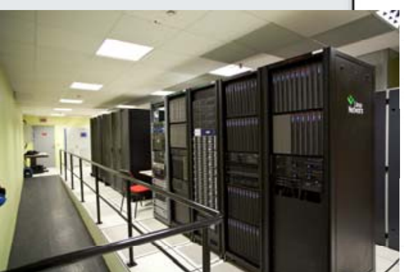

IAP cellar

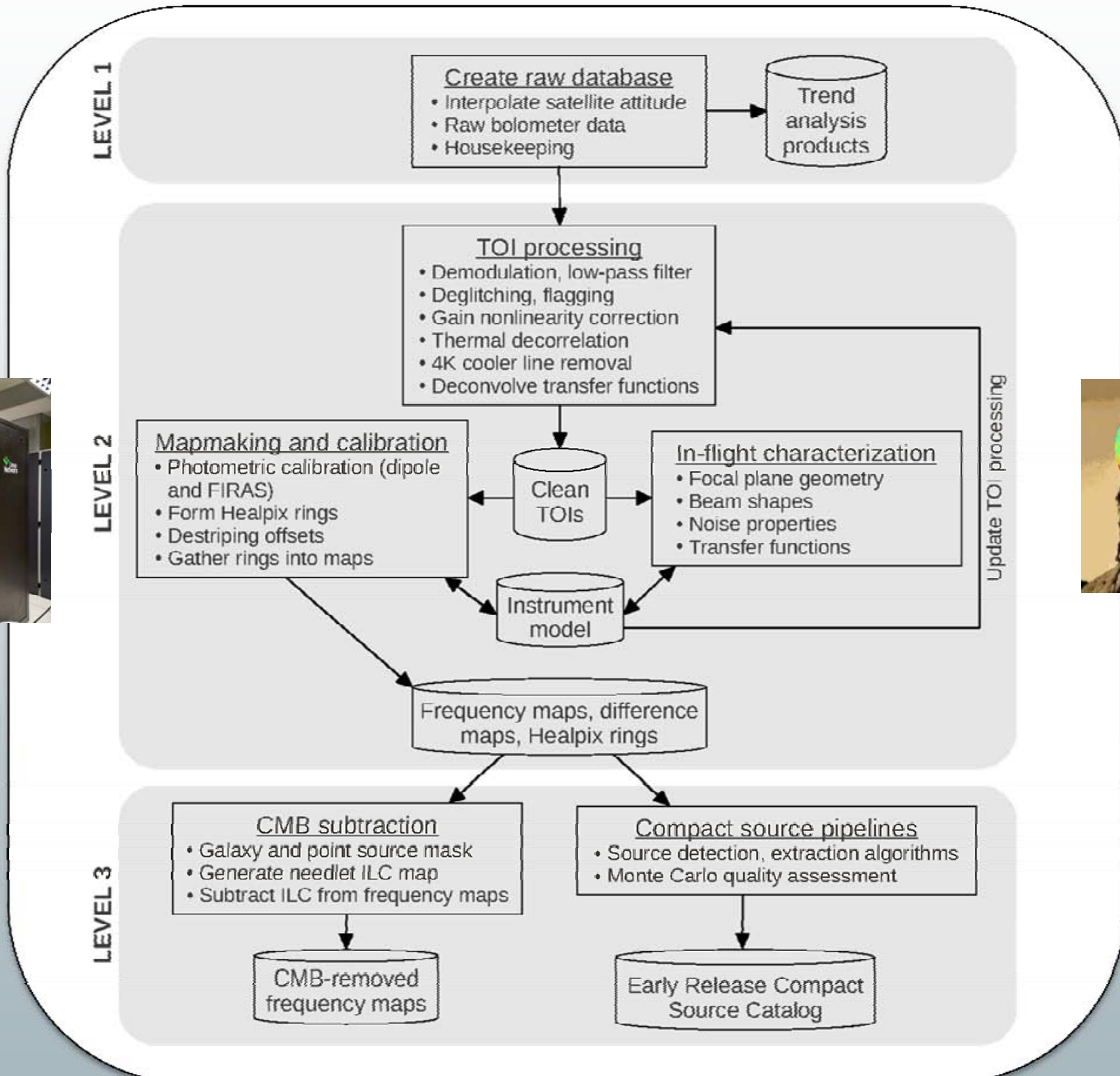

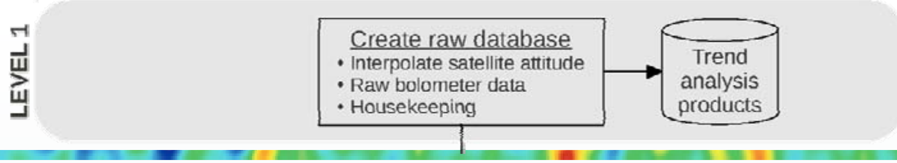

- L1 received 4 x10^8 telemetry packets:
  - *29%, 6% and 4% for the housekeeping of respectively the satellite, the Sorption Cooler System and HFI (25 425 HK pars followed out of 63 100) and*
  - *61% for HFI science data. Only 20 packets lost from L2.*
- 4.7 x 10^9 time samples for 72 detectors, i.e. 334 x 10^9 detector samples from the first 295 days of survey
- Decompress, QLA and update/append Time Ordered Information objects (TOIs) in reference database.
- Attitude History File of the Satellite quaternion pointings at 8Hz linearly interpolated daily at Time-of-Sample of the bolometers and stored for later On-the-fly generation of any pointing using the Focal Plane Geometry.

Raw Detector TOI (Time Ordered Information)

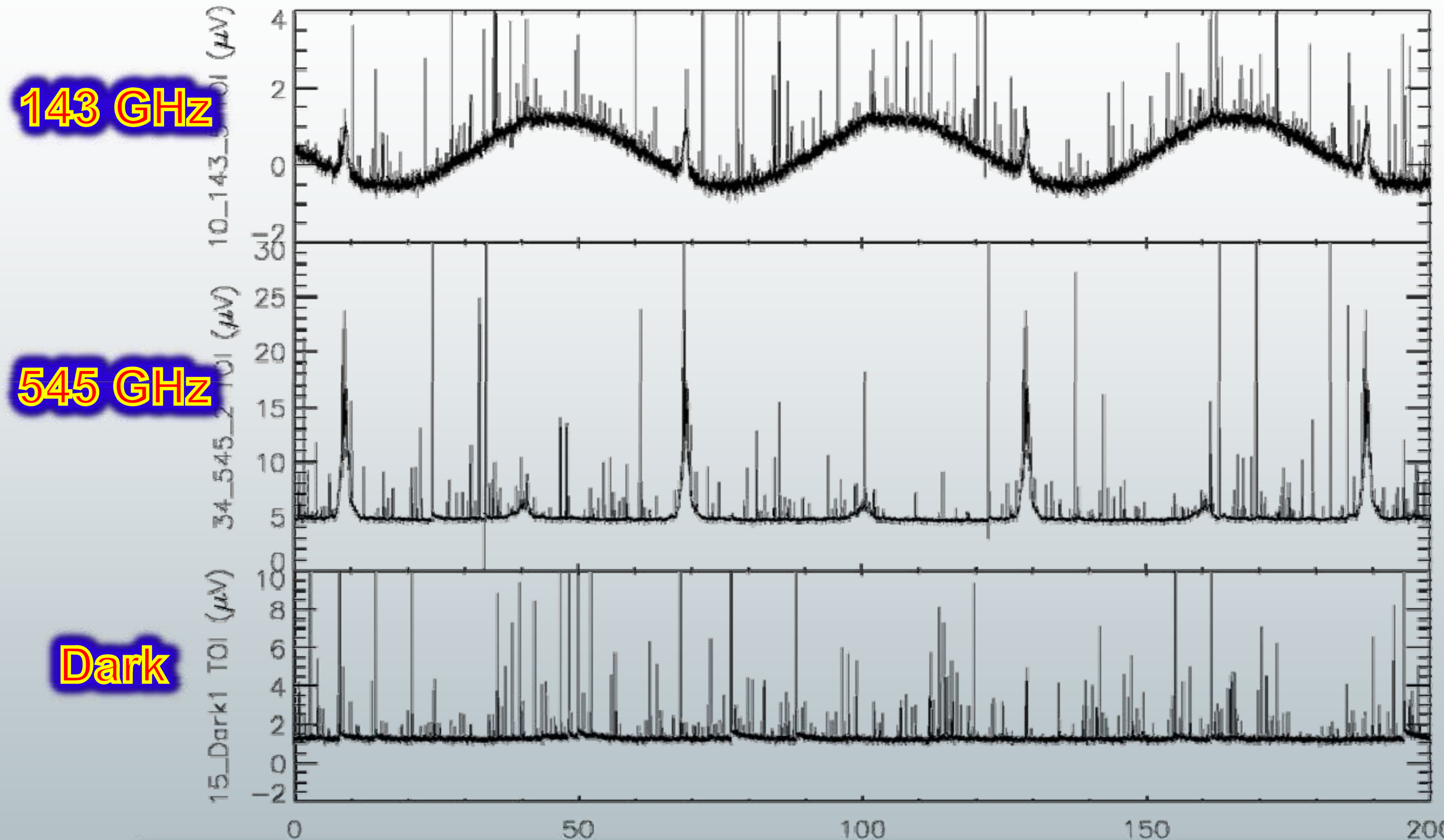

3 minutes of quasi 'raw" data (i.e. only demodulated).The Solar (cosmological) dipole is clearly visible at 145GHz with a 60 seconds period (the satellite rotates at 1 rpm), while the Galactic plane crossings (2 per rotation) are more visible at 545 GHz than at 143 GHz. The Dark bolometer sees no sky signal, but displays a similar population of glitches from cosmic rays.

"Glitchology" (1/2)

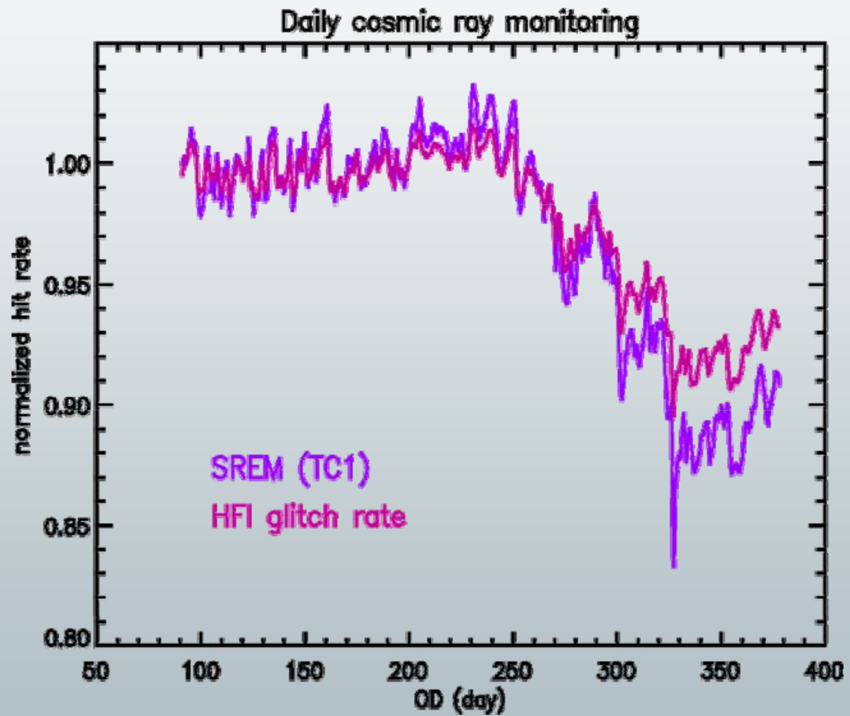

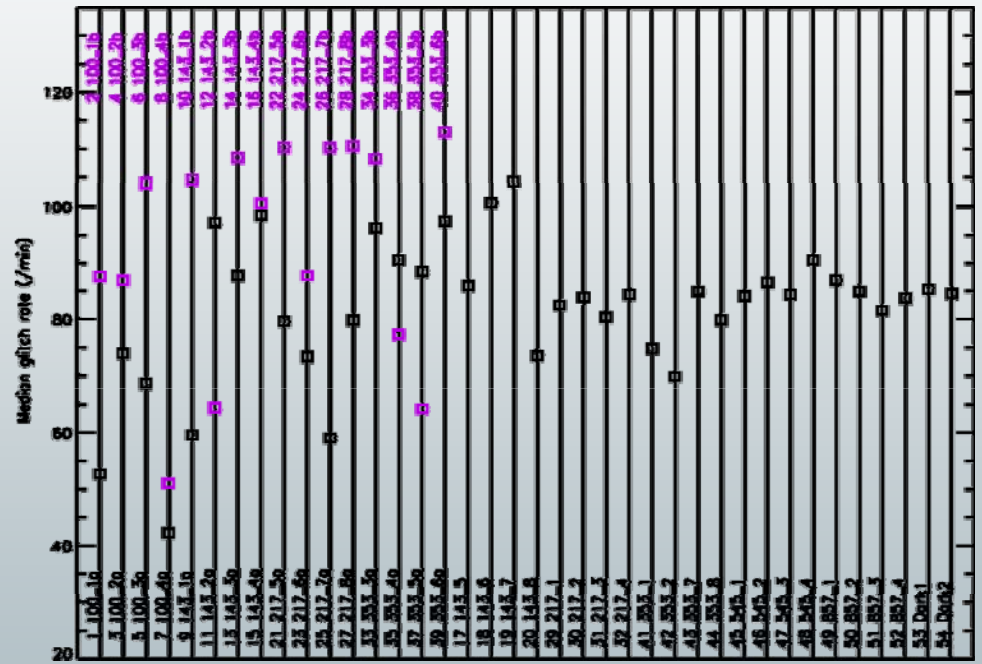

Glitches are induced by Cosmic Rays, at a rate ~ 80/minute

Et voila!

(skipping 12 summary slides of TOI processing...)
(Deglitching, T decor., nonlin corr., 4Klines, TD deconv., RTS)

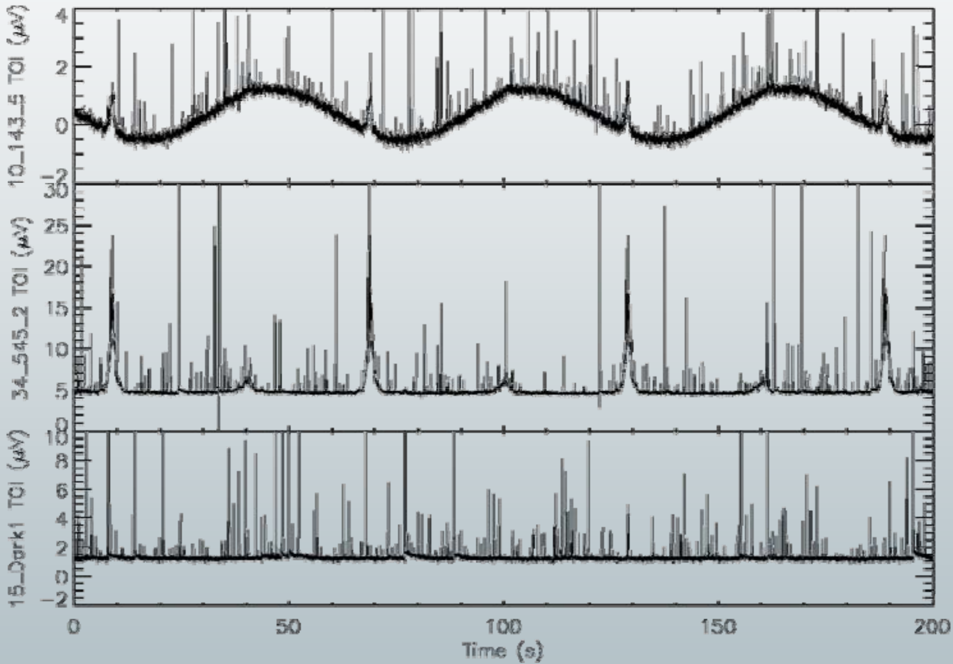

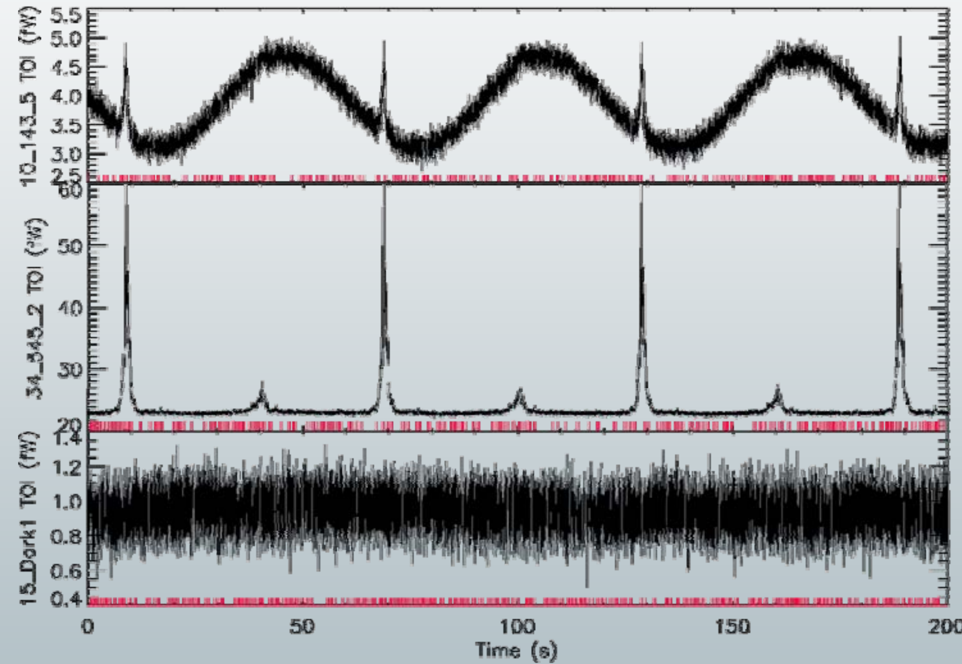

Scanning Mars

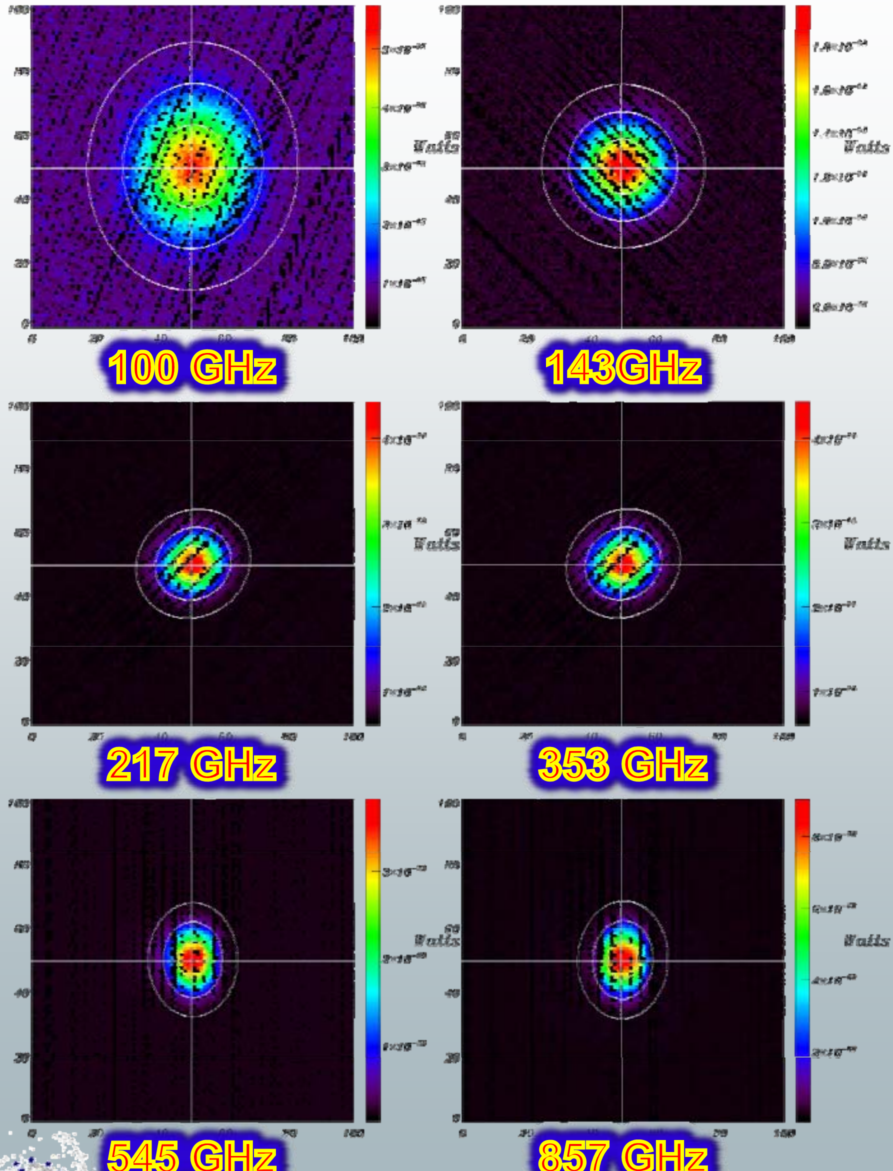

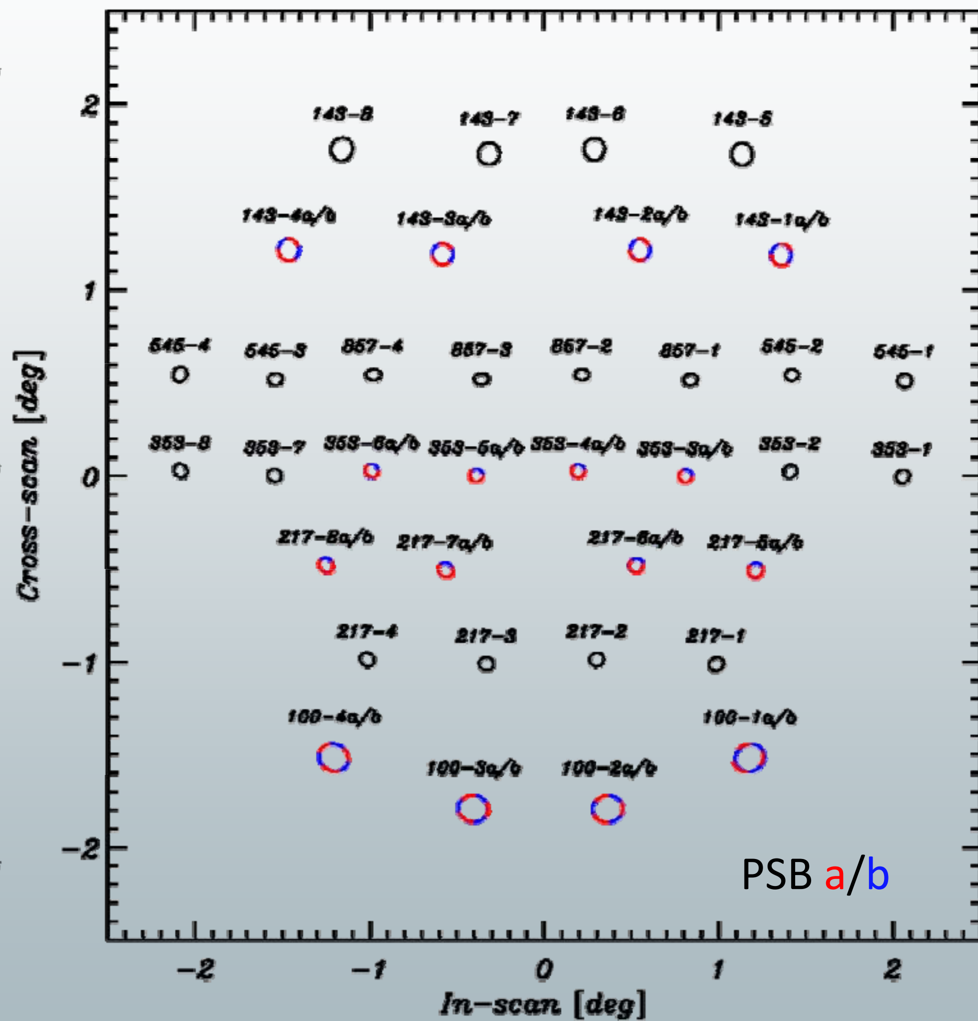

½ difference maps

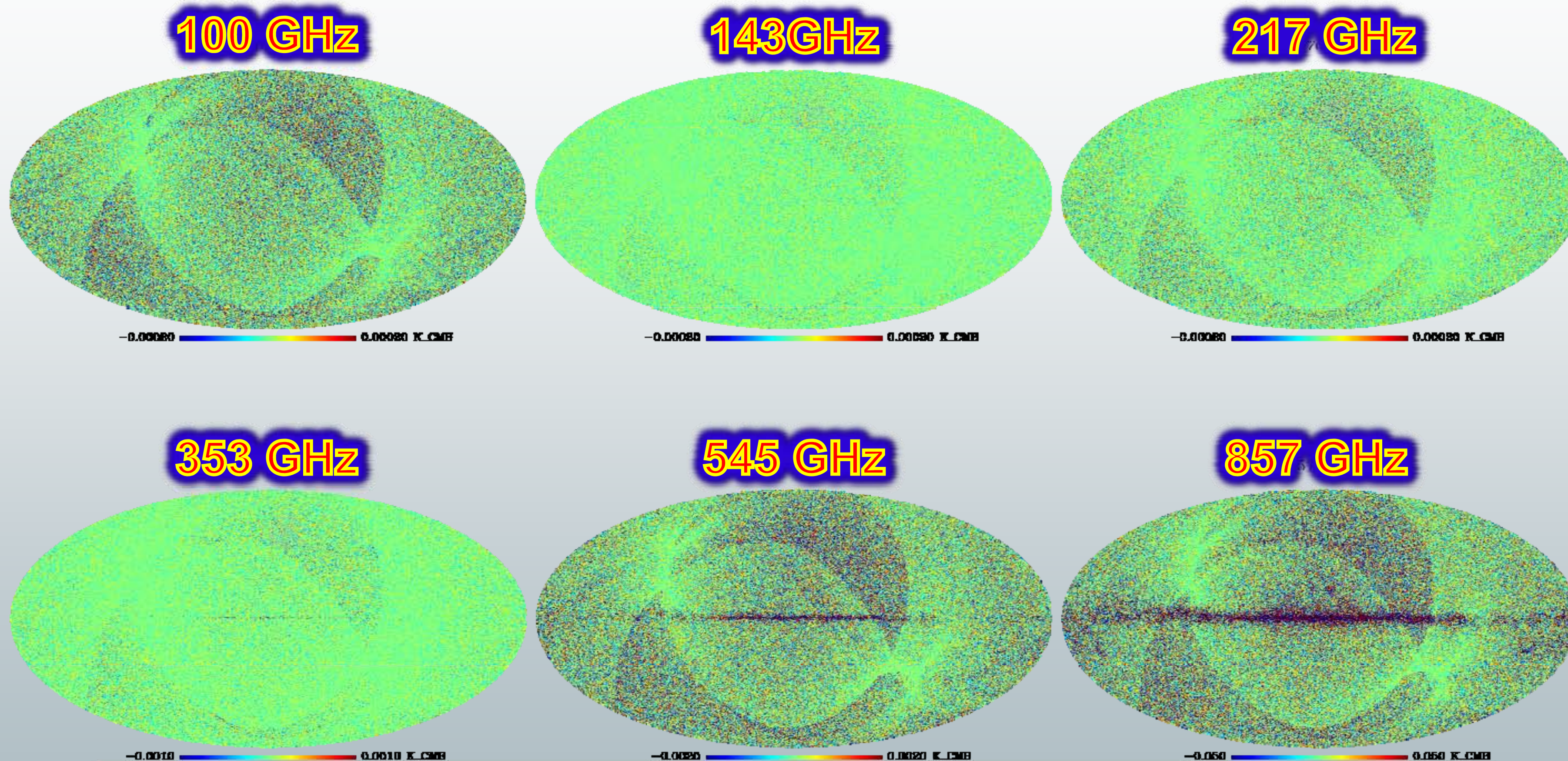

One can build 2 maps at each frequency out of the first or the second half of the data acquired during each stable pointing period of ~40mn.
In forming half difference maps, slowly varying effect on 20mn tiescale are subtracted. But it does provide a good view of the high frequency residuals.

½ difference maps spectra

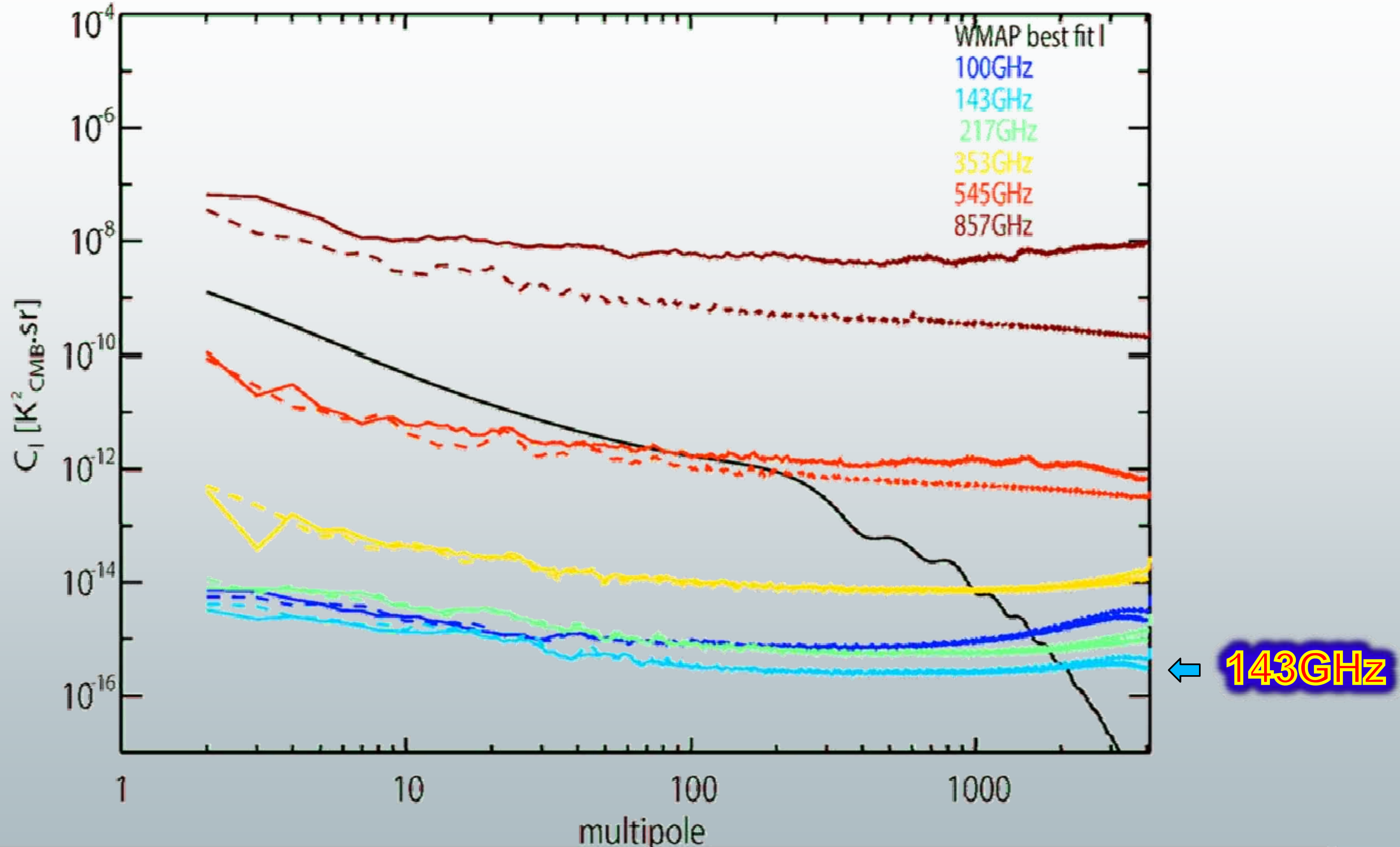

The C(l) of the ½ difference maps offer a synthetic view on the map residuals, at least at small scales. Dashes are for a 40% masked sky. c_{WN} is computed from the mean level between l=100 and l=1000

C_{wn} versus BB values

[µK degree]

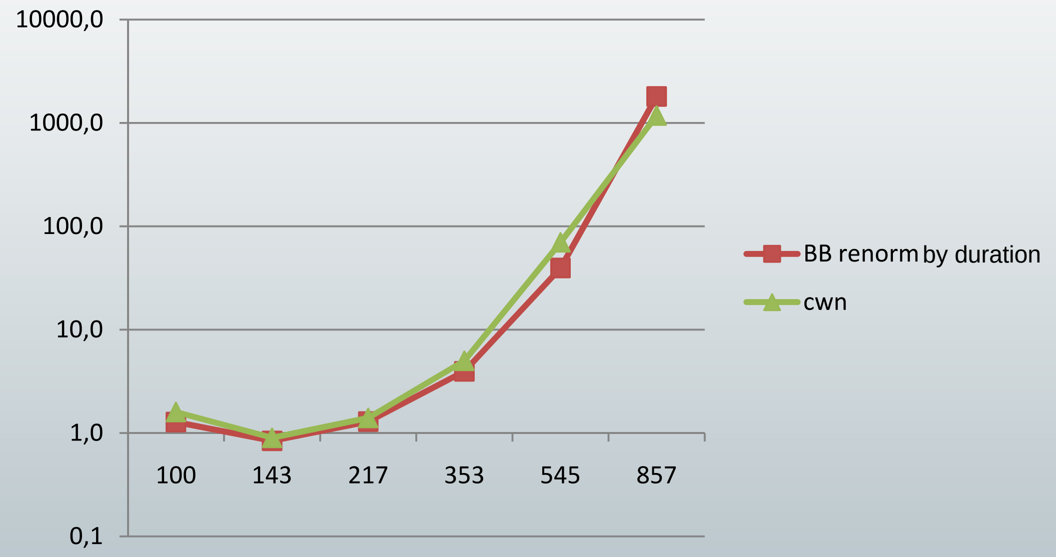

The combination of residual excess low frequency noise and better than the goals NETs leads to current maps whose high frequency noise is rather close to goal values ☺

CMB removal (DX4→ DR2)

In common with LFI, we compared 6 methods and picked a Needlet based ILC, masking very little of the data.

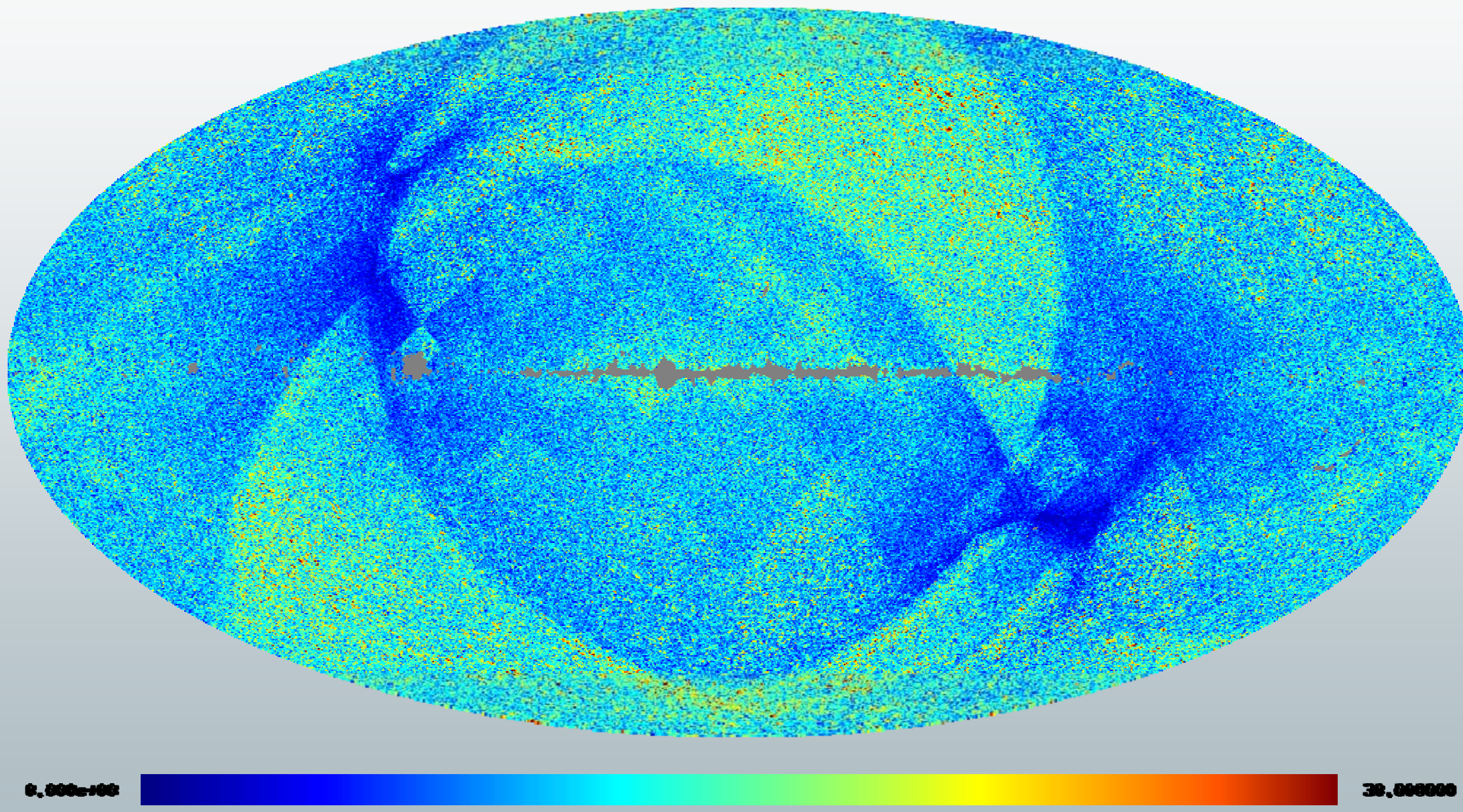

The same operations performed on the channel maps were performed on the ½ difference maps, offering a view on the residual in the CMB template removed from the maps (σ=11μK).

The HFI foregrounds sky

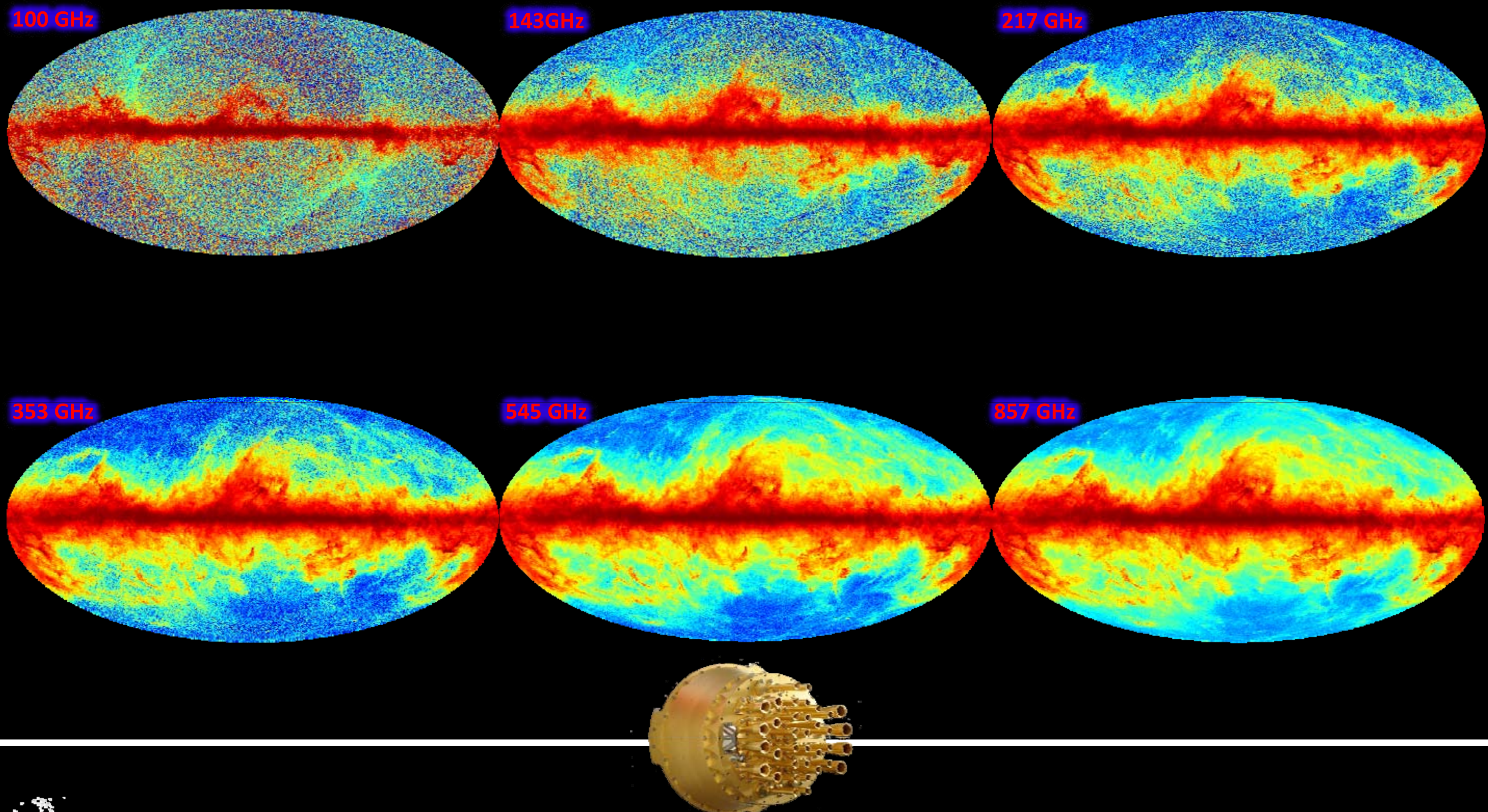

The Planck Foregrounds sky

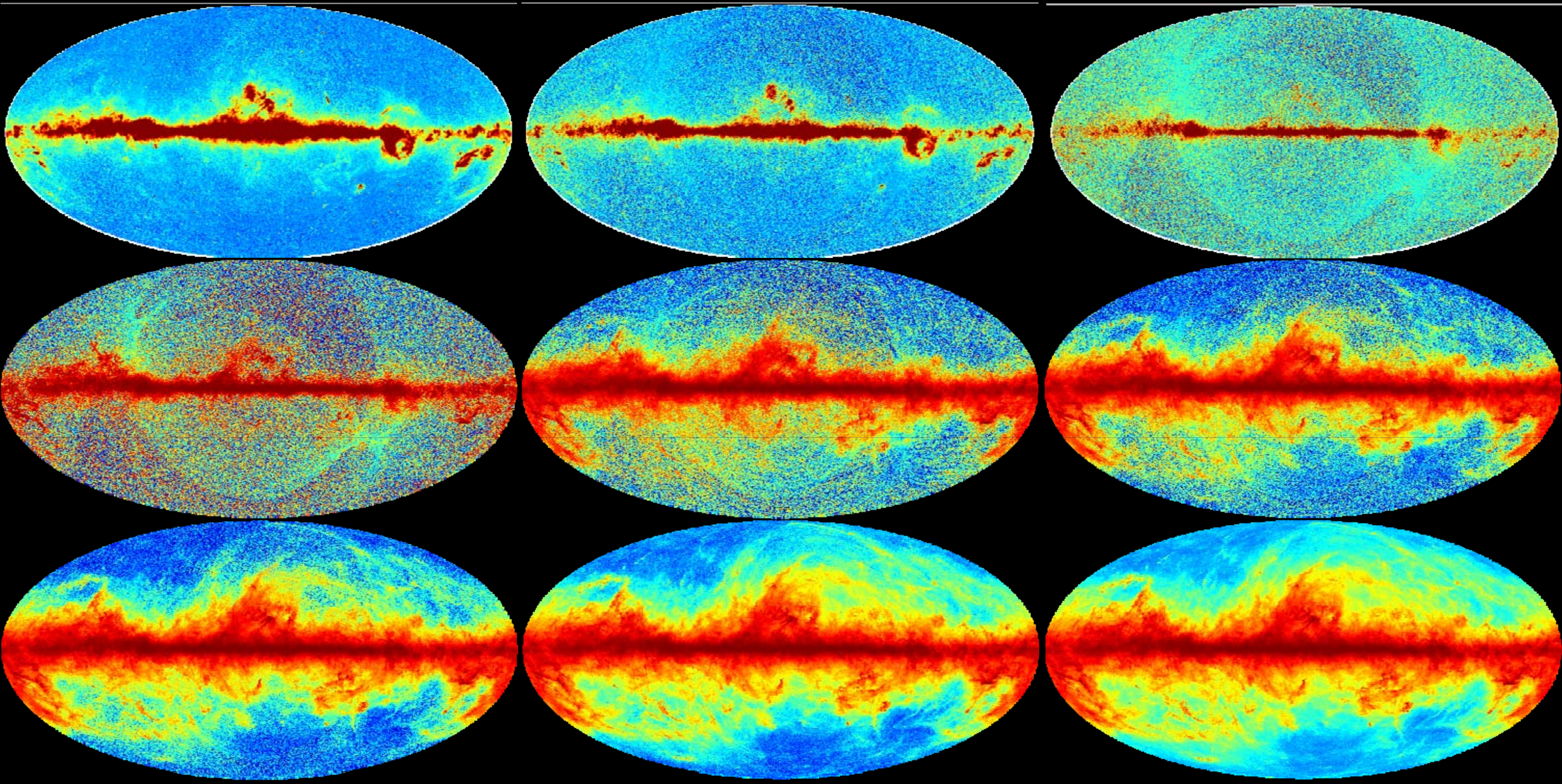

Planck Early Release Compact Source Catalogue

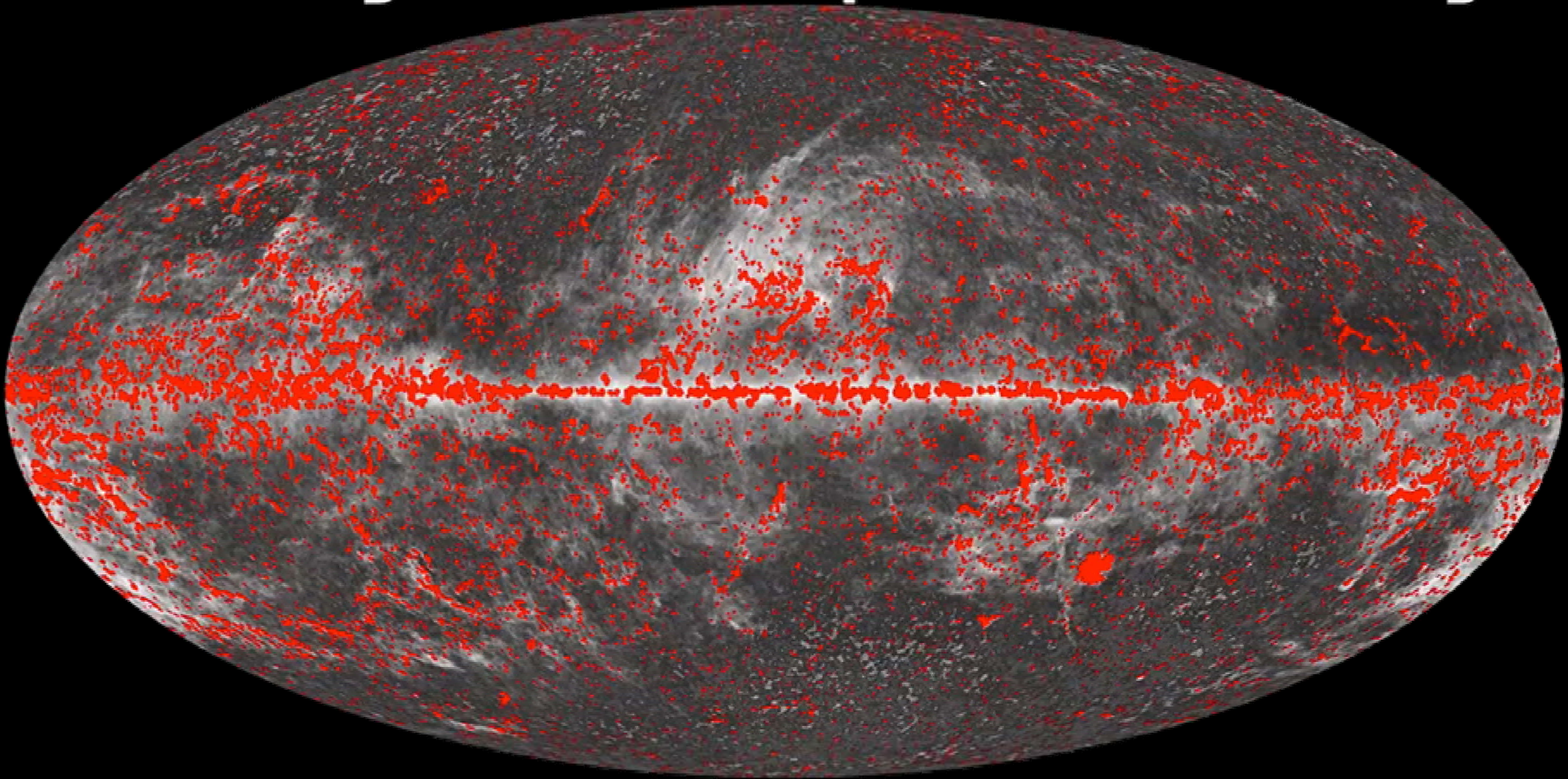

All compact sources

The Planck Foregrounds sky

Planck Early Release Compact Source Catalogue

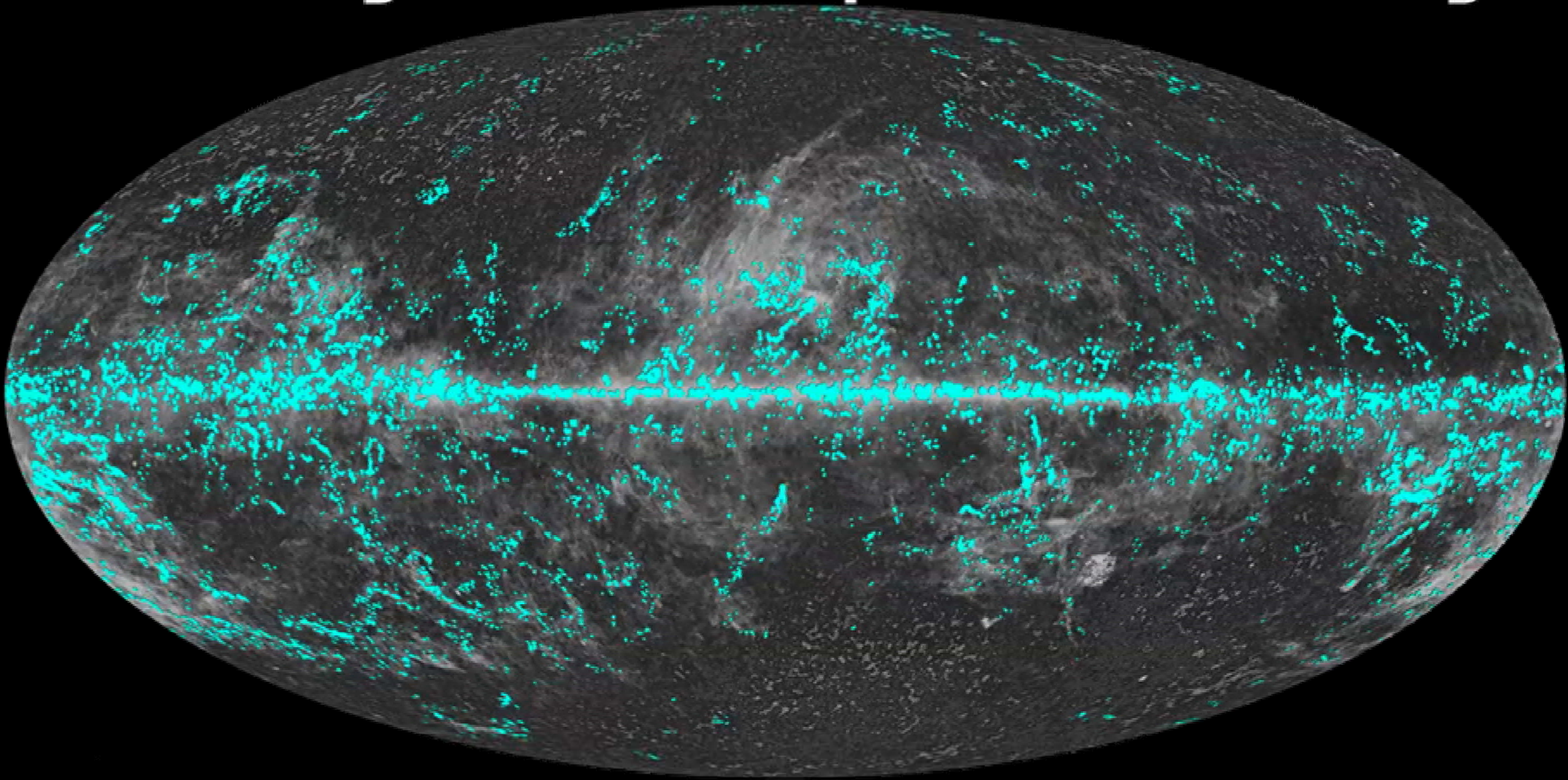

Galactic sources

The Planck Foregrounds sky

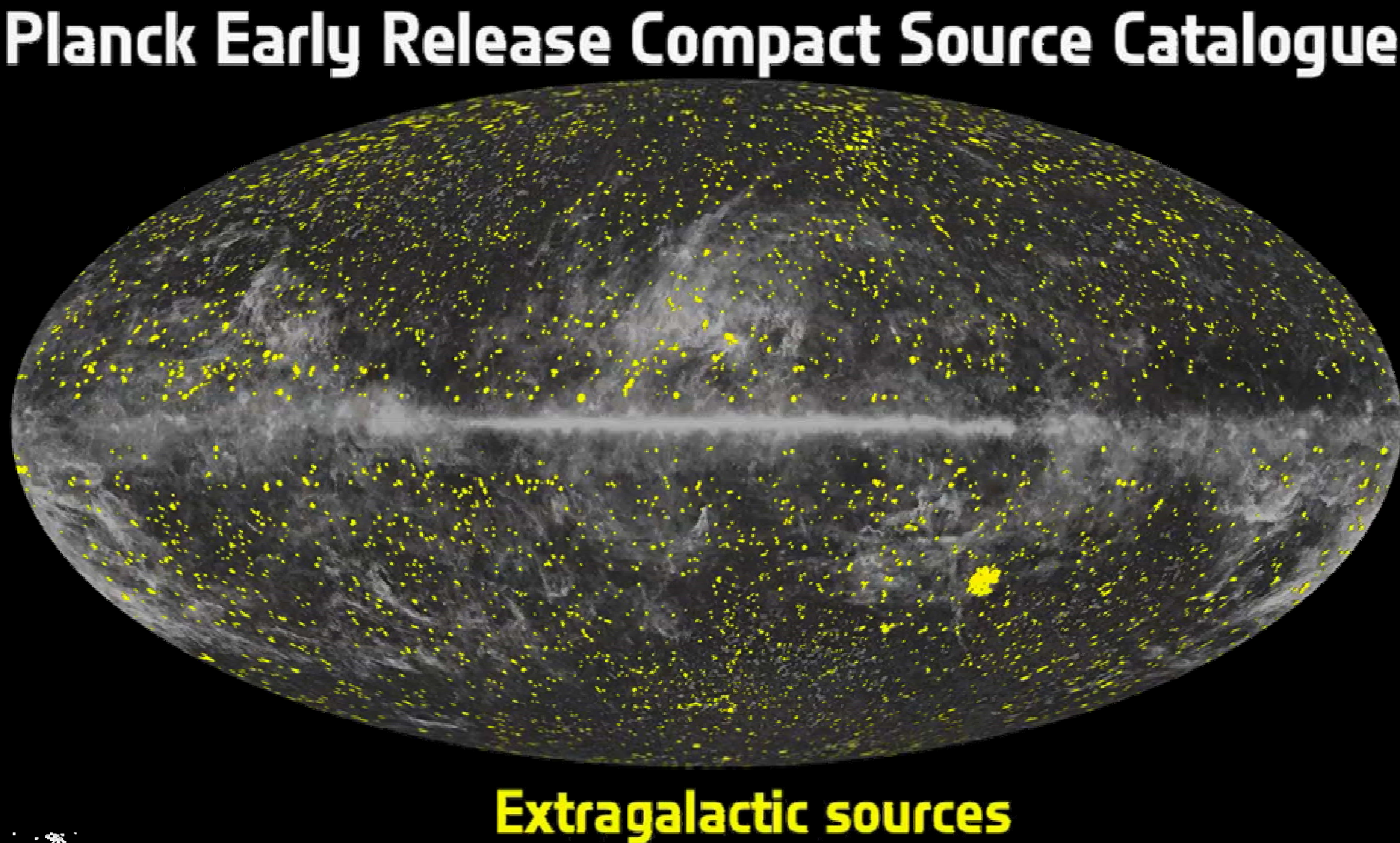

THE ERCSC Pipeline

Step 1

- Take all-sky Intensity and Covariance Maps from 1.6 sky surveys, convert to K_{RJ}

Step 2

- Run 4 source detection codes on maps
- Generate RMS noise map using a 2deg moving annulus from source subtracted map

Monte-Carlo Analysis

- Inject artificial point sources into maps
- Rerun 4 detection codes
- Study extracted properties of artificial sources after excluding “real” sources from Step 2

Cut 1

- Apply SNR cut (FLUX/RMS noise) so ERCSC requirements are met on artificial sources >90% reliability all sky
- Flux density uncertainty<30% and position accuracy <FWHM/5
- Apply same SNR cut per frequency to real sources (SNR varies with freq.)

Cut 2

- Reject spurious sources such as hot pixels, instrumental artifacts, planet sidelobes
- Select 2 algorithms which have the largest # of sources in the >90% reliability cat.
- PowellSnakes (30-143 GHz; P. Carvalho et al. 2009) and Sextractor (217-857 GHz; Bertin & Arnouts 1996)

Validation

- Use external catalogs such as QSOs, WMAP, VLA
- Use predictive flux catalog from pre-selected bright sources
- Compare catalogs from jacknife tests which include only half the data

ERCSC

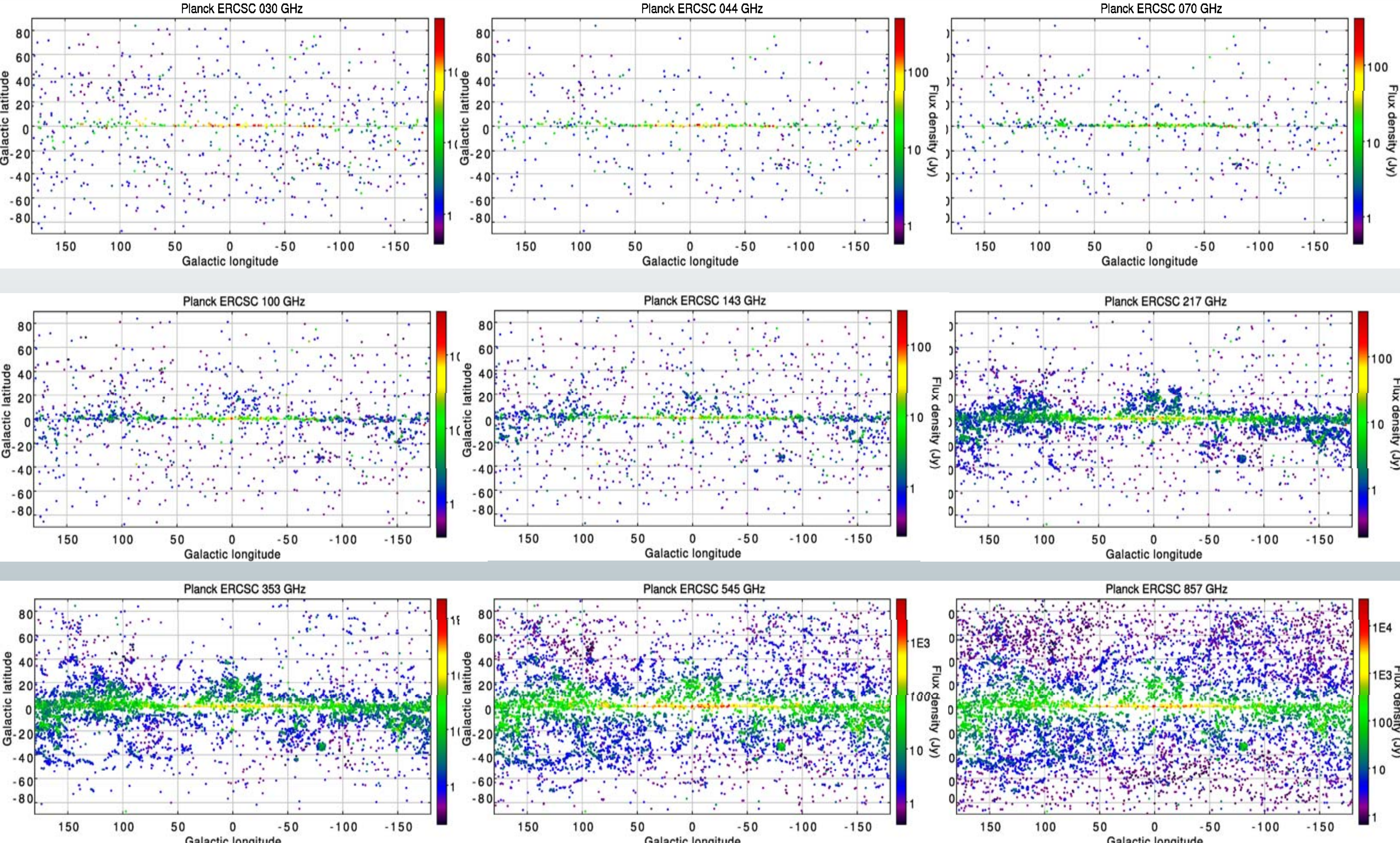
Planck ERCSC 030 GHz
Planck ERCSC 044 GHz
Planck ERCSC 070 GHz
Planck ERCSC 100 GHz
Planck ERCSC 143 GHz
Planck ERCSC 217 GHz
Planck ERCSC 353 GHz
Planck ERCSC 545 GHz
Planck ERCSC 857 GHz
Galactic latitude
Galactic longitude
Flux density (Jy)

An ERCSC Gallery

Planck Early Release Compact Source Catalog

PER030 (30 GHz)

ILC model of CMB subtracted

Catalog: ERCSC_f030.fits (706 sources) sorted by GLON

Origin: U.S. Planck Data Center

Date: 2010-09-04

Map: /attic/ercsc/RUNS/p4.0_ILC/MAPS/LFI_030.fits

Image width: 2.20 deg

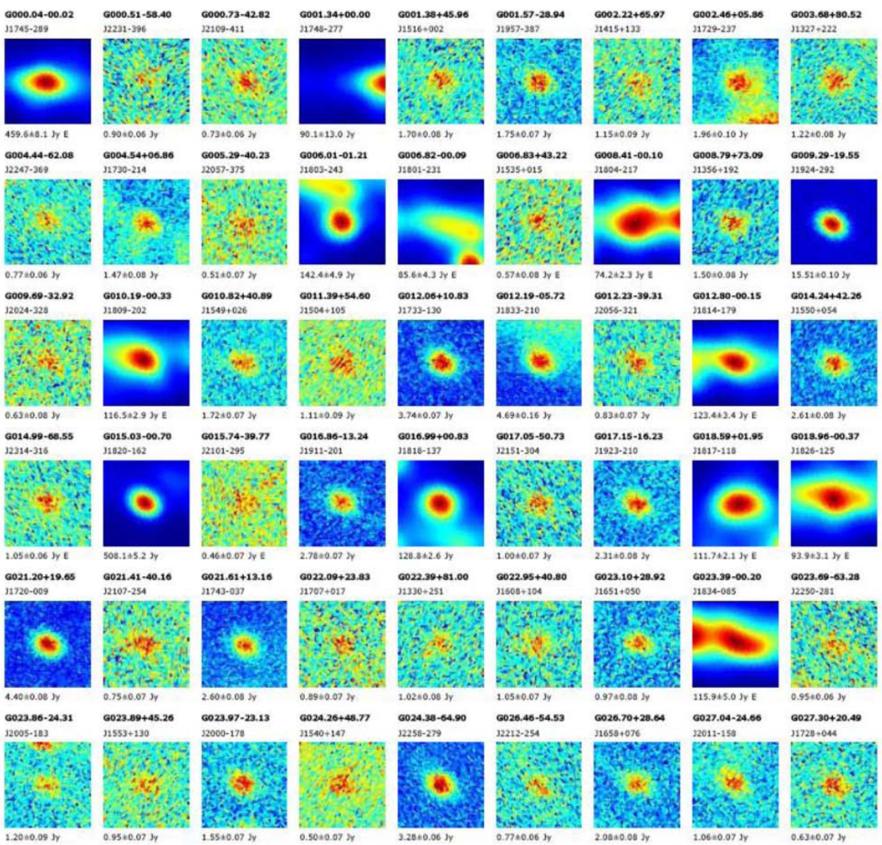

Planck Early Release Compact Source Catalog

PER143 (143 GHz)

ILC model of CMB subtracted

Catalog: ERCSC_f143.fits (1778 sources) sorted by GLON

Origin: U.S. Planck Data Center

Date: 2010-09-04

Map: /attic/ercsc/RUNS/p4.0_ILC/MAPS/HFI_143.fits

Image width: 0.47 deg

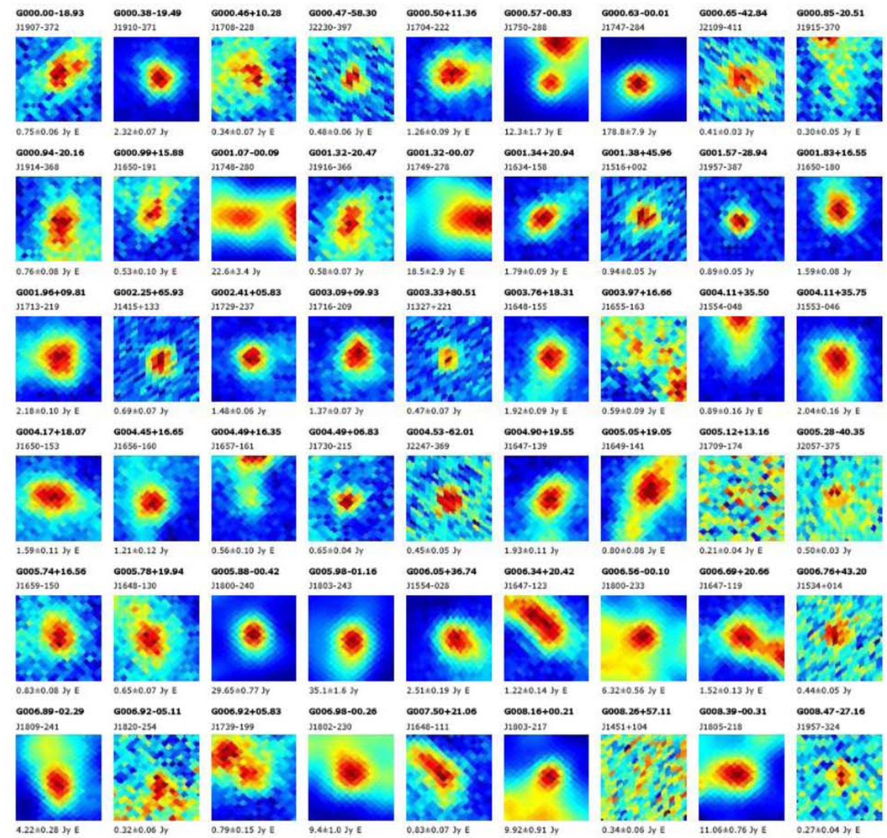

ERCSC columns

Column Name	Description
Identification	
NAME	Source name
FLUX	Flux density (mJy)
FLUX_ERR	Flux density error (mJy)
CMBSUBTRACT	Flag indicating detection of source in CMB subtracted maps
EXTENDED	Flag indicating that source is extended
DATESOBS	UTC dates at which this source was observed
NUMOBS	Number of days this source observed
CIRRUS	Cirrus flag based on 857 GHz source counts
Source Position	
GLON	Galactic longitude (deg) based on extraction algorithm
GLAT	Galactic latitude (deg) based on extraction algorithm
POS_ERR	Standard deviation of positional offsets for sources with this SNR (arcminute)
RA	Right Ascension (J2000) in degrees transformed from (GLON,GLAT)
DEC	Declination (J2000) in degrees transformed from (GLON,GLAT)
Effective beam	
BEAM_FWHMMAJ	Elliptical Gaussian beam FWHM along major axis (arcmin)
BEAM_FWHMMIN	Elliptical Gaussian beam FWHM along minor axis (arcmin)
BEAM_THETA	Orientation of Elliptical Gaussian major axis (measured East of Galactic North)
Morphology	
ELONGATION	Ratio of major to minor axis lengths
Source Extraction Results	
FLUXDET	Flux density of source as determined by detection method (mJy)
FLUXDET_ERR	Uncertainty (1 sigma) of FLUXDET (mJy)
MX1	First moment in X (arcmin)
MY1	First moment in Y (arcmin)
MX2	Second moment in X (arcmin^2)
MXY	Cross moment in X and Y (arcmin^2)
MY2	Second moment in Y (arcmin^2)
PSFFLUX	Flux density of source as determined from PSF fitting (mJy)
PSFFLUX_ERR	Uncertainty (1 sigma) of PSFFLUX (mJy)
GAUFLUX	Flux density of source as determined from 2-D Gaussian fitting (mJy)
GAUFLUX_ERR	Uncertainty (1 sigma) of GAUFLUX (mJy)
GAU_FWHMMAJ	Gaussian fit FWHM along major axis (arcmin)
GAU_FWHMMIN	Gaussian fit FWHM along minor axis (arcmin)
GAU_THETA	Orientation of Gaussian fit major axis
Quality Assurance	
RELIABILITY	Fraction of MC sources that are matched and have photometric errors $< 30\%$
RELIABILITY_ERR	Uncertainty (1 sigma) in reliabiliy based on Poisson statistics
MCQA_FLUX_ERR	Standard deviation of photometric error for sources with this SNR
MCQA_FLUX_BIAS	Median photometric error for sources with this SNR
BACKGROUND_RMS	Background point source RMS obtained from threshold maps (mJy)
Bandfilling (857 GHz catalog only)	
BANDFILL217	217 GHz Aperture Photometry Flux Density at 857 GHz Source Position (mJy)
BANDFILL217_ERR	Uncertainty in BANDFILL217
BANDFILL353	353 GHz Aperture Photometry Flux Density at 857 GHz Source Position (mJy)
BANDFILL353_ERR	Uncertainty in BANDFILL353
BANDFILL545	545 GHz Aperture Photometry Flux Density at 857 GHz Source Position (mJy)
BANDFILL54_5ERR	Uncertainty in BANDFILL545

ERCSC characteristics

Freq [GHz]	30	44	70	100	143	217	353	545	857
λ [μm]	10000	6818	4286	3000	2098	1382	850	550	350
Sky Coverage in %	99.96	99.98	99.99	99.97	99.82	99.88	99.88	99.80	99.79
Beam FWHM [arcmin][a]	32.65	27.00	13.01	9.94	7.04	4.66	4.41	4.47	4.23
# of Sources	705	452	599	1381	1764	5470	6984	7223	8988
# of $\lvert b\rvert > 30^\circ$ Sources	307	143	157	332	420	691	1123	2535	4513
$10\sigma^b$ [mJy]	1173	2286	2250	1061	750	807	1613	2074	2961
$10\sigma^c$ [mJy]	487	1023	673	500	328	280	249	471	813
Flux Density Limit[d] [mJy]	480	585	481	344	206	183	198	381	655

b : Flux density of the median > 10 sigma at b> 30deg
(sig = photometric uncertainty of the source)

c : Flux density of the faintest > 10 sigma at b> 30deg

d : faintest source at b> 30deg

ERCSC sensitivity

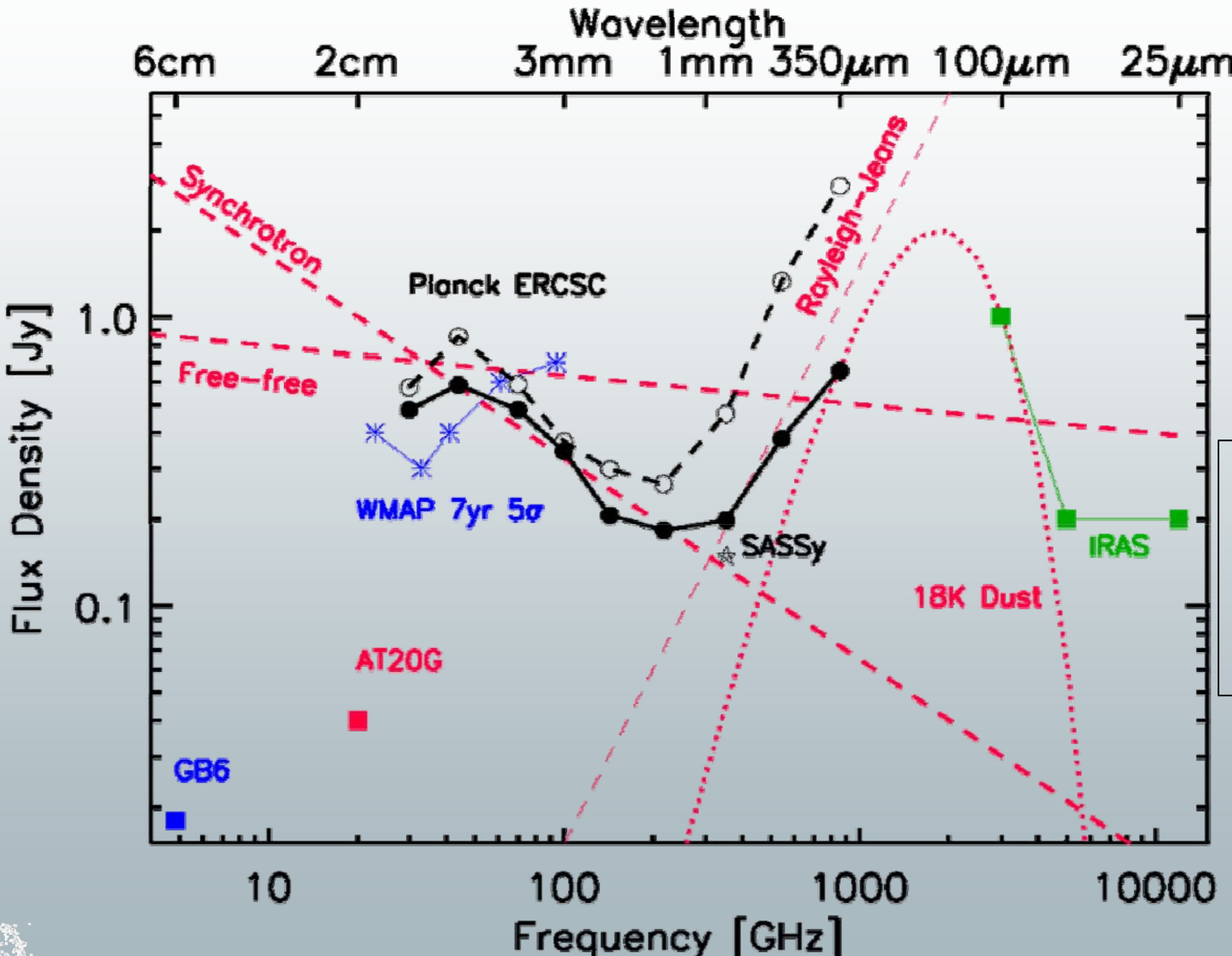

Planck Galactic Plane |b|<10 deg

Planck Extragalactic |b|>30 deg

Planck finds WMAP sources

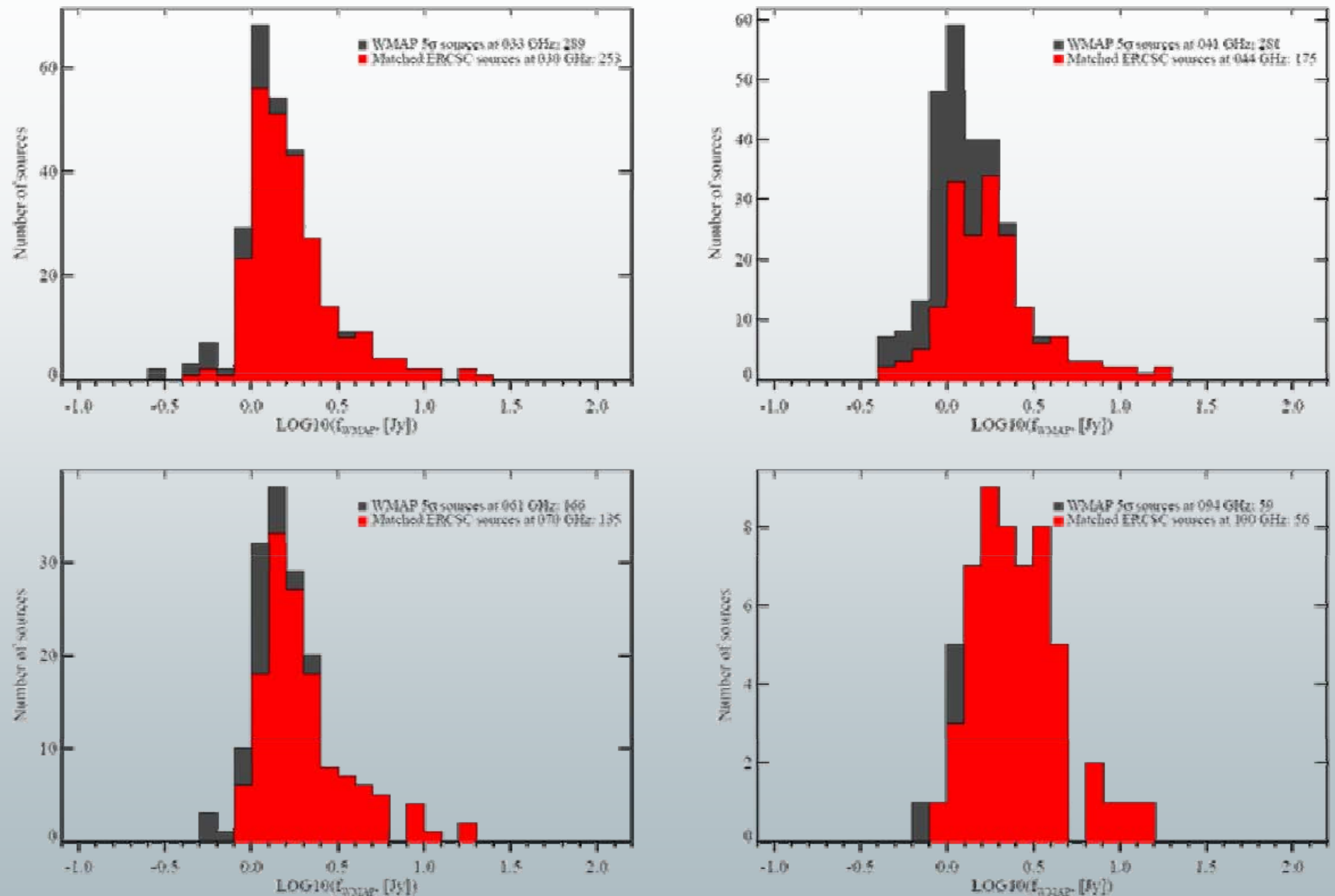

Fig. 10. Histogram distribution of *WMAP* flux densities for all *WMAP* 5σ sources in each band (gray region). The sources that are detected in the ERCSC catalogs are shown as the red histogram. Some of the *WMAP* sources have been missed because of source variability.

And some more...

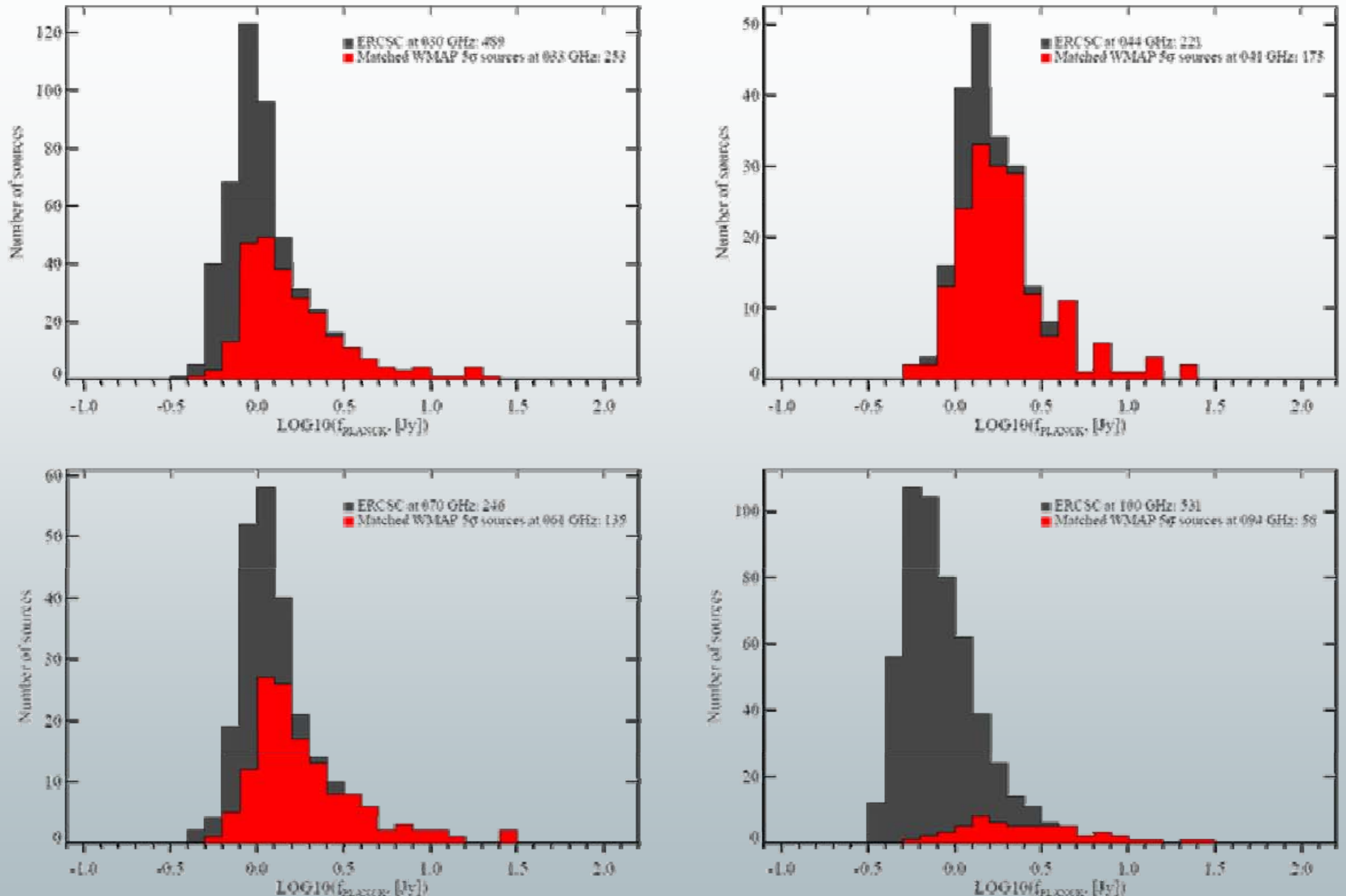

Fig. 11. Histogram distribution of ERCSC flux densities at each band in gray. ERCSC sources that are matched with *WMAP* 5σ sources in a similar band are shown as the red histogram. The *WMAP* 7 year point source catalog mask (see text) has been applied to the ERCSC catalogs to ensure the same sky coverage.

Quasar matches and position offsets

30 GHz

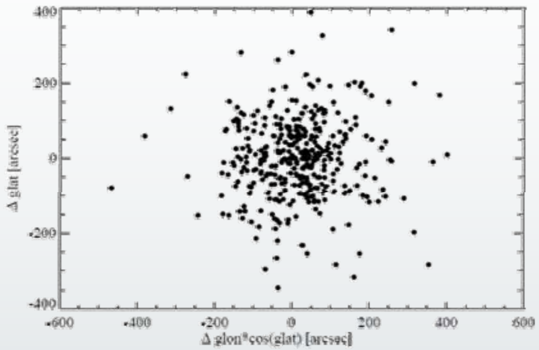

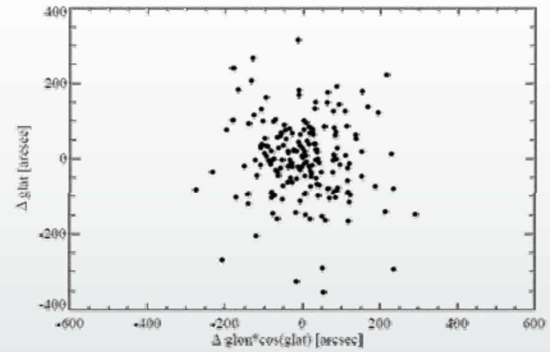

44 GHz

70GHz

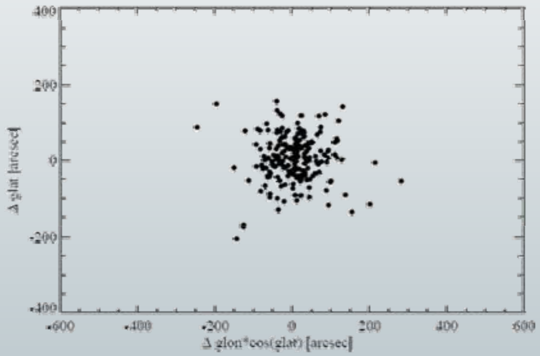

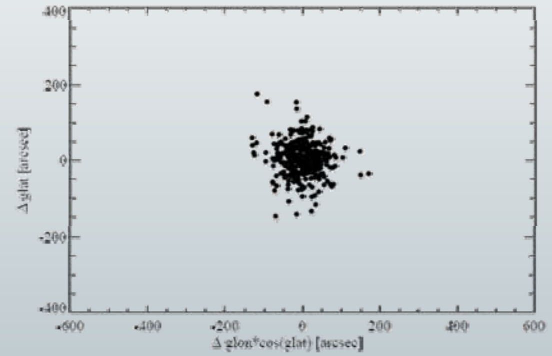

100 GHz

±10’

143GHz

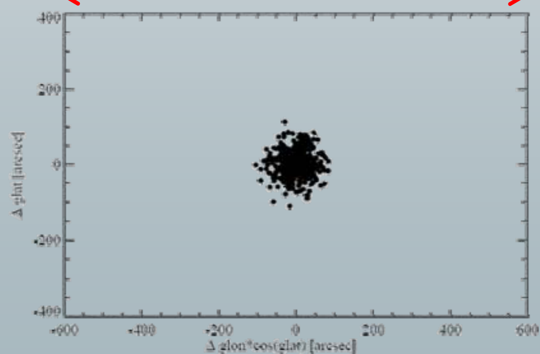

NB: similar at 353GHz. Numbers too small at higher ν

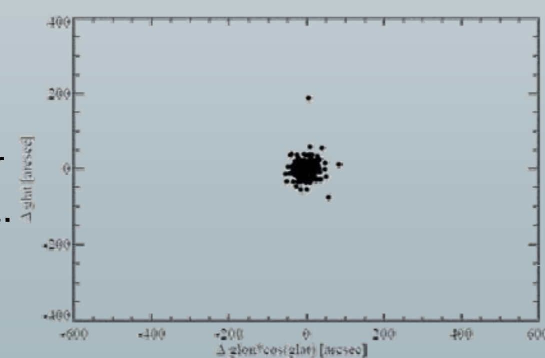

217GHz

Spectral index between 2 ν

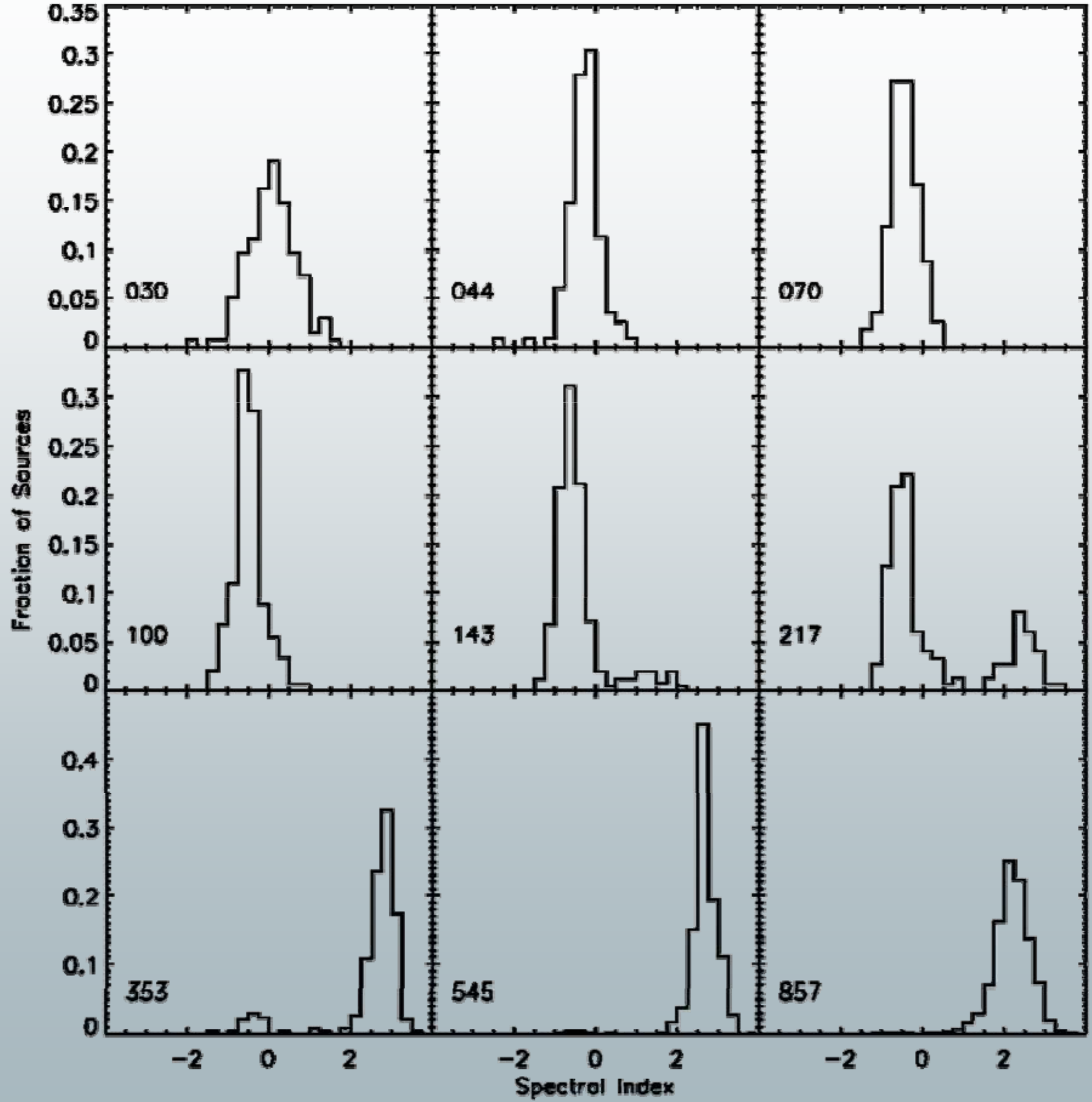

Obviously many relatively flat spectrum radio-sources, visible till 217GHz

Euclidean normalized differential number counts

Versus predictions by the de Zotti et al. (2005) model

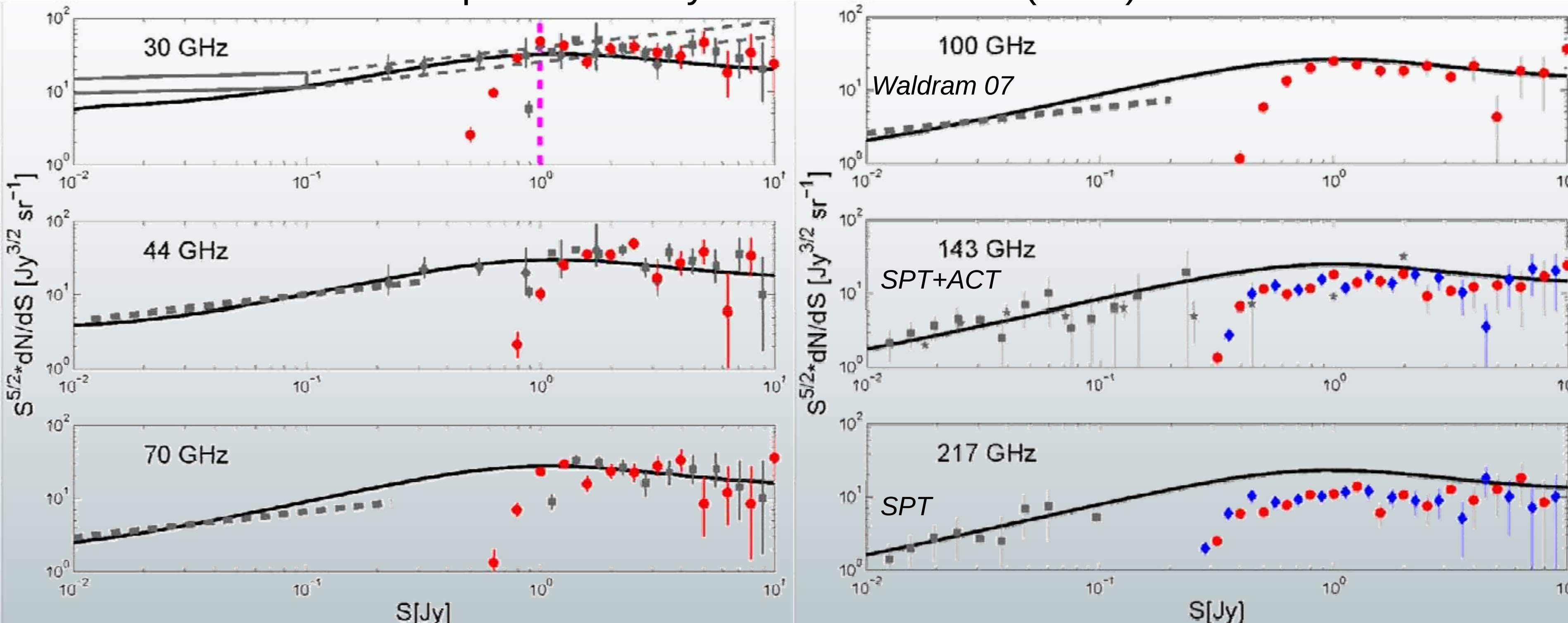

LFI: red circles with Poisson error bars show the counts of sources with counterparts in our reference 30GHz sample (completeness till ~1Jy, purple)

HFI: the blue diamonds show the counts obtained after removing sources with 143–217GHz spectral index indicative of dust emission.

The de Zotti et al. (2005) model over-predicts the bright counts by a factor of about 2 at 143GHz and about 2.6 at 217GHz, while it is consistent with the fainter SPT (Vieira et al. 2010) and ACT (Marriage et al. 2010) counts. The discrepancy between the model and our current data is due to a steepening of the spectra of ERCSC sources above about 70GHz

Spectral steepening above 70GHz

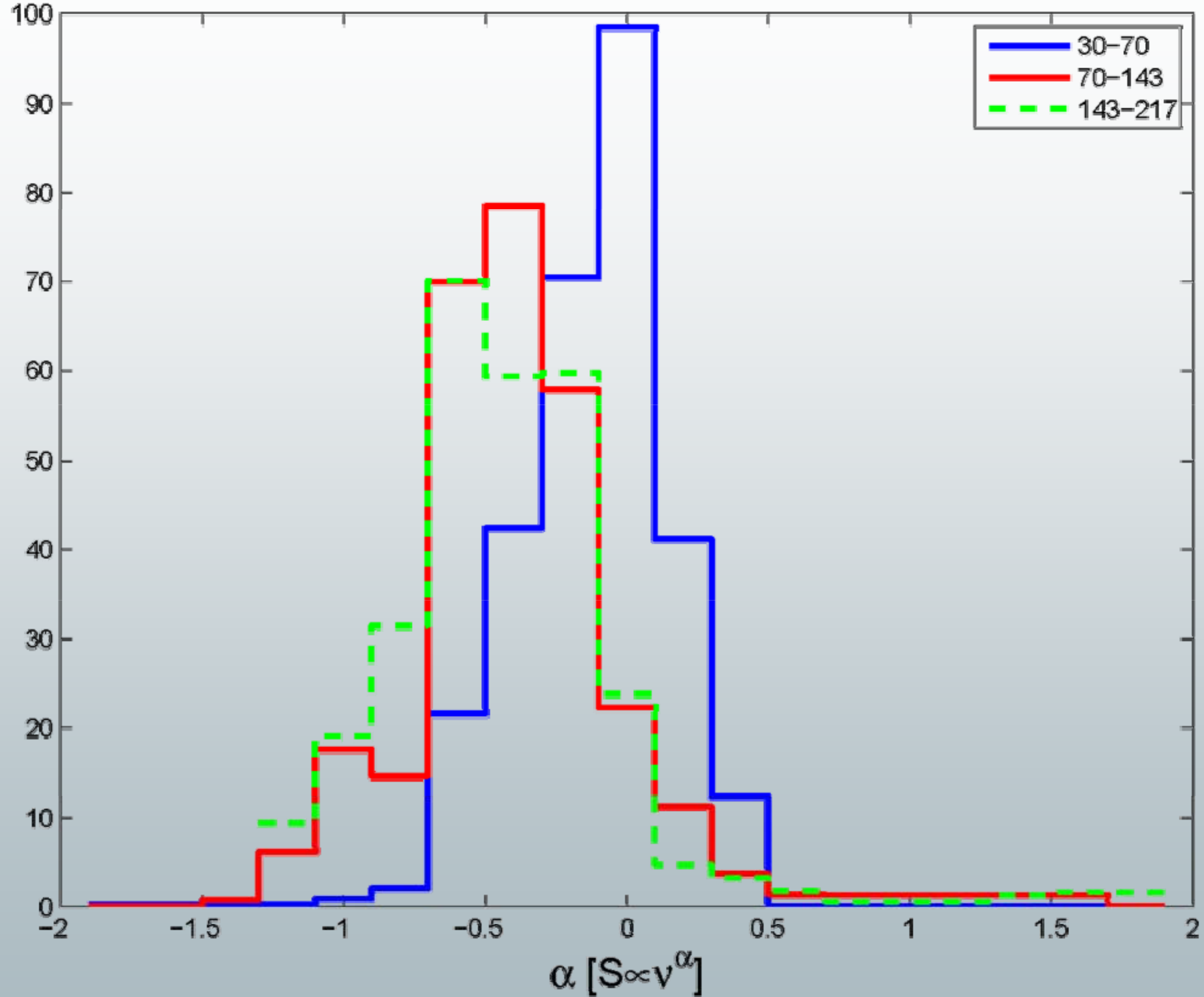

Spectral index distributions for different frequency interval calculated by taking into account all sources selected at 30GHz with S > 1 Jy. There is clear evidence for a steepening above 70GHz.

Early Cold Core (ECC) catalog

- A warm template from the IRAS 100 micron map is subtracted from each of the 353, 545 and 857 GHz images and a source detection run on each band.
- The single frequency sources are merged together using a matching threshold of 5'
- The S/N>4 in each band
- A modified black body is fit to the multiband photometry
- Only SNR>15 sources are found to have robust fit parameters from the MC: 915 sources with T<14K

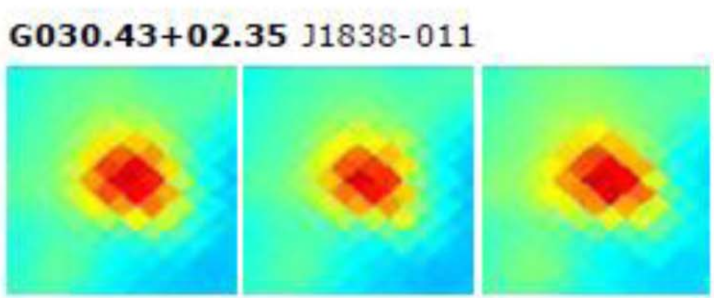

353-IRAS 545-IRAS 857-IRAS

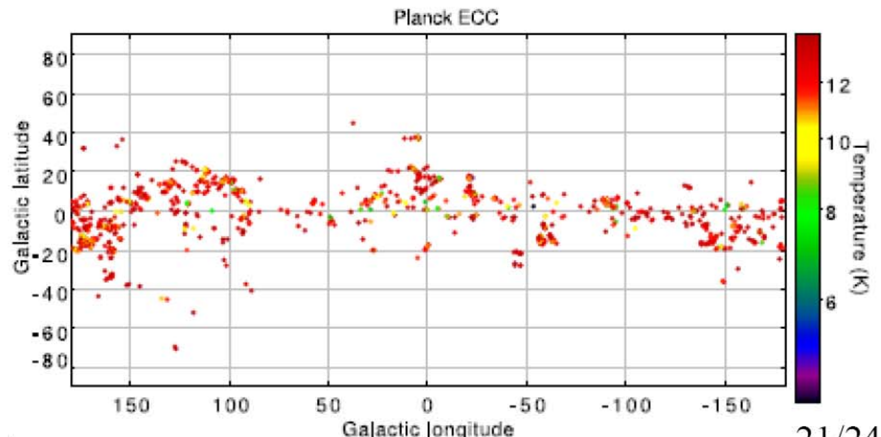

See Planck Collaboration 2011r & s
Science results in 2011q-u

The Sunyaev-Zeldovich effect

Comments on Astrophysics and Space Physics 1972

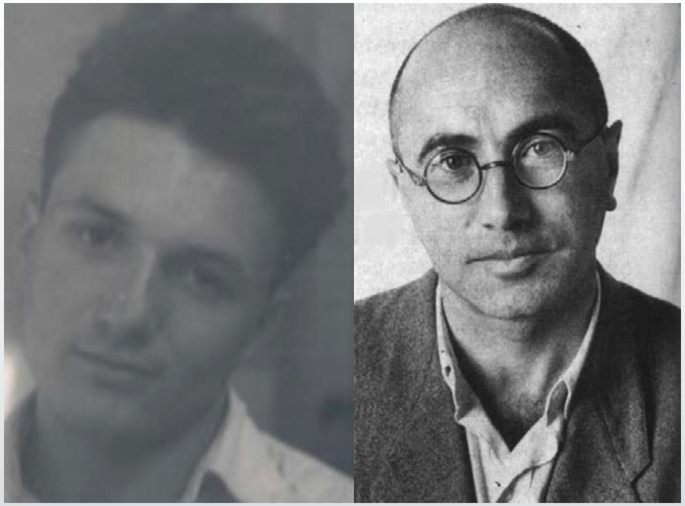

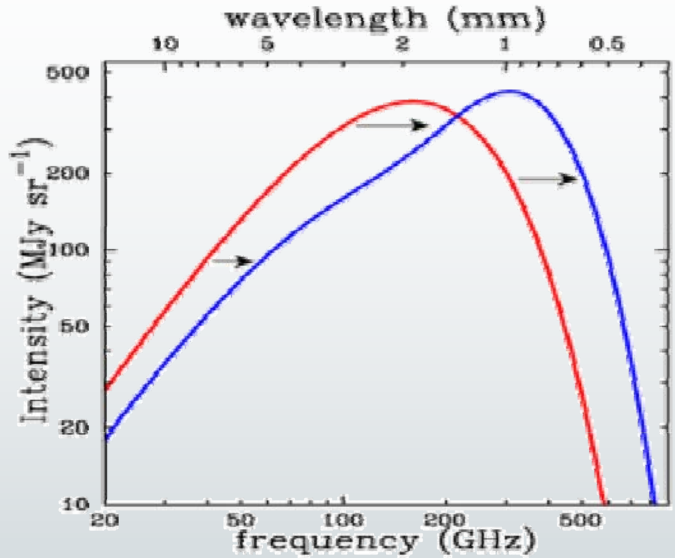

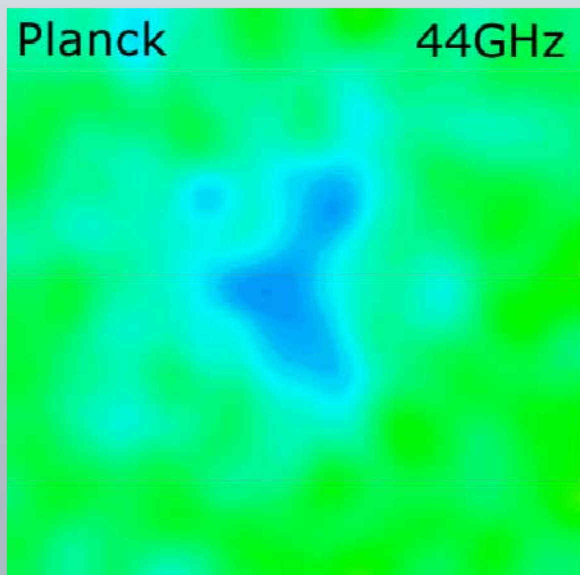

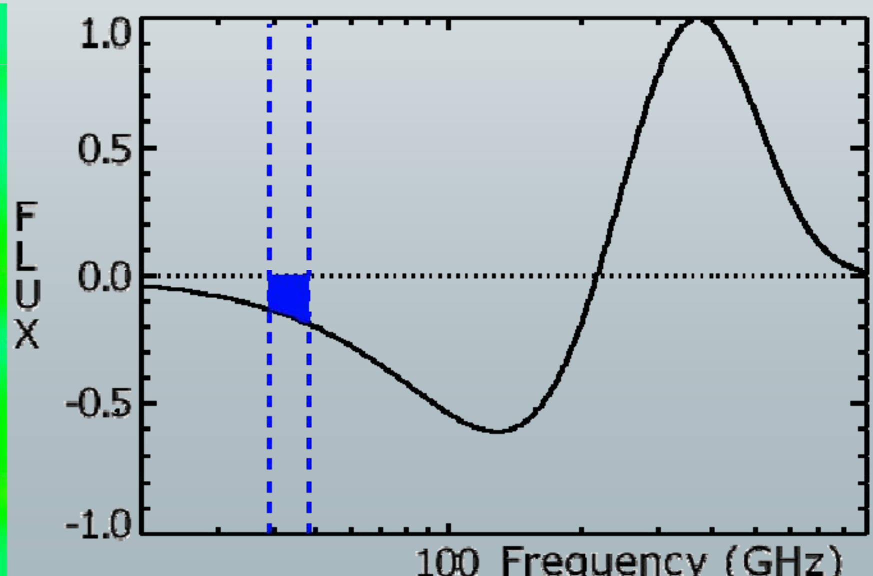

Coma y map versus X-ray contours

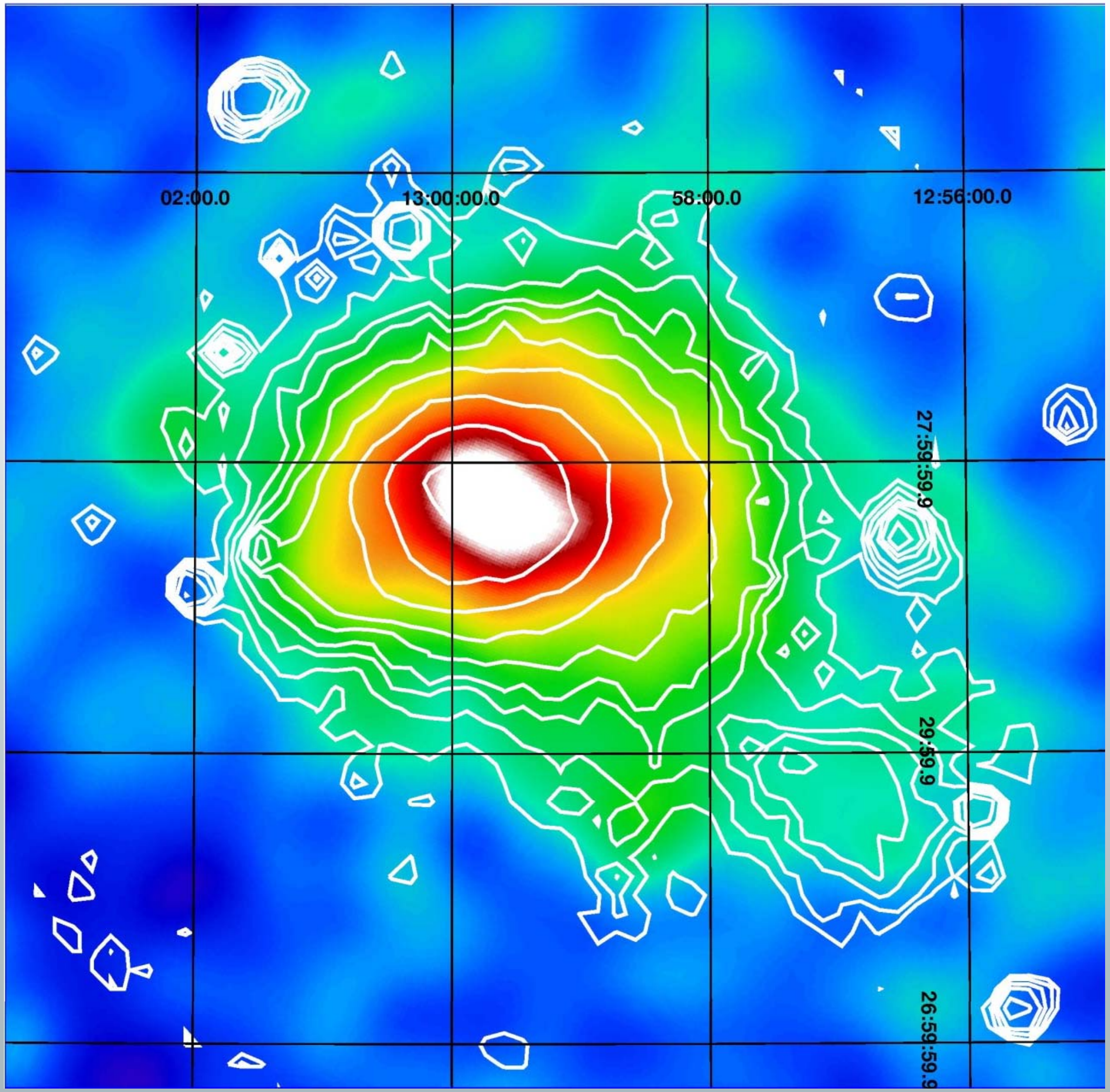

Early SZ (ESZ) catalogue

- ~1000 objects in blind search
- Culled to 199 robust objects

- The very first all-sky sample, includes 199 clusters, 30 are new
- The largest cluster sample observed in the microwaves

- Z < 0.6
- Large fraction are X-ray confirmed
- 1st detection of SZ effect in majority o ROSAT clusters

- Unique capability of detecting the rarest and most massive clusters

- See PC 2011d, e, f, g, h

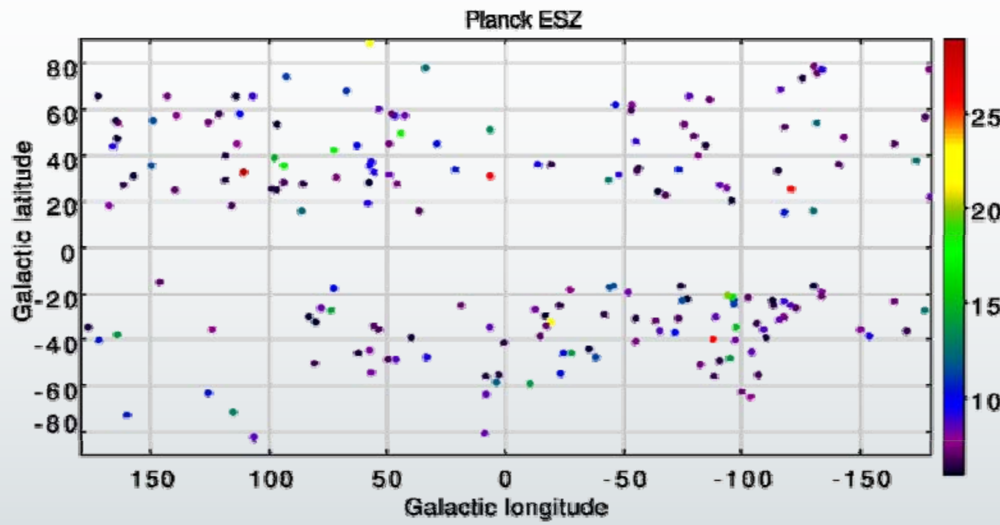

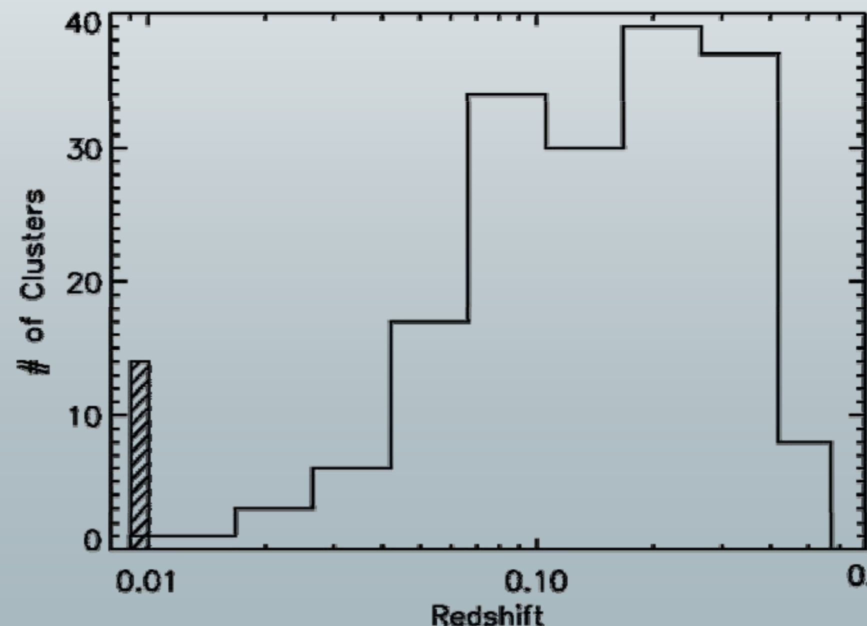

THE ERCSC

- The Early Release Compact Source Catalog (ERCSC) is an early, >90% reliability catalog based on 1.6 sky coverages
- Produced and released with a rapid turnaround (<9 months)
- Consists of 9 single frequency catalogs as well as bandfilled217-857 GHz entries for each 857 GHz source
- Includes the Early Cold Cores (ECC) and Early SZ-cluster (ESZ) catalogs
- More than 15 000 unique sources including stars with dust shells, cold molecular cloud cores, radio galaxies, blazars, infrared luminous galaxies, Galactic ISM features, SZ clusters
  - *Beware of CO contamination for Galactic sources at 100 GHz*
- Available from ESA Planck Legacy Archive and NASA's Infrared Science Archive (IRSA) starting Jan 11, 2011
- Interesting astrophysics is evident in the ERCSC
- Ripe for follow-up with Herschel, SOFIA, ALMA, VLA etc.

The Planck SZ sky

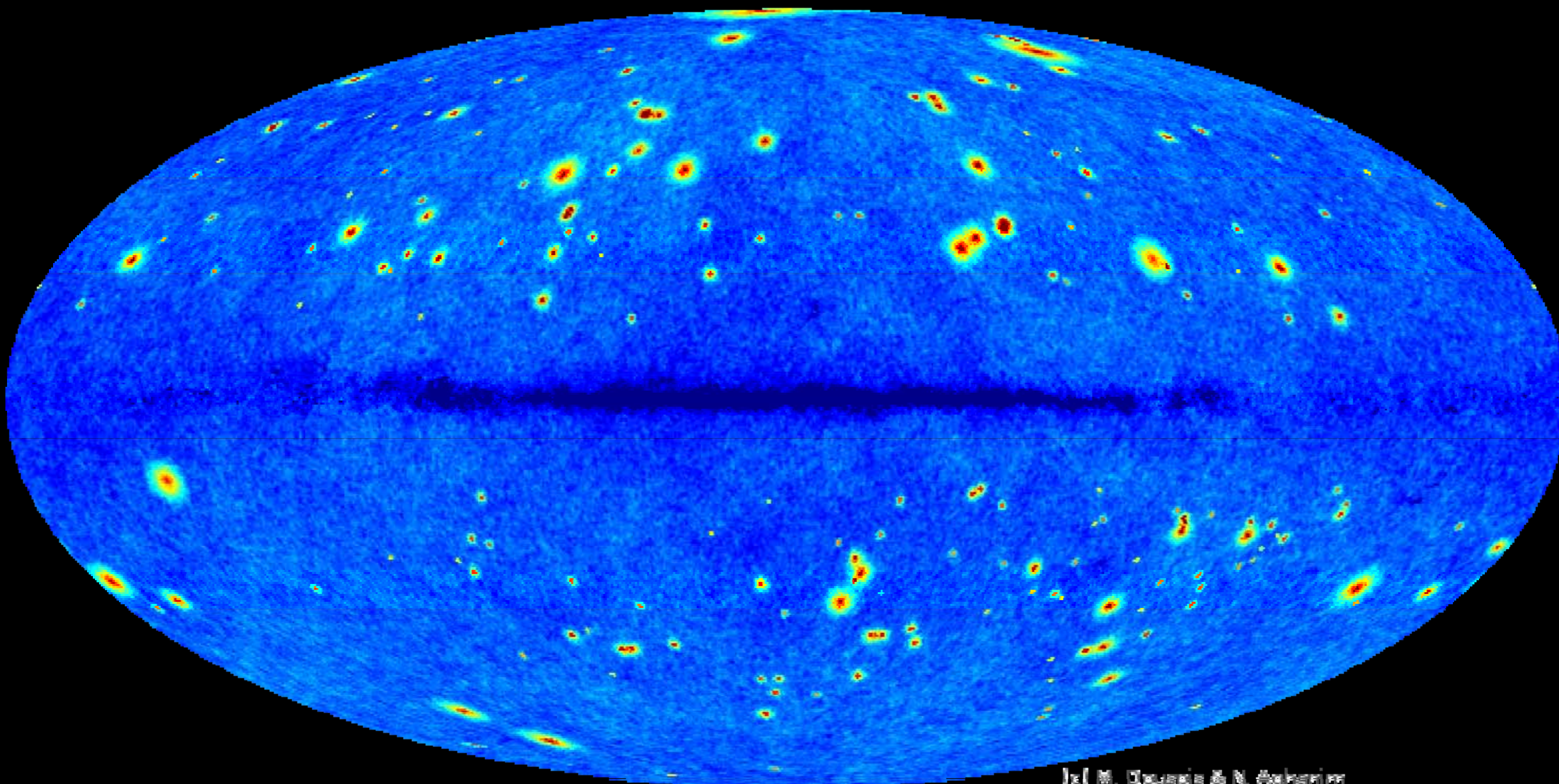

(c) M. Douspis & N. Aghanim

“Raw” versus cleaned @ various S/N

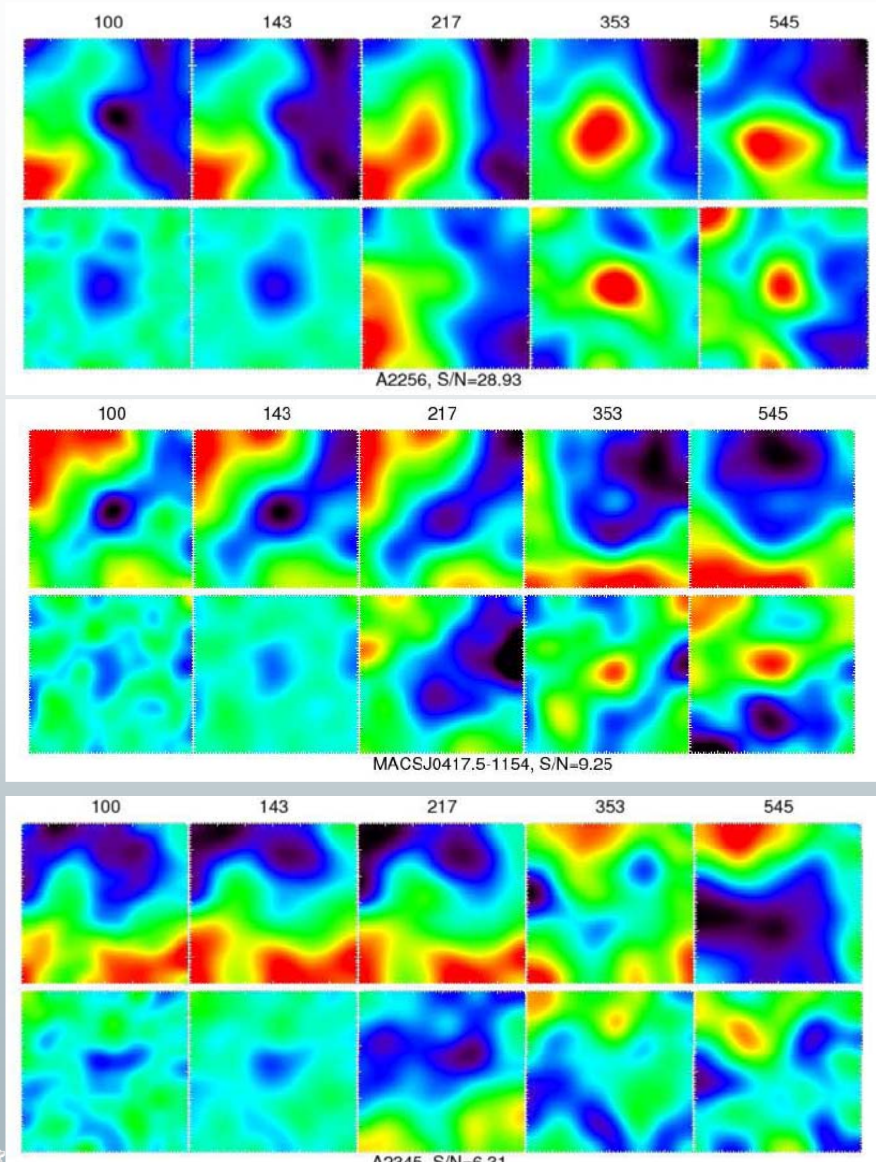

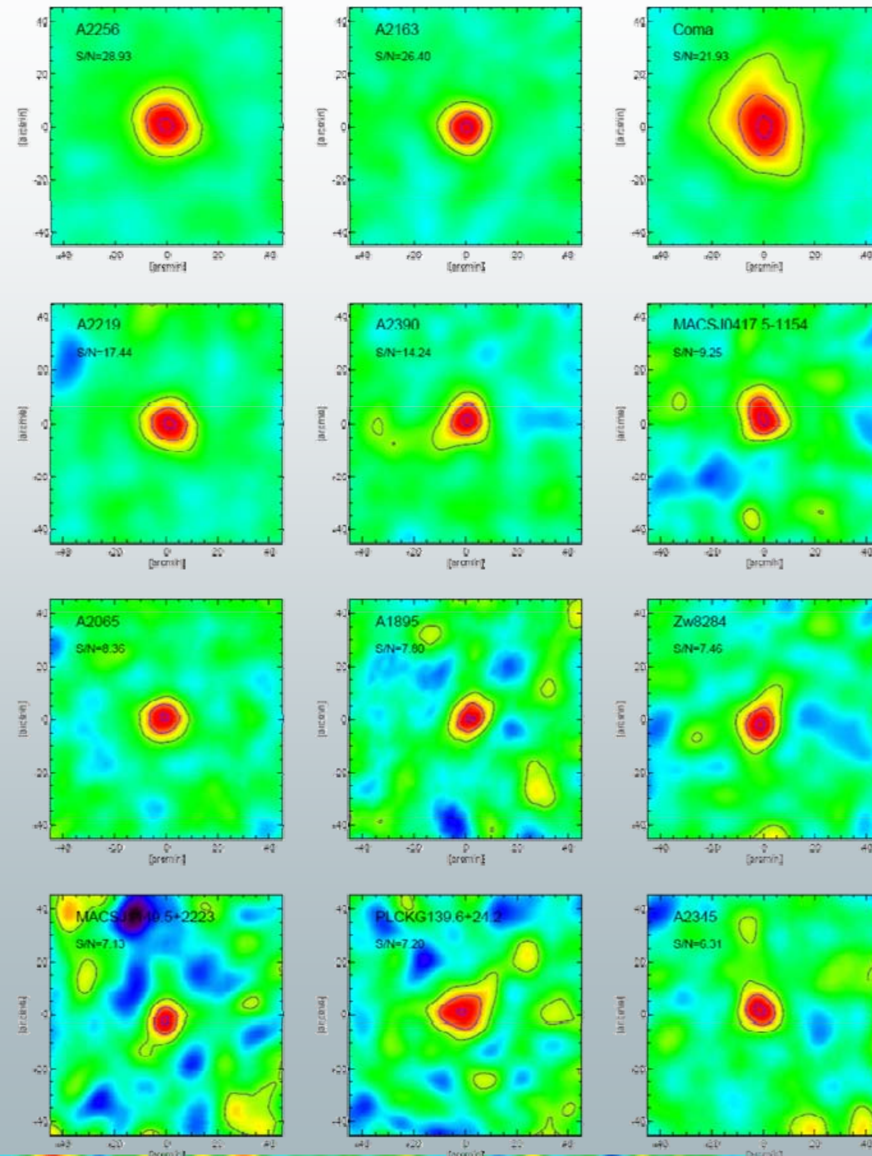

XMM-Newton follow-up / validation

Planck → Discovery of candidate new clusters

XMM-Newton observations → Confirmation of 21 candidates as new clusters with low luminosities and disturbed morphologies.

Planck may be revealing a population of massive dynamically perturbed objects, under-represented in X-ray surveys.

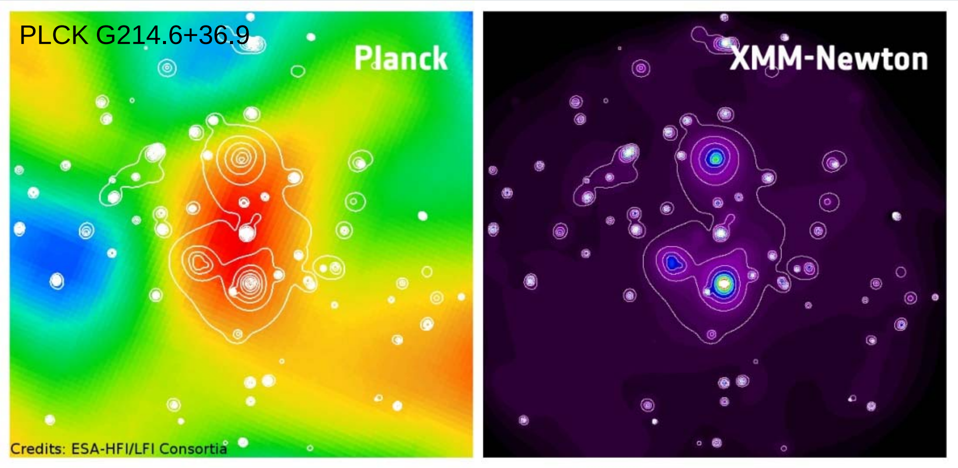

The first super cluster discovered through SZ effect
z_{opt}=0.45/0.46±0.02/0.45; z_X=0.45 (A) A:kT ~3.6 keV θ_{500}=2.2'

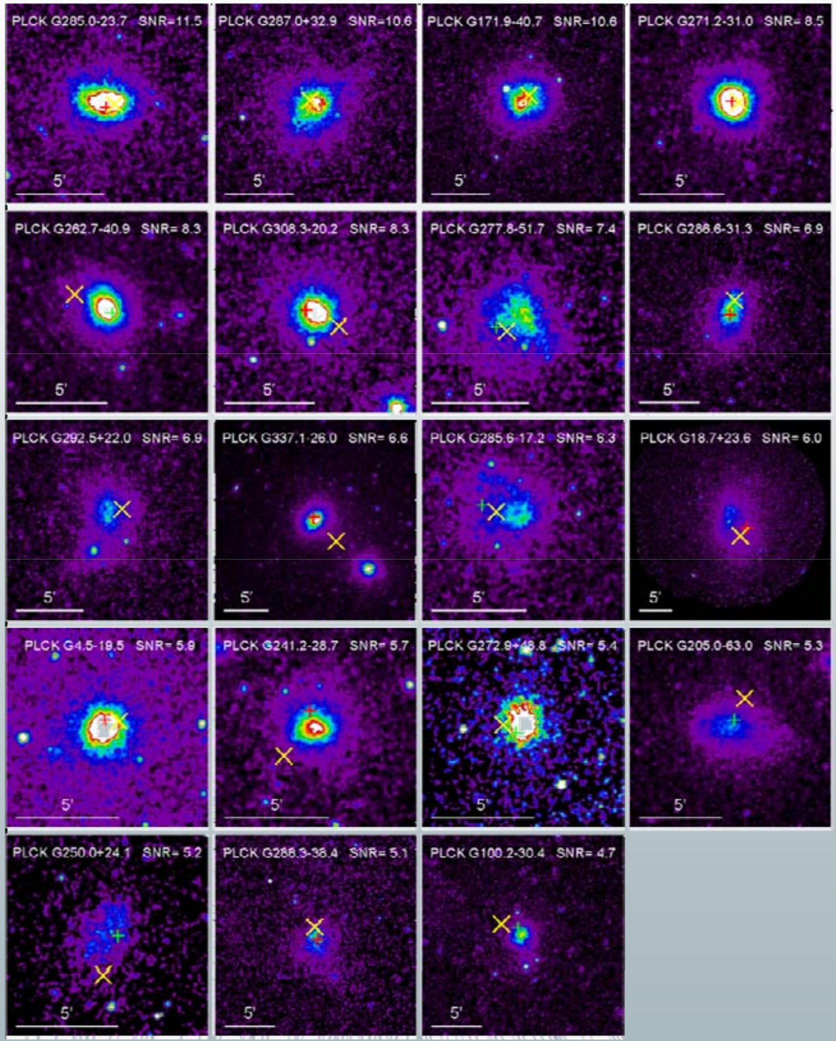

Consistency and more

- X and Y probe the same component (the hot gas), but differently

- X: $E_x \propto \int_{vol} n_e^2 \Lambda(T)\, dv$

- Y crash course: Compton y-parameter (Compton = γ+e ➔ γ+e)
  $y = \int_{los} n_e (T_e - T_\gamma)/m_e c^2\, \sigma T\, d\,los \sim \int p_e\, d\,line\text{-}of\text{-}sight$
- *y governs Thermal SZ effect:*
  $\Delta T/T = y * (x(e^x+1)/(e^x-1)-4)$, $x = h\nu/T_\gamma$
  $\Delta I_\nu = \Delta T/T * x^4 e^x/(e^x-1)^2$; → $-2y$, 0@217, xy
  $(Y = \int y(\theta,\phi)\, d\Omega \sim E_{th} / D_A^2 \sim (E_{grav} - P_{kinetic,\,etc} V + 3 P_s V)/2\, D_A^2)$
  (VIRIAL THEOREM: $E_{grav} \sim G M_g M/R \sim M^{5/3}$ dark matter dominated)

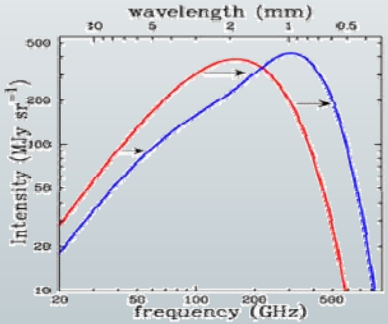

- *And Kinetic SZ (kSZ)*
  $\Delta T/T = \int n_e\, ve_{||} /c\, \sigma\, T\, d\, los \sim \int J_e \,.\, Dr$
  $(\int kSZ(\theta,\phi)\, d\Omega \sim M_{gas} V_{bulk} / DA^2)$

➔ *Can predict Y from X under some hypotheses*

X-ray baseline model

Based on observed scaling relations and structural properties of REXCESS

Ingredient 1:
L-M relation
(Pratt et al. 2009)

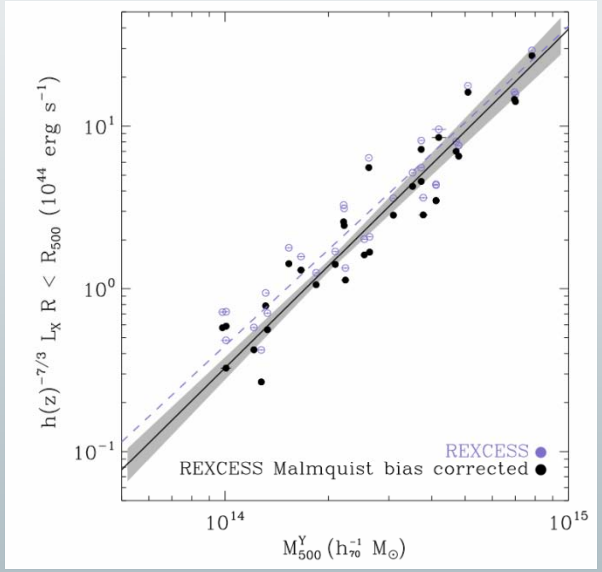

Ingredient 2:
Average ICM density
profile (Croston et al. 2008)

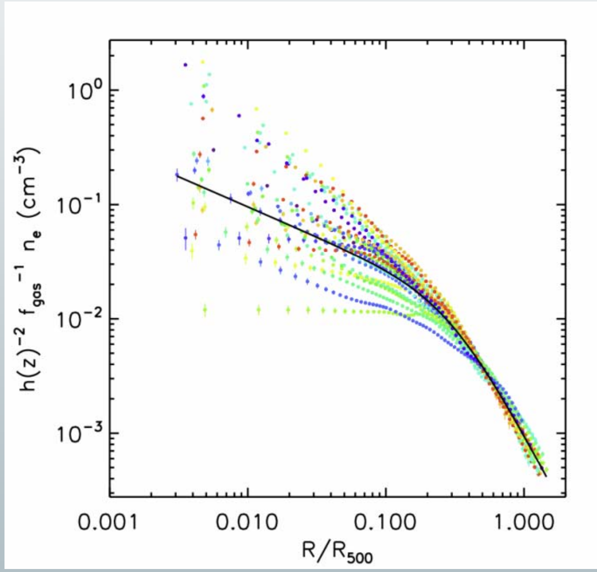

Ingredient 3:
Universal pressure
profile (Arnaud et al. 2010

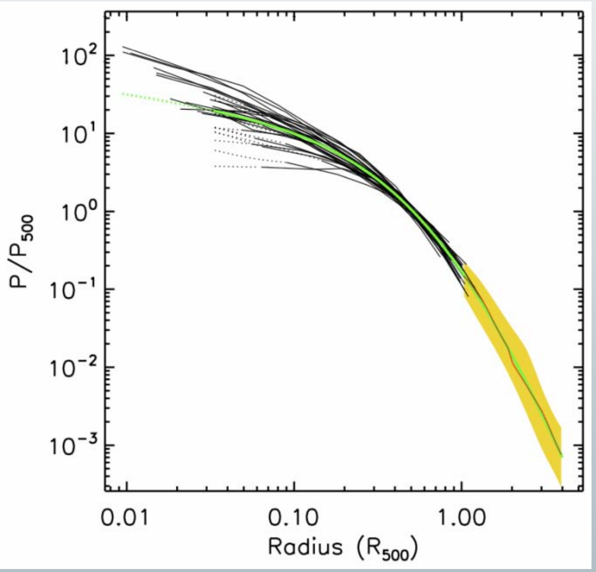

L_{500}, z ➔ M_{500}, R_{500}, Profile, predicted Y_{500}

Planck clusters vs other samples

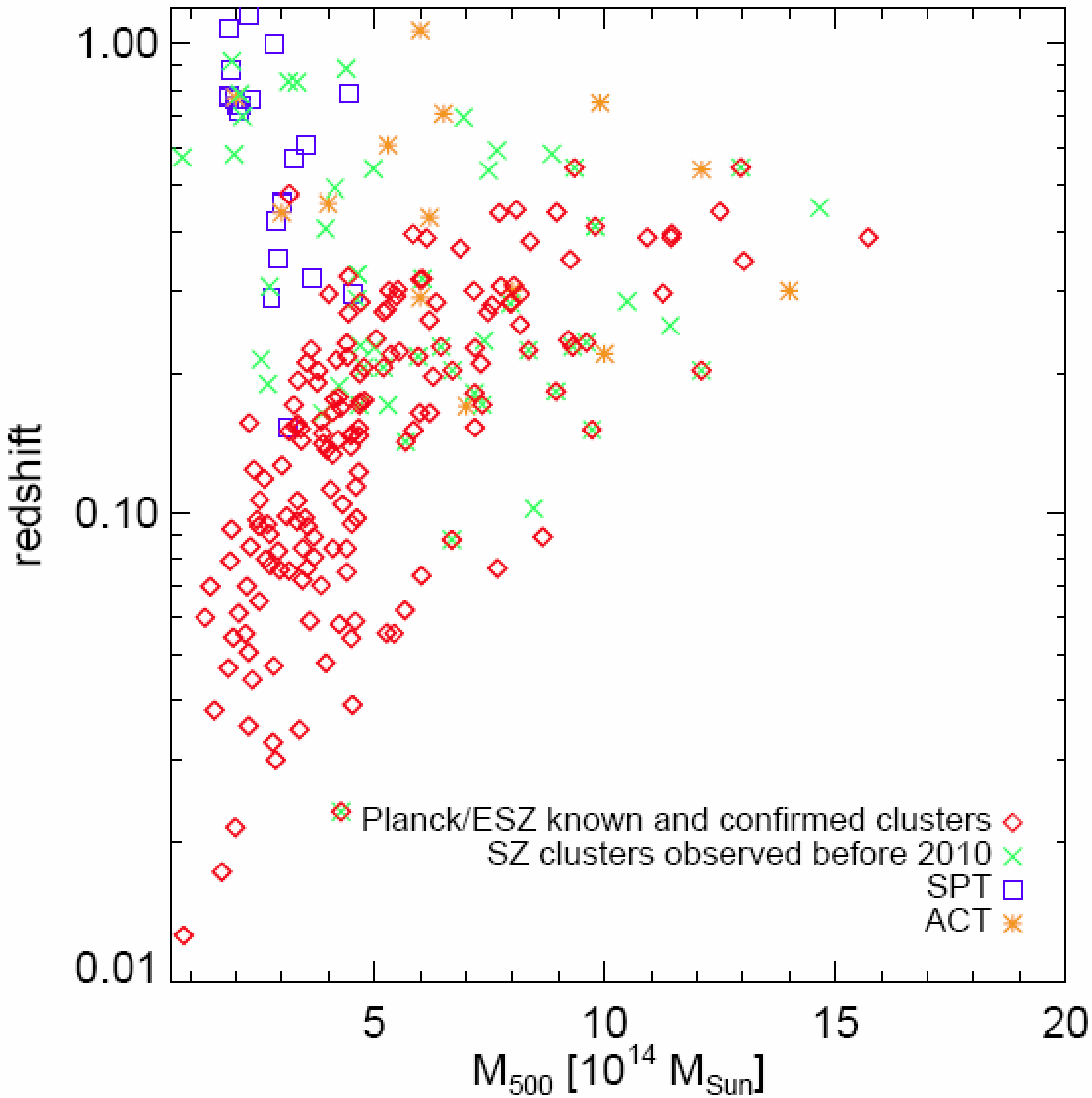

Scaling relation SZ versus X-ray luminosity

Use Multi-frequency Matched Filter (MMF) at positions of the **M**eta-**C**atalogue of **X**-ray detected **C**lusters (~ 1600 MCXC clusters)

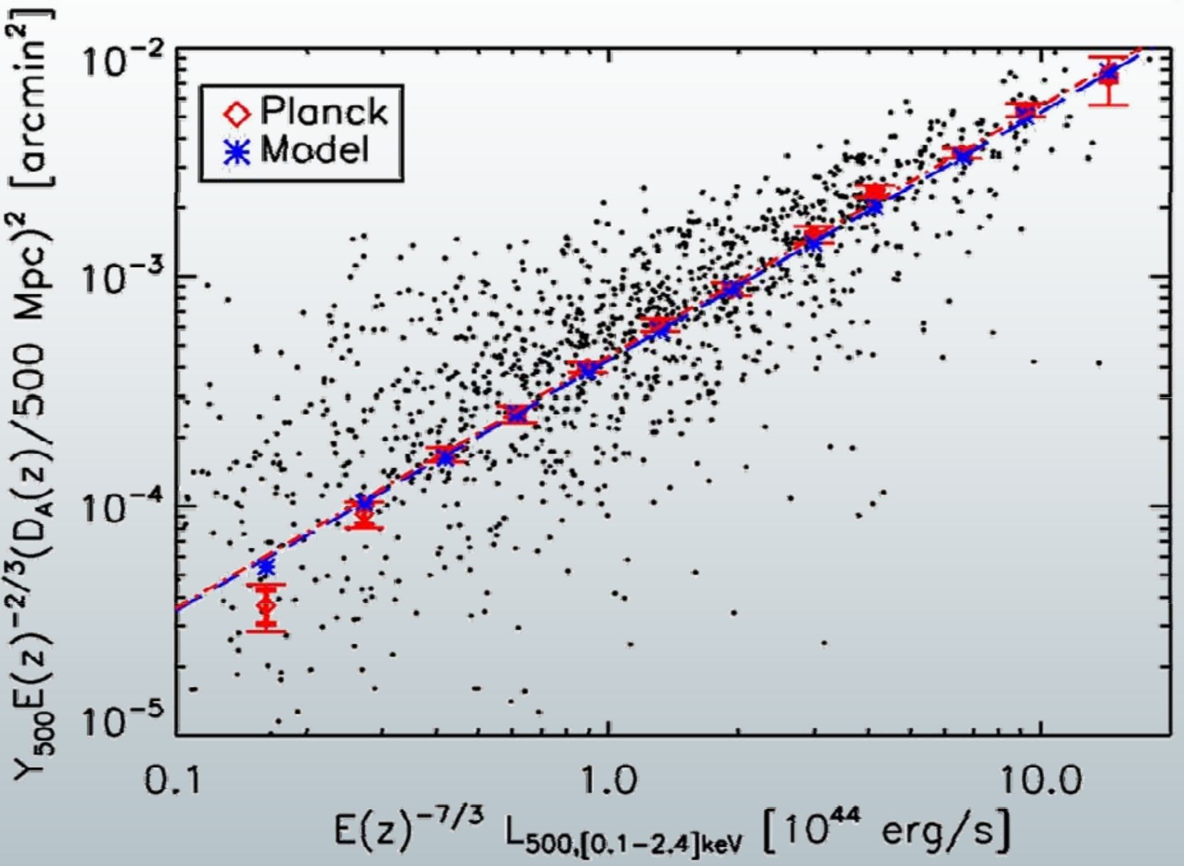

NB: Same conclusion drawn from individual Planck measurement on a selected sub-sample of 62 ESZ clusters with high-quality XMM-Newton archival data

- perfect agreement between X-ray-based predicted and measured SZ signals
- Planck shows that there are **no missing hot baryons**
  (a 5 years debate, closed because Planck error bars are about 10 times smaller than WMAP ones)
- The overall view of the properties of the hot gas in clusters is consistent

Comparison with optical clusters

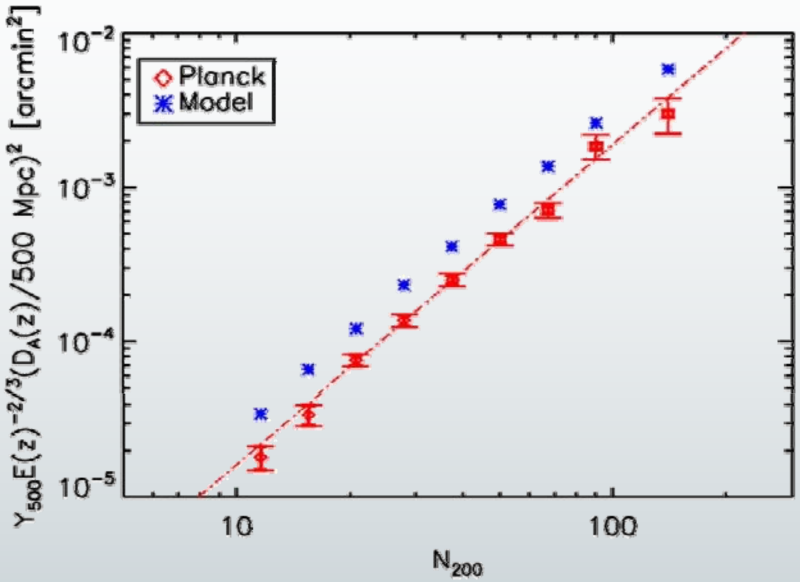

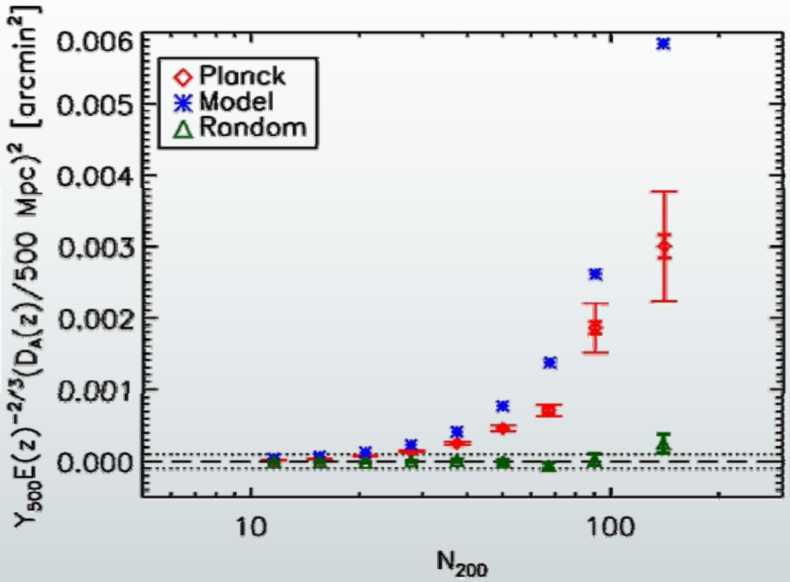

- *First* comparison *of* the SZ signal and the galaxy content of clusters on about 13000 optical clusters from the MaxBCG of SDSS
- In contrast to the X-ray SZ studies, the SZ signal is lower that expected from theoretical predictions
- The origin of the difference needs further investigation and will tell us more on the population of clusters and structure formation

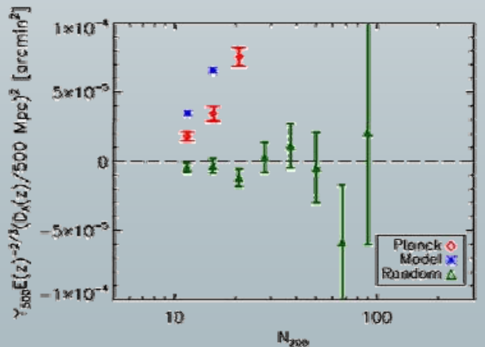

No contradiction with X ray

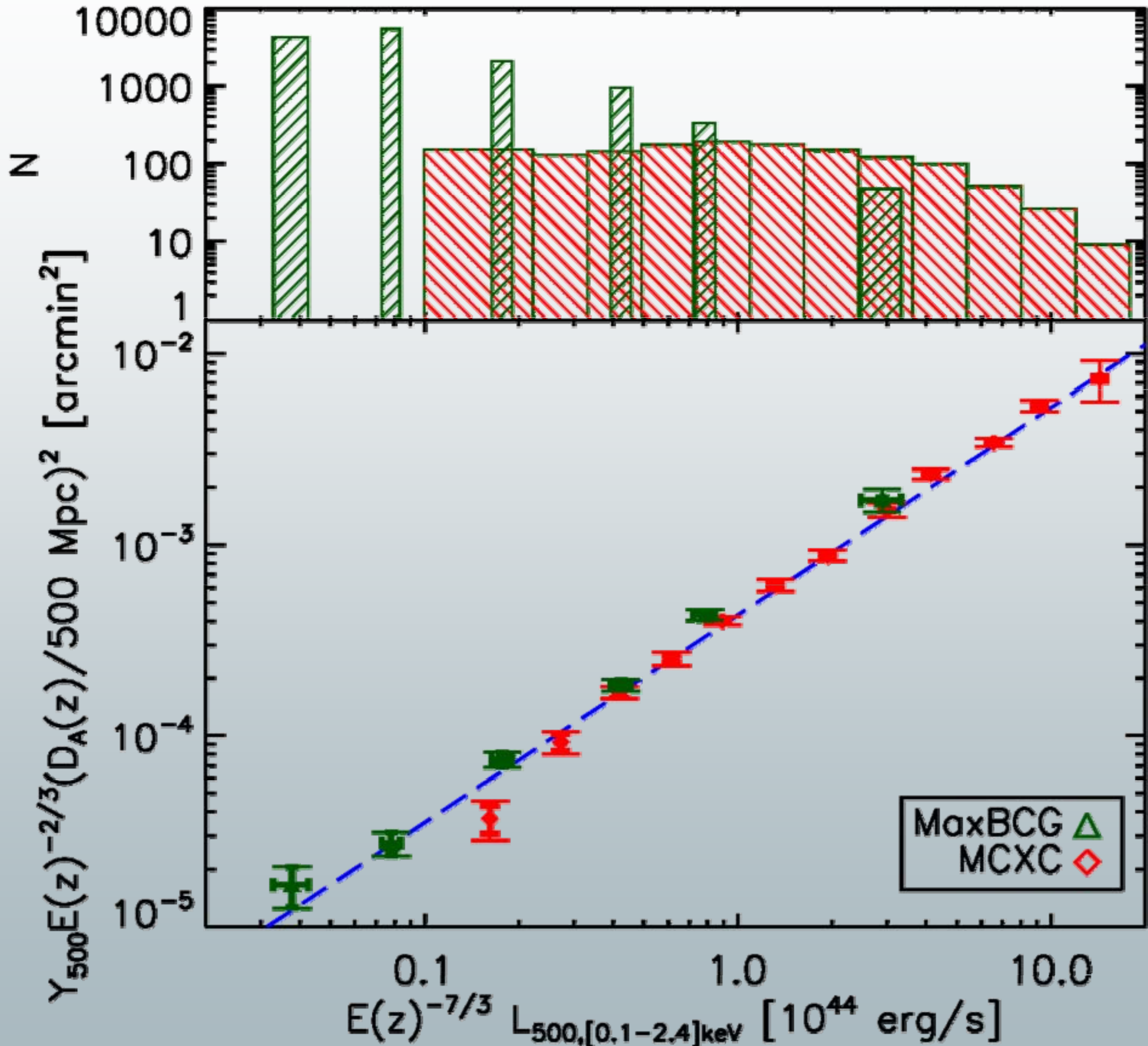

Blue dashed line: Model L-M + M-Y

Note that this goes to really small L_{500} (M_{500})

Back to Galaxies...

- We now know that a large part of the (integrated) light from galaxies is actually in the infared/summ (z+reprocessing)
- Diffraction law: confusion rules this field

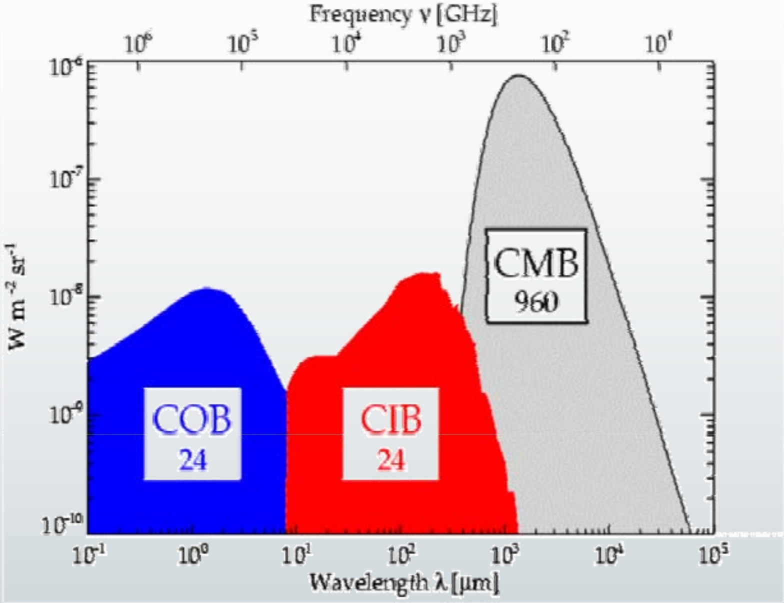

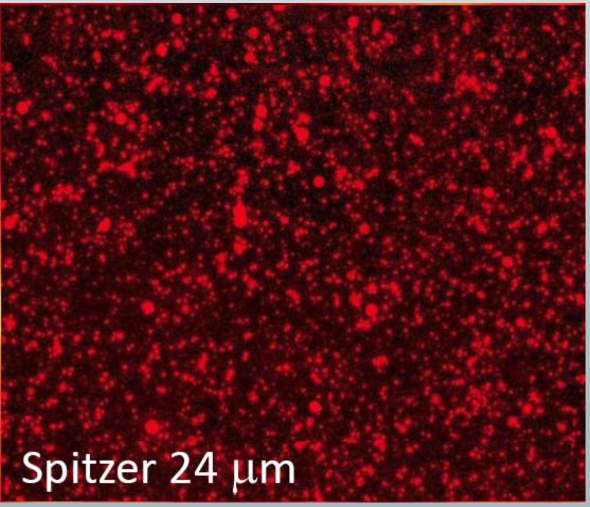

CIB 80% resolved

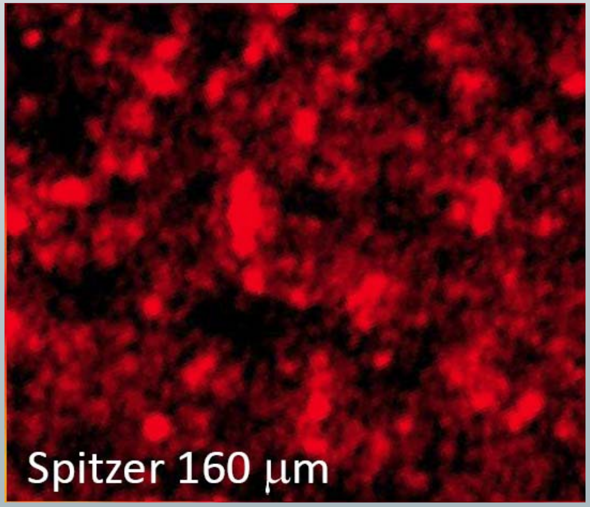

CIB 15% resolved

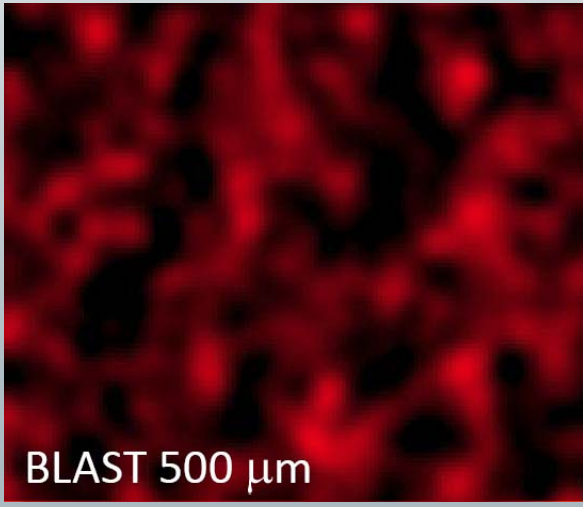

CIB <1% resolved

A saving grace: the negative K-correction

1. when a galaxy is very far - thus much younger- its radiation is redshifted to lower frequencies
2. it is also becoming dimmer and thus difficult to observe
3. in the far infrared and microwave the resolution of telescopes is far less than in the optical
4. **the steep decrease of luminosity with wavelength helps detecting the associated structures in the CIB at high redshifts**

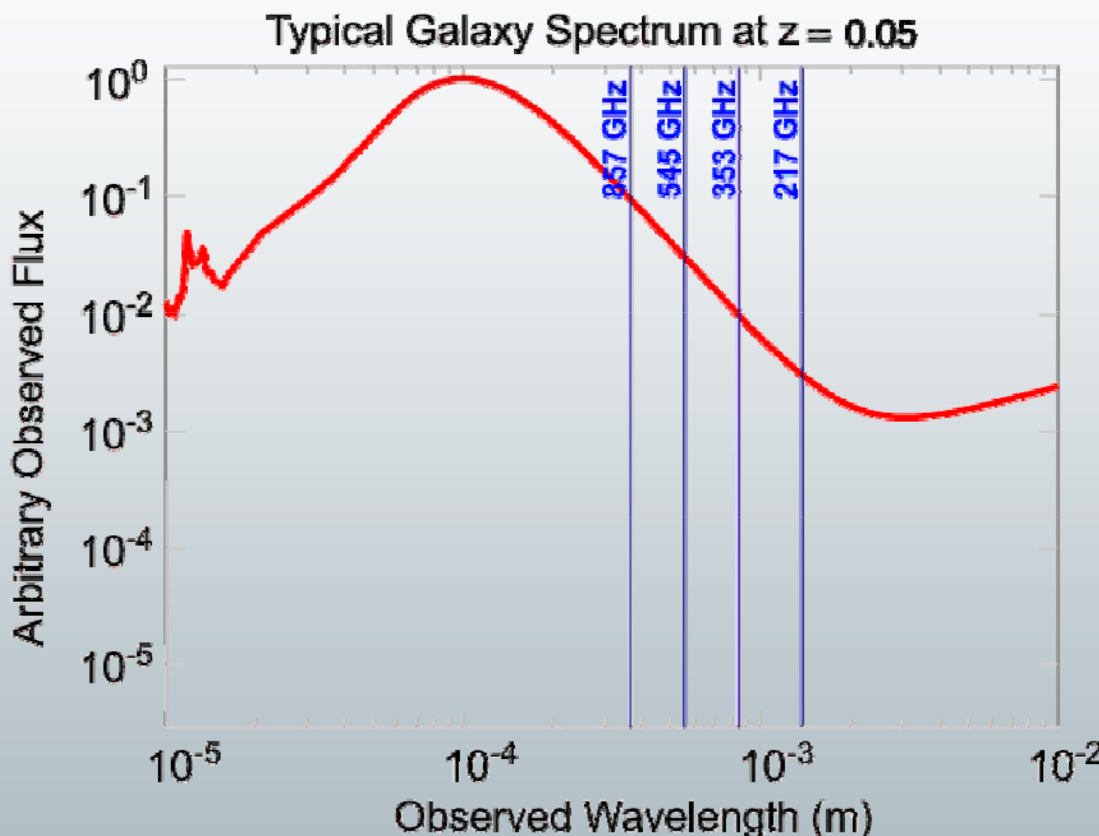

The CIB spectrum

- The contribution from large redshifts can become dominant at lower frequencies
- At 217 GHz, the models indicate that galaxies at z>2 dominates over lower redshift ones (less than 3 billion years)

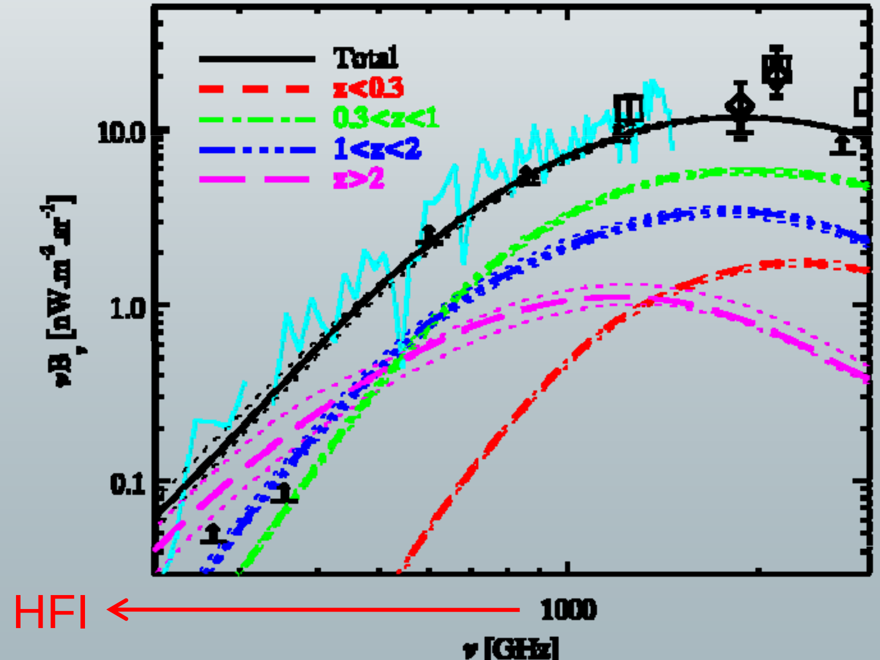

Bétermin+ model

Let's go for it ☺

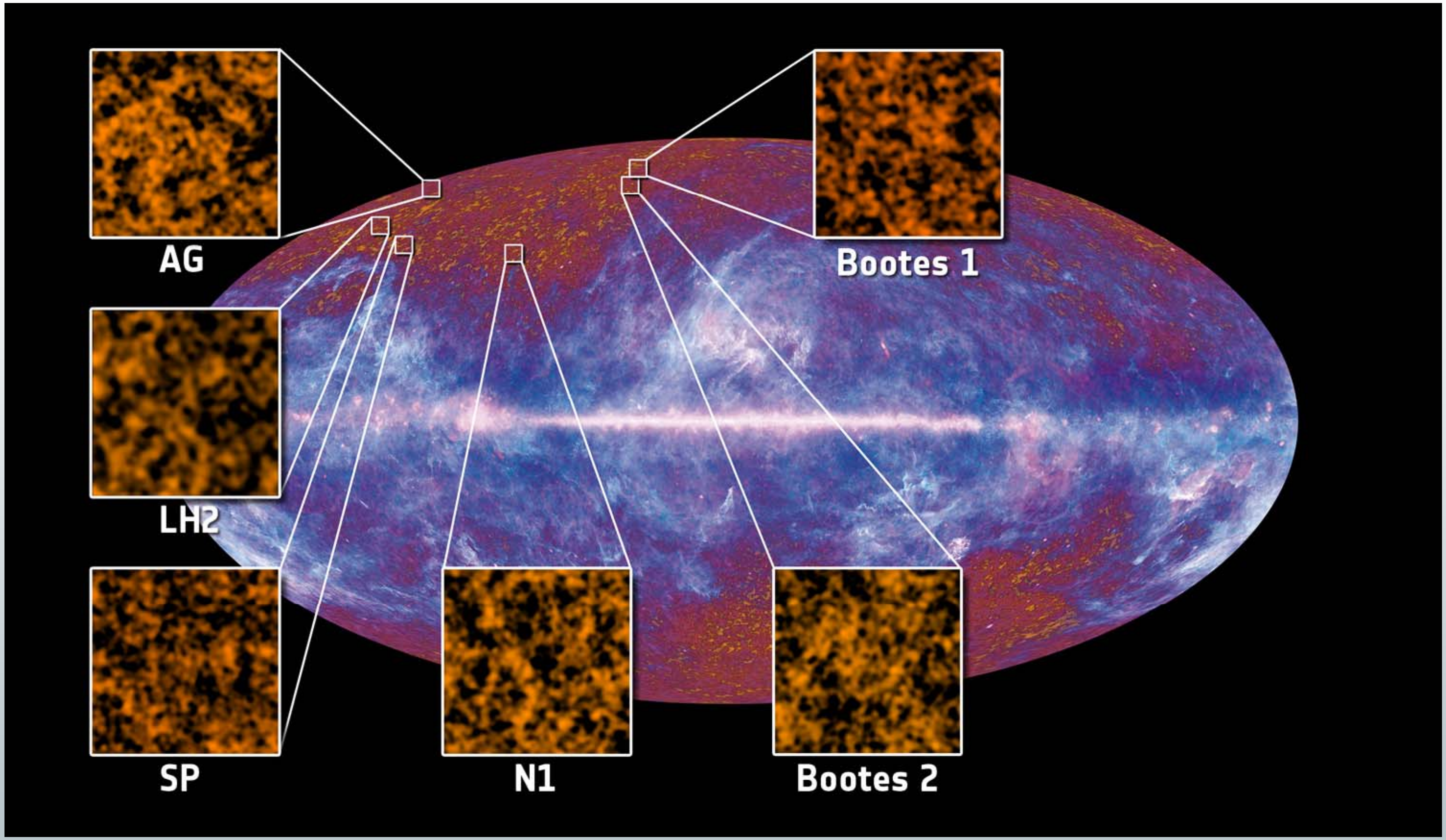

6 high Galactic latitude fields with very low dust contamination : <N(HI)> = 0.7-1.8 10^{20} at/cm^2

- Two contaminants: CMB background and Galactic dust foreground!
- Cleaning based on templates removal (& ERCSC source masking)
  - HFI (Wiener-filtered) 143 GHz
  - HI GBT data for dust (martin+2011)

Removing dust

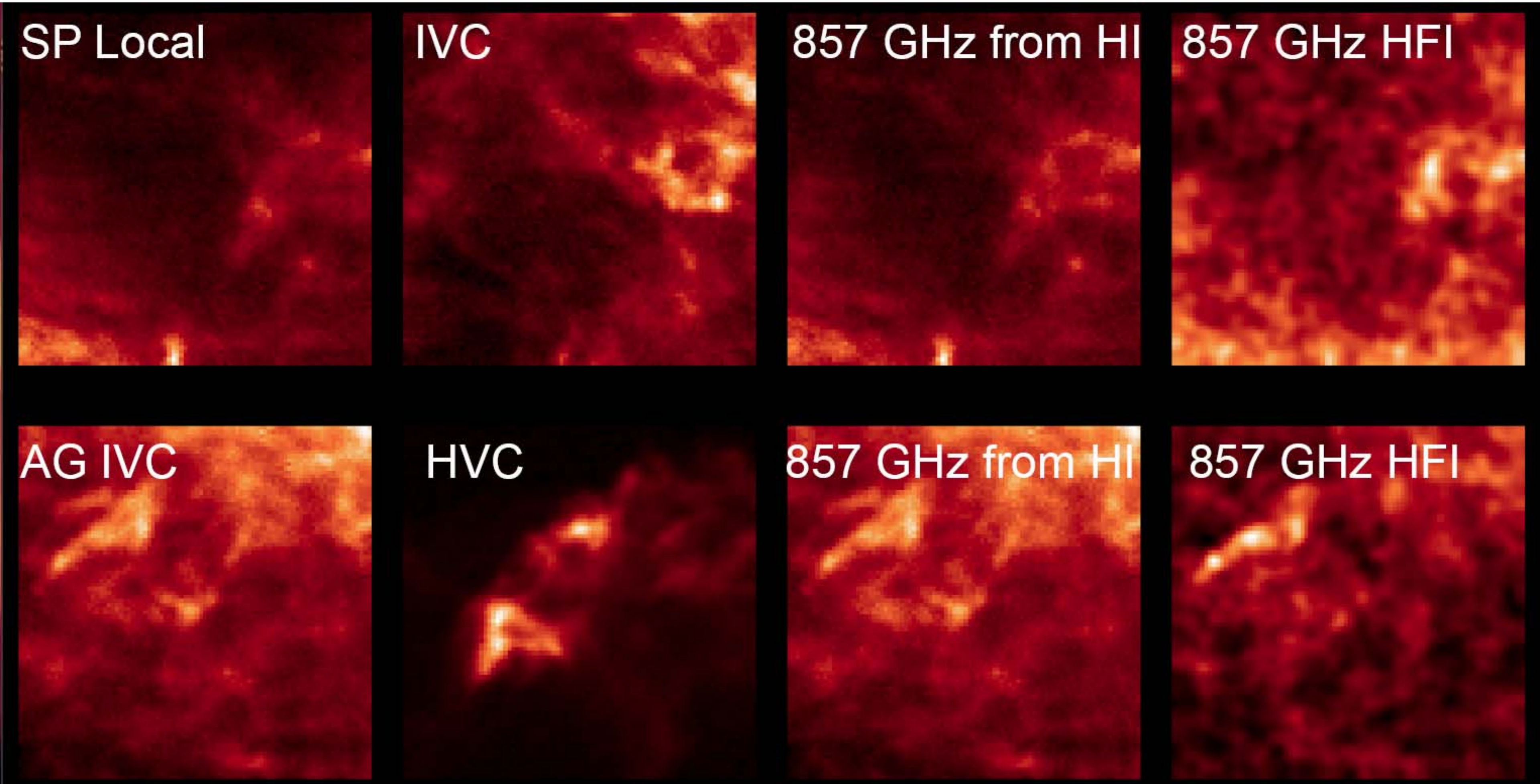

$$I_\nu(x,y) = \sum_i \alpha_\nu^i N_{HI}^i(x,y) + C_\nu(x,y)$$

HI = best dust tracer in the diffuse sky

Decompose emission at each HFI ν on each of the components (local, IVC and HVC)

The cleaning

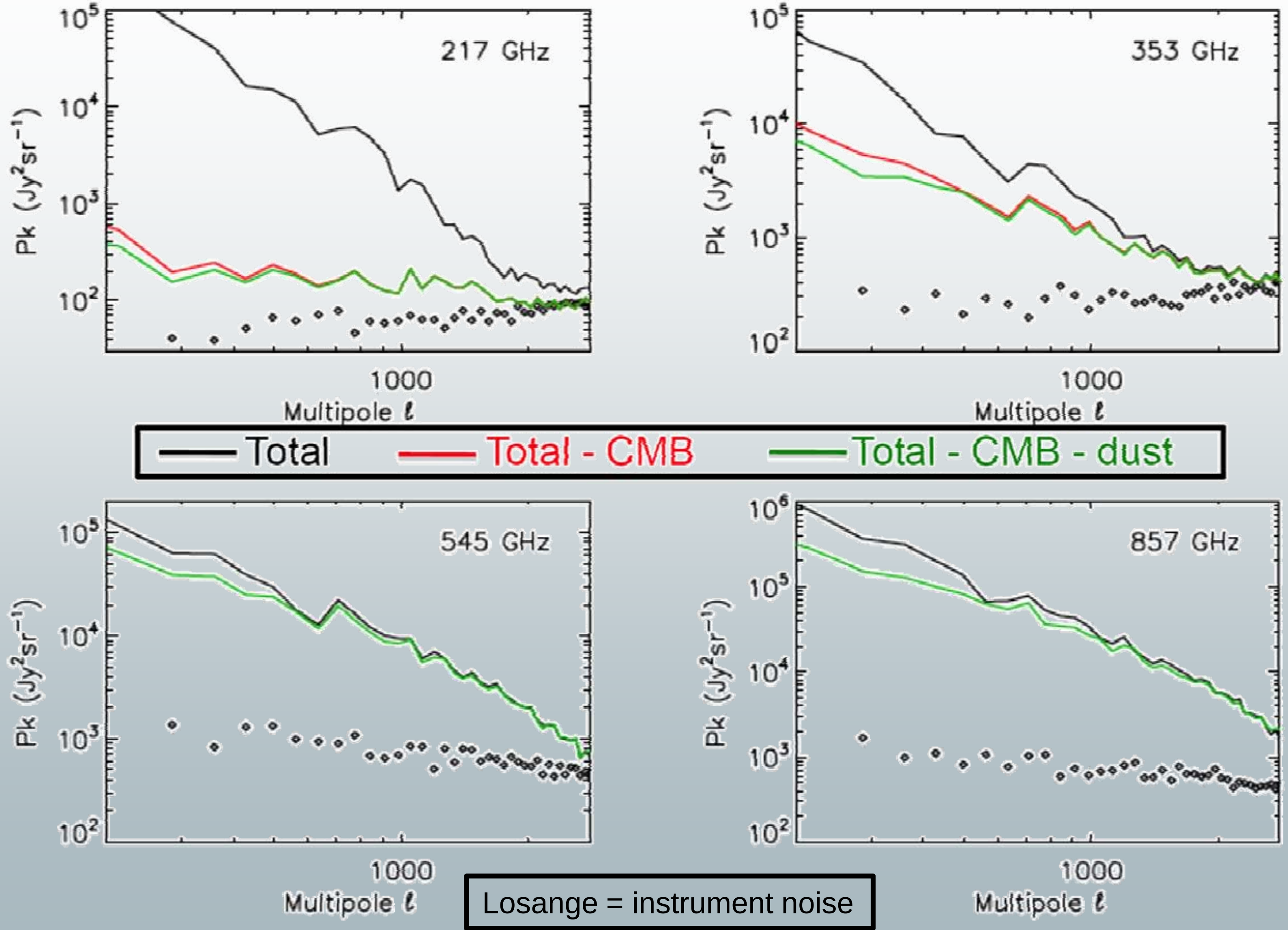

CIB appearance versus frequency

1. As we move towards lower frequencies we see structures in the universe closer and closer to the galaxy formation period
2. The same structures are seen in successive bands illustrating the high signal to noise
3. we expect the lowest Planck frequency CIB maps (217 Ghz) shows structures formed less than 2 billion years after the big bang

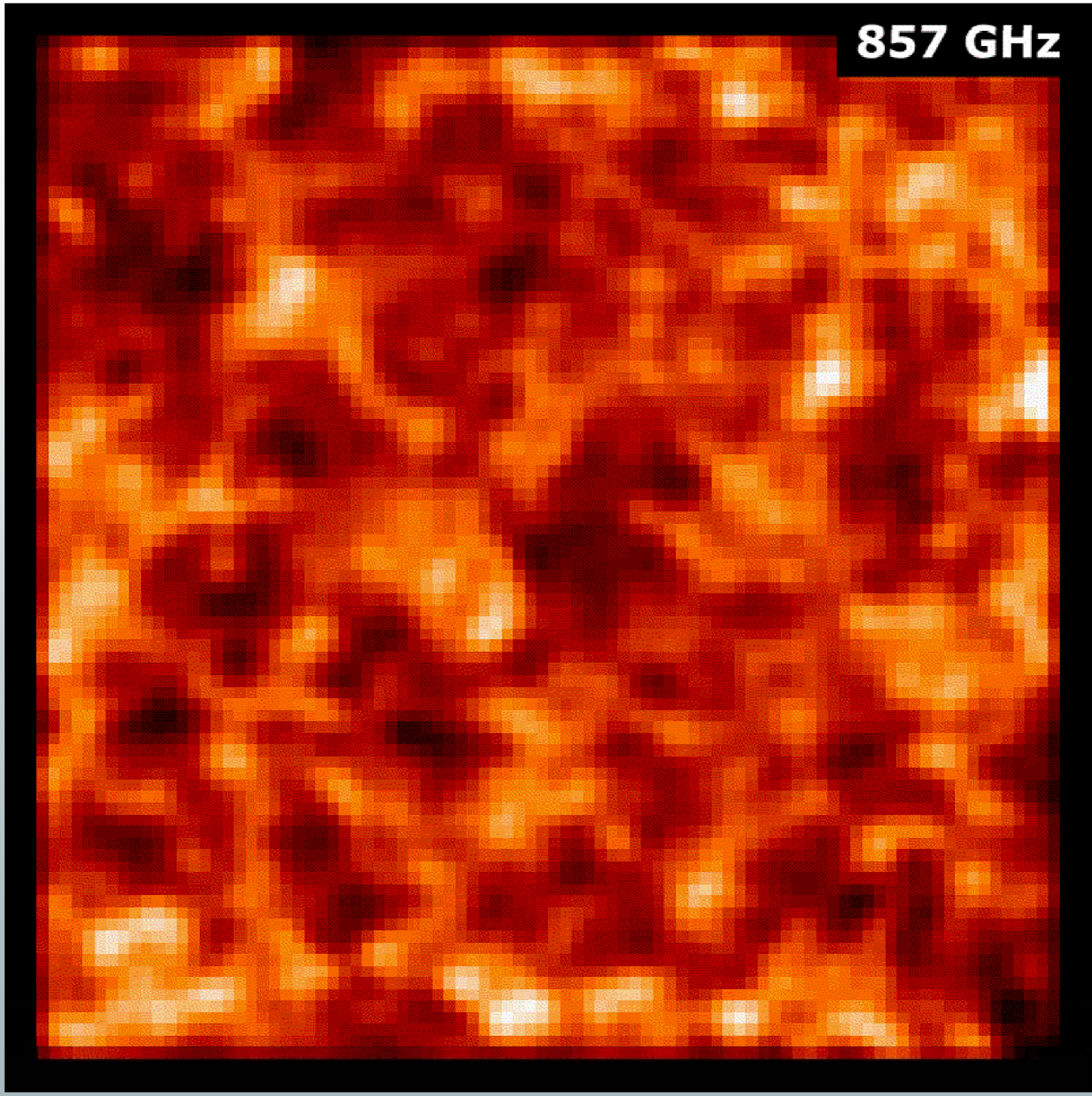

Models tend to differ at high-z...

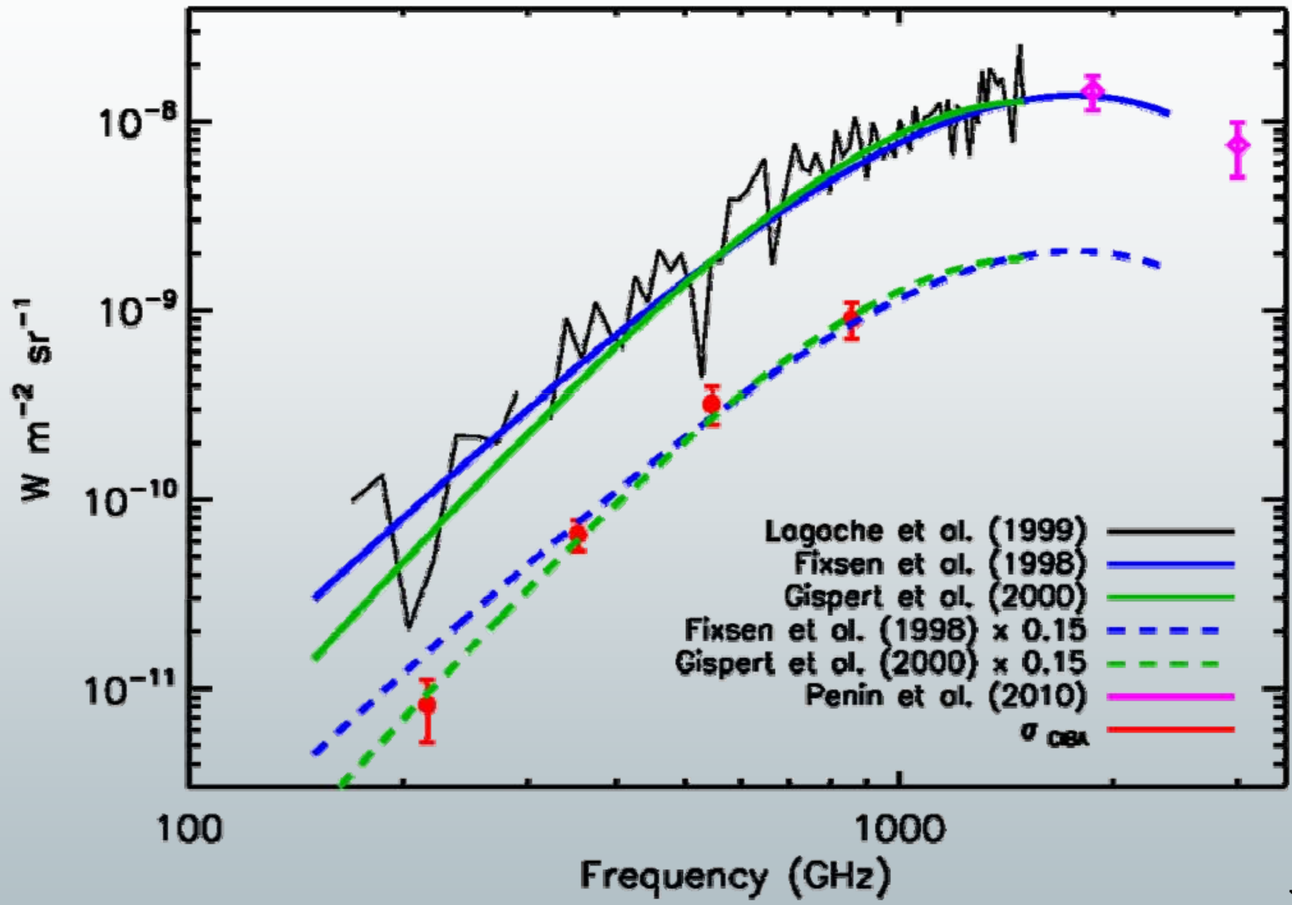

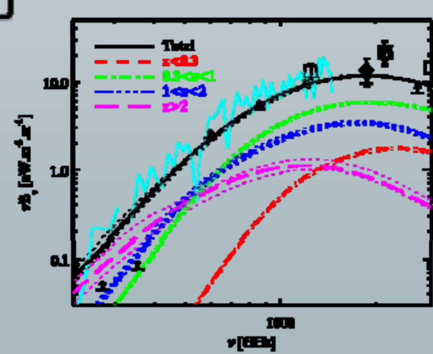

CIB power spectra

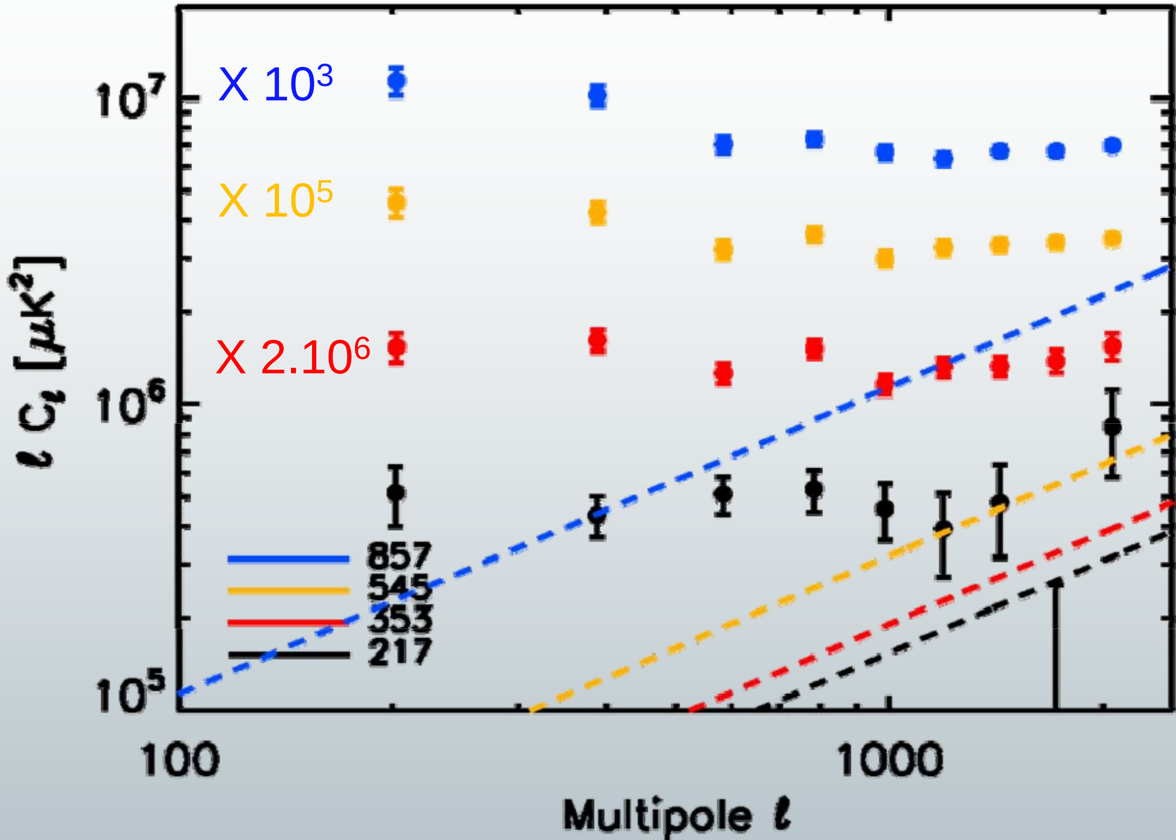

Field-combined CIB anisotropy power spectra at 217, 353, 545 & 857GHz.

The dashed line shows the expected sum of the dusty and radio galaxy shot-noise power. The power spectra at 217, 353, and 545GHz have been arbitrary scaled to allow for a better comparison between frequencies

BLAST & SPT (217 GHz) versus HFI

The green dashed line corresponds to the SPT shot noise and the green dot-dashed line to the clustering model of Hall et al. (2010), the sum of the two being the continuous green line.

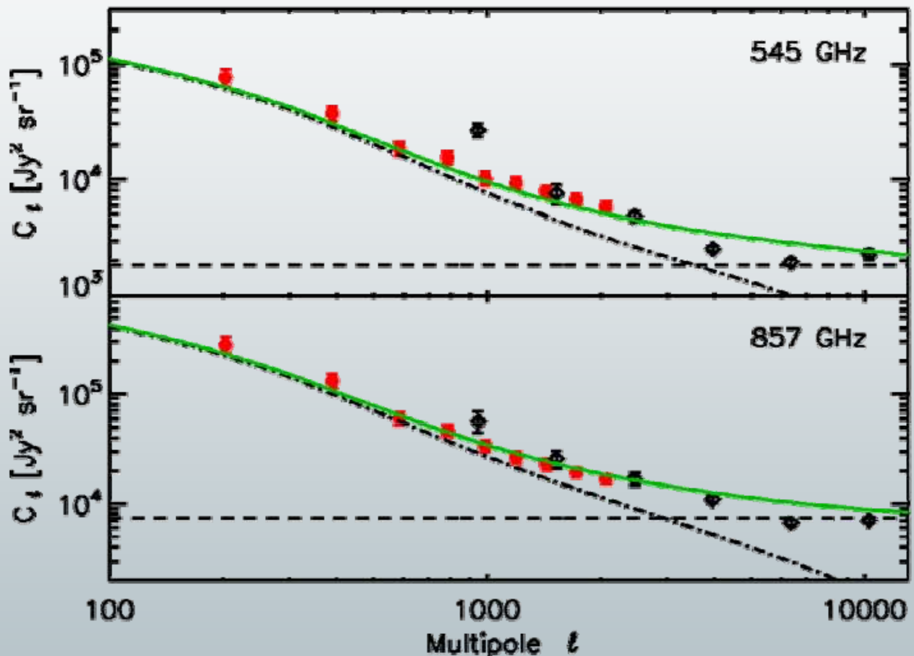

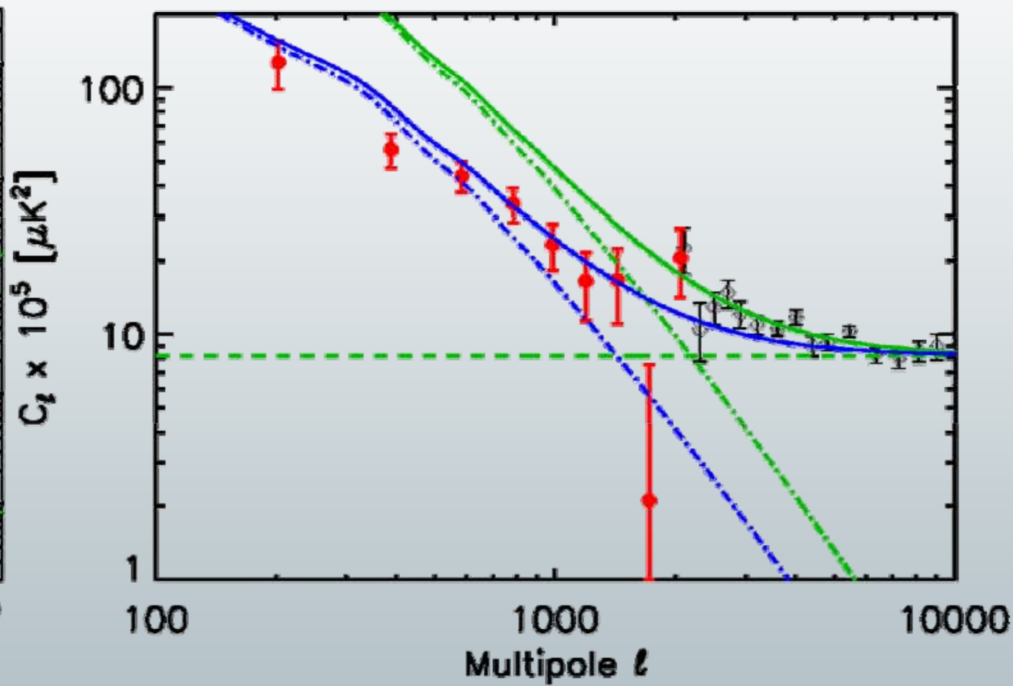

NB: BLAST values are color-corrected using the CIB mean spectrum (1.05 @ 857 & 0.7 @ 545 GHz)

SPT clustering model overpredicts by a factor $\simeq$ 2.4 the HFI power at $\ell = 800$.

When normalised by this factor (dash-dotted line) the clustering+shot noise (continuous line) now under-predicts the SPT data points (a signature of non-linear contributions?)

Counts and HOD

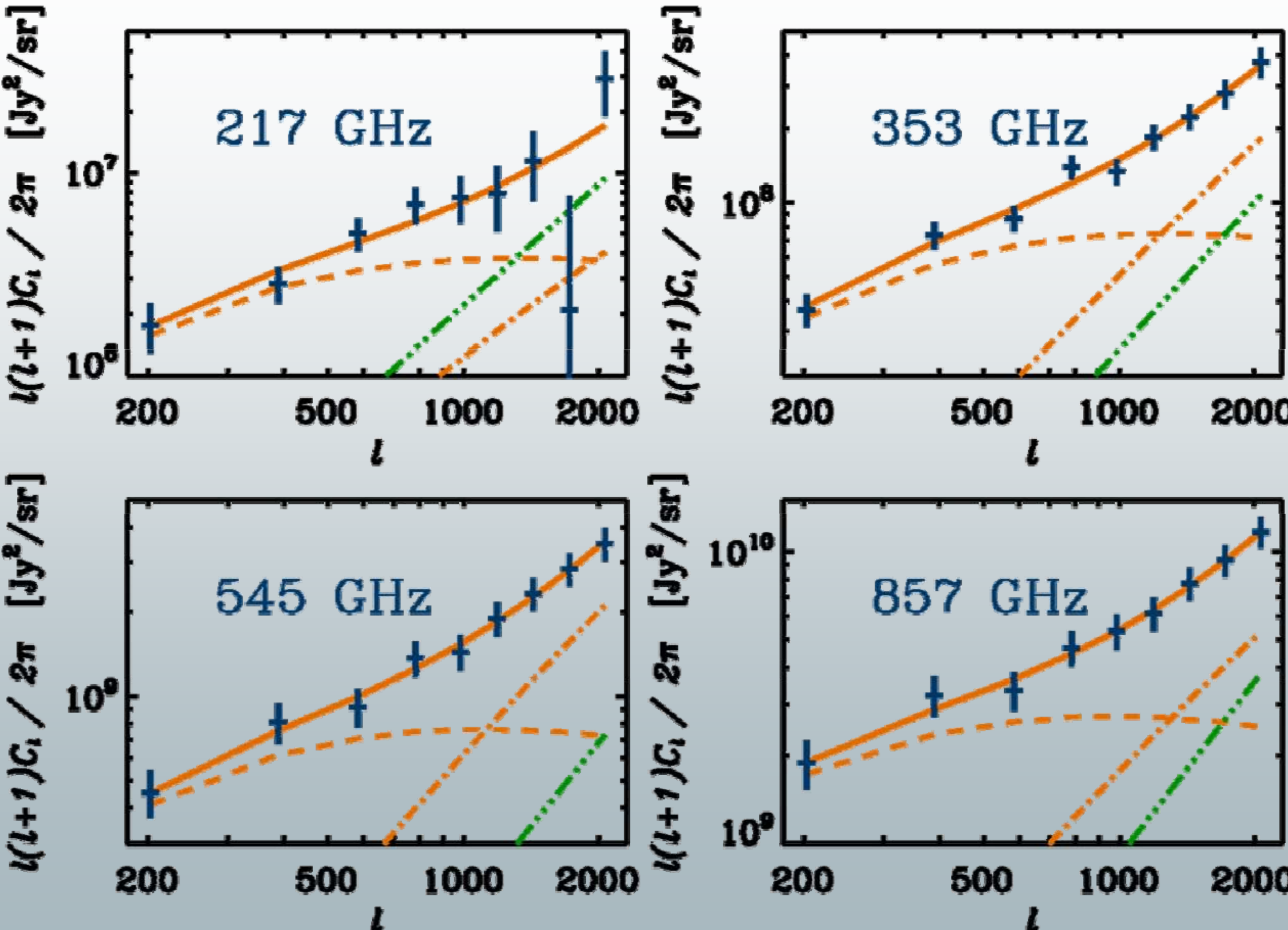

Hard to go further in modelling

Frequency (GHz)	A	n	χ^2 /(#bins-#params)
217	47.38 ± 4.91	-1.04 ± 0.12	1.07
353	993.7 ± 34.07	-1.03 ± 0.05	1.26
545	(103.7 ± 4.34) ×10^2	-1.08 ± 0.06	0.51
857	(36.09 ± 1.44) ×10^3	-1.17 ± 0.06	0.61

Table 6. Power-law model best-fit parameters for each frequency as well as the reduced χ^2. The errors corresponds to the 1σ Gaussian error including statistical and systematic errors.

Halo Model HOD (Halo Occupation Density model)

$$C_\ell^{\nu\nu'} = \int_0^{3.5} dz \frac{d\chi}{dz} \frac{a^2}{\chi^2} \bar{j}_\nu(z) \bar{j}_{\nu'}(z) P_{gg}(k = \ell/\chi, z) + \left(j_{\rm eff}^{\nu\nu'}\right)^2 \int_{3.5}^{7} dz \frac{d\chi}{dz} \frac{a^2}{\chi^2} P_{gg}(k = \ell/\chi, z)$$

Need z-evolution of luminosity function $\bar{j}_\nu(z) = (1+z) \int_0^{S_{\rm cut}} dS\, S\, \frac{d^2N}{dS\, dz}$

But of course, as is, degeneracies → constraints in a larger plan

Conclusions

- Planck works well. HFI exceeds expectations
- First 10 months of data (Aug13->Jun6th): reprocessed, ERCSC and first scientific analysis all in 6 months.
- ERCSC (~15000 sources, 189 SZ clusters) fullfills expectations

- 25 papers unveiled at Planck2011 à la Vilette (& AAS & astroph)
- Disclaimer: very incomplete / biased subsample of these 25 papers.
- Radio-source models steepen too early: miss the high end (217GHz)
- Lots of Cold Cores... The net has been drawn, now to exploit the catch
- An incredible ensemble for dust / ISM studies (AME, dark gaz... uncovered)
- A new reference sample for SZ studies.: high mass / rare objects
  - *Finding new (interacting/multiple) objects*
  - *Full consistency with X-ray data (Y vs X)*
  - *Surprise with optically selected clusters (and unprecedented very low masses)*
- CIB anisotropies very well measured
  - *Power detected from 10' to 120' at 4 frequencies*
  - *Interesting comparison with other determinations ☺*
  - *Further constraints on Galaxy formation models*
- Stay tunes : the nominal mission is inj the can, downstairs (data dec 13th)

The first 25 (a to y)

Title	Authors
Planck early results 01: The Planck mission	Planck Collaboration
Planck early results 02: The thermal performance of Planck	Planck Collaboration
Planck early results 03: First assessment of the Low Frequency Instrument in-flight performance	Mennella et al.
Planck early results 04: First assessment of the High Frequency Instrument in-flight performance	Planck HFI Core Team
Planck early results 05: The Low Frequency Instrument data processing	Zacchei et al.
Planck early results 06: The High Frequency Instrument data processing	Planck HFI Core Team
Planck early results 07: The Early Release Compact Source Catalogue	Planck Collaboration
The Explanatory Supplement to the Planck Early Release Compact Source Catalogue	Planck Collaboration
Planck early results 08: The all-sky early Sunyaev-Zeldovich cluster sample	Planck Collaboration
Planck early results 09: XMM-Newton follow-up for validation of Planck cluster candidates	Planck Collaboration
Planck early results 10: Statistical analysis of Sunyaev-Zeldovich scaling relations for X-ray galaxy clusters	Planck Collaboration
Planck early results 11: Calibration of the local galaxy cluster Sunyaev-Zeldovich scaling relations	Planck Collaboration
Planck early results 12: Cluster Sunyaev-Zeldovich optical scaling relations	Planck Collaboration
Planck early results 13: Statistical properties of extragalactic radio sources in the Planck Early Release Compact Source Catalogue	Planck Collaboration
Planck early results 14: Early Release Compact Source Catalogue validation and extreme radio sources	Planck Collaboration
Planck early results 15: Spectral energy distributions and radio continuum spectra of northern extragalactic radio sources	Planck Collaboration
Planck early results 16: The Planck view of nearby galaxies	Planck Collaboration
Planck early results 17: Origin of the submillimetre excess dust emission in the Magellanic Clouds	Planck Collaboration
Planck early results 18: The power spectrum of cosmic infrared background anisotropies	Planck Collaboration
Planck early results 19: All-sky temperature and dust optical depth from Planck and IRAS – constraints on the "dark gas" in our Galaxy	Planck Collaboration
Planck early results 20: New light on anomalous microwave emission from spinning dust grains	Planck Collaboration
Planck early results 21: Properties of the interstellar medium in the Galactic plane	Planck Collaboration
Planck early results 22: The submillimetre properties of a sample of Galactic cold clumps	Planck Collaboration
Planck early results 23: The Galactic cold core population revealed by the first all-sky survey	Planck Collaboration
Planck early results 24: Dust in the diffuse interstellar medium and the Galactic halo	Planck Collaboration
Planck early results 25: Thermal dust in nearby molecular clouds	Planck Collaboration

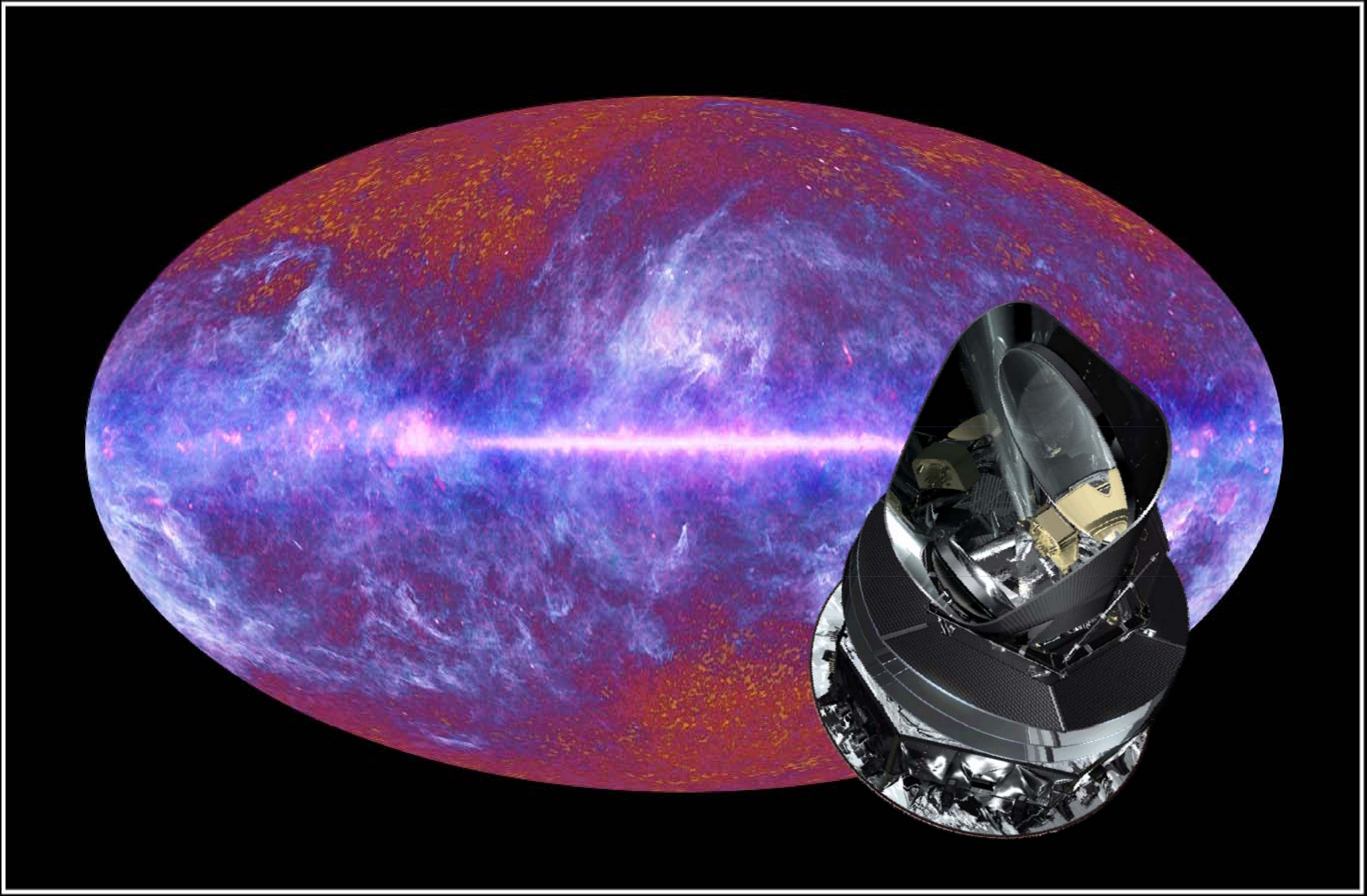

The Planck one-year all-sky survey